THE ROLE OF HEPARAN SULFATE PROTEOGLYCANS DURING DEVELOPMENT OF THE ZEBRAFISH LATERAL LINE

by
Caitlin Moira Fox

A dissertation submitted to Johns Hopkins University in conformity with the requirements for the degree of Doctor of Philosophy

Baltimore, Maryland
October 2016

Abstract

The lateral line is a sensory system that aquatic organisms use to sense local water currents in their environment using mechanosensory neuromasts. It makes for an excellent model system in which to study cell signaling and collective cell migration, given its superficial location just beneath the epidermis, and the variety of genetic tools available in zebrafish. Development of the posterior lateral line is spearheaded by the posterior lateral line primordium (PLLP), which is a group of about 120 cells that collectively migrate from the ear to the tip of the tail between 24 and 48hpf. As it migrates, the PLLP periodically deposits sensory organs from its trailing end. Two signaling systems play important roles in patterning the cells of the PLLP, working in concert to assemble protoneuromasts and mediate migration. Wnt signaling maintains a population of largely mesenchymal cells in the leading domain, and also initiates transcription of two Fgf ligands, while repressing the Fgf receptor. The Fgf ligands are delivered to trailing cells, where they activate their receptor and downstream signaling induces epithelialization and protoneuromasts formation. Fgf also acts as a migrational cue for trailing cells to follow the leading migratory cells.

Heparan sulfate proteoglycans (HSPGs), embedded in the cell membrane and distributed throughout the extracellular matrix, are known to widely regulate signaling pathways, including Wnt and Fgf signaling. HSPGs are composed of a core protein with covalently linked heparan sulfate chains, which are heavily modified by a series of enzymes during synthesis. I examined the role of Syndecan4 (Sdc4), a type of core protein and 3-*O*-sulfation, a rare modification made to heparan sulfate, in regulating signaling of

the PLLP. My findings indicate that both Sdc4 and 3-*O*-sulfation promote Fgf signaling and the downstream processes of protoneuromast formation and cell migration.

I demonstrate that *sdc4* is expressed in the trailing domain of the PLLP, where it is negatively regulated by Fgf signaling. Morpholino-mediated knockdown of *sdc4* interferes with protoneuromast formation and significantly slows the speed of migration, both of which most likely result from weak Fgf signaling. In *sdc4* mutants, I also show that Fgf signaling is compromised. *Sdc4* mutants are more vulnerable to manipulation of Fgf signaling, exhibiting decreased migration speed when treated with low doses of various inhibitors of Fgf. In addition to their susceptibility to Fgf signaling inhibition, *sdc4* mutant PLLP migration is slower after *sdc3* knockdown.

In addition to the importance of particular core proteins, I show that specific modifications to the heparan sulfate chain also support Fgf signaling. Two 3-*O*-sulfotransferases, *hs3st3b1a* and *hs3st3b1b*, are expressed in the leading domain of the PLLP. Wnt signaling activates expression of both genes, and Fgf is a co-activator of *hs3st3b1b*. Knockdown of *hs3st3b1a* causes a decrease in Fgf signaling and impaired protoneuromast formation. *Hs3st3b1a*/*hs3st3b1b* double mutants show a similar phenotype, with a decrease in the number of neuromasts deposited by the PLLP.

The sum of these results suggests a regulatory mechanism for Fgf signaling in which core syndecan proteins and 3-*O*-sulfation modifications are both active. Hs3st3b1a and Hs3st3b1b are present in the leading domain, where Fgf signaling is not typically active, due to repression of the Fgf receptor. However, leading cells do produce the Fgf3 and Fgf10 ligands, which activate FgfR1, present on trailing cells. Given the evidence that Hs3st3s regulate Fgf signaling, it seems plausible that they play some role in the effective

delivery of the Fgf ligands to trailing cells. Meanwhile, Sdc4 is present on trailing cells, and regulates reception of the Fgf ligands, possibly as an independent receptor or as a co-receptor to FgfR1. Thus, Sdc4, and 3-*O*-sulfated HSPGs cooperate to support Fgf signaling and the downstream processes of protoneuromast assembly and collective cell migration.

Thesis advisor/reader: Ajay Chitnis, MD, PhD

Reader: Rejji Kuruvilla, PhD

Acknowledgements

First and foremost, I would like to thank my mentor, Dr. Ajay Chitnis, for accepting me into his laboratory and encouraging me every day to be a better scientist. I am privileged to have learned from such a brilliant and enthusiastic scientist, not to mention an excellent chef. Although communication with one's mentor is not always easy, he continually strived to be the best advisor and always wanted the best for me. In particular, he supported me in my pursuit of career exploration outside of academic research, and for that, I cannot possibly thank him enough.

Thank you to the past and present members of the Chitnis lab, who always made the lab welcoming. I am especially grateful to Gregory Palardy, Dr. Damian Dalle Nogare, and Dr. Uma Neelathi, who showed me kindness and endless patience in teaching me new protocols and helping me trouble-shoot problems, no matter how trivial. I also thank the staff in the fish facility for providing our animals with such excellent care and for always making time to answer my questions.

I am hugely thankful to my committee members, Drs. Marnie Halpern, Rejji Kuruvilla, Matthew Hoffman, and Matthew Kelley for all of their research advice over the years. They understand the circuitous routes research can take, and were always there to provide suggestions or help point me in a new direction.

Graduate school, and the inevitable question of what career move comes afterward, is no easy feat, and I would be remiss not to thank those scientists and administrators who provided me with emotional support and career guidance. To the former directors of the JHU-NIH Graduate Partnership Program, Drs. Orna Cohen-Fix and Michael Lichten, I am indebted to you for your understanding, guidance, and support. I would also like to thank

Drs. Philip Wang and Philip Ryan (Phil 1 and Phil 2), from the NIH Office of Intramural Training and Education, who provided me with a multitude of career exploration opportunities and supported me in my job hunt.

Last, but so very, very far from least, I would like to thank my family. My husband, Brett Fox, has stood steadfastly by me for eleven years. When we started dating in college, little did he know that he would end up married to a graduate student, but he has been, and always will be, my champion. He has shown me nothing but unwavering love, always supporting me in my devotion to science and encouraging me in my career aspirations. Finally, I am eternally grateful to my first fans, my parents, Diana and Steven Younts. They have always been my gold standard for what it means to have a successful career and, more importantly, a fulfilling life. In the first grade, my mom taught me the value of doing the extra credit portion of my homework, and they have both encouraged me to excel every day since.

Table of Contents

Abstract ii

Acknowledgements v

List of Tables ix

List of Figures x

Chapter 1: Introduction 1
- **1.1 The posterior lateral line of zebrafish** 1
- **1.2 Cell-cell signaling in the posterior lateral line primordium** 3
  - Wnt and Fgf signaling 3
  - Chemokine signaling 6
  - Notch signaling 8
- **1.3 Structure of heparan sulfate proteoglycans** 11
  - General structure and function 11
  - Core proteins in the zebrafish genome and their expression in the PLLP 12
- **1.4 Biosynthesis of heparan sulfate glycosaminoglycan chains** 14
  - Initiation 14
  - Polymerization 15
  - Modification 16
- **1.5 Regulation of cell-cell signaling by heparan sulfate proteoglycans** 18
- **1.6 Aims of this thesis** 22

Chapter 2: Syndecan4 mediates cell differentiation and migration via Fgf signaling in the zebrafish lateral line primordium 24
- **2.1 Introduction** 24
  - Syndecan4 structure, signaling capabilities, and function 24
  - Syndecan4 as a regulator of Fgf signaling 25
  - Syndecan4 as a regulator of chemokine signaling 26
- **2.2 Results** 28
  - *Sdc4* is expressed in the trailing domain of the PLLP and suppressed by Fgf signaling 28
  - Knockdown of *sdc4* interferes with protoneuromast formation and slows PLLP migration 32
  - *Sdc4* morphants exhibit weak Fgf signaling 34
  - Ectopic expression of *sdc4* causes dorsalization of zebrafish embryos 34
  - *Sdc4* mutants have a normal pattern of neuromasts despite changes in signaling 37
  - Inhibiting Fgf signaling within the PLLP in *sdc4* mutants suggests a role for Sdc4 in migration 40
  - Sdc3 works with Sdc4 to support neuromast formation and PLLP migration 43
- **2.3 Discussion** 44
- **2.4 Appendix** 52

Chapter 3: 3-*O*-sulfated heparan sulfate supports Fgf signaling in the zebrafish lateral line 53
- **3.1 Introduction** 53
  - Rarity and types of 3-*O*-sulfation 54
  - Specific roles for 3-*O*-sulfation 55
- **3.2 Results** 57
  - Wnt signaling activates expression of two Hs3st3 enzymes in the leading domain. 57

Knockdown of *hs3st3*s results in fewer neuromasts. 61
Knockdown of *hs3st3b1a* decreases the size of the Fgf signaling domain. 65
Overexpression of *hs3st3*s causes dorsalization of zebrafish embryos. 67
Hs3st3b1a/*hs3st3b1b* mutants have fewer neuromasts than wild-types. 69
3.3 Discussion 70
3.4 Appendix 76
Chapter 4: Concluding remarks and future directions 77
Chapter 5: Materials and Methods 83
5.1 Solutions 83
5.2 Zebrafish 84
5.3 CRISPR mutants and genotyping 84
5.4 Morpholinos and chemical inhibitors 85
5.5 *In situ* hybridization 86
In situ probes and hybridization protocol 86
In situ image analysis 87
5.6 Morpholino and mRNA microinjection 88
5.7 Microscopy 88
5.8 Statistical analysis 89
References 90
Curriculum Vitae 100

List of Tables

Table 5.3.1: gRNA oligos 85

Table 5.3.2: PCR Primers 85

Table 5.4.1: Morpholinos 86

Table 5.4.2: Chemical inhibitors 86

List of Figures

Figure 1.1.1: As the PLLP migrates, neuromasts are deposited from the trailing edge 2

Figure 1.2.1: Wnt and Fgf work together signaling direct the mesenchymal to epithelial transition that forms protoneuromasts 4

Figure 1.2.2: Chemokine signaling guides directional migration of the PLLP, while Fgf is a migrational cue for trailing cells 7

Figure 1.2.3: Notch and Fgf signaling specify the central cell of the rosette as a hair cell progenitor 9

Figure 1.3.1: There are three classes of HSPG core proteins 13

Figure 1.4.1: Heparan sulfate glycosaminoglycan chains are synthesized in a step-wise manner by a series of enzymes 15

Figure 2.2.2: Sdc4 is expressed in the trailing domain of the primordium..... 28

Figure 3.2.2: Fgf signaling suppresses sdc4 expression 29

Figure 2.2.3: Intensity of *sdc4* expression is increased in *cxcl12a* morphants 31

Figure 2.2.4: Sdc4 morphants have fewer neuromasts 32

Figure 2.2.5: Sdc4 morphant primordia have fewer forming protoneuromasts..... 33

Figure 2.2.6: *Sdc4* morphants exhibit weak Fgf signaling..... 35

Figure 2.2.7: Overexpression of sdc4 causes ectopic activation of Fgf signaling..... 36

Figure 2.2.8: *Sdc4* mutants have a normal pattern of neuromast deposition, despite changes in Wnt and Fgf signaling..... 38

Figure 2.2.9: *Sdc4* mutants have increased expression of chemokine receptors 39

Figure 2.2.10: Inhibition of Fgf signaling in *sdc4* mutants causes migration defects 42

Figure 2.2.11: Knockdown of sdc3 causes migration defects in *sdc4* mutants 44

Figure 3.2.1: Hs3st3b1a and hs3st3b1b are expressed in the leading domain..... 58

Figure 3.2.2: Wnt activates expression of *hs3st3b1a* and *hs3st3b1b* 60

Figure 3.2.3: *Hs3st3* morphants have fewer deposited neuromasts..... 62

Figure 3.2.4: *Hs3st3b1a* morphants have fewer neuromasts and their deposition appears to be delayed 63

Figure 3.2.5: *Hs3st3b1a* morphants have fewer protoneuromasts..... 64

Figure 3.2.6: *Hs3st3b1a* morphants have decreased Fgf signaling 66

Figure 3.2.7: *Hs3st3b1a* morphants have decreased Fgf signaling 67

Figure 3.2.8: Overexpression of *hs3st3* mRNA causes dorsalization..... 68

Figure 3.2.9: *Hs3st3b1a*/*hs3st3b1b* double mutants have fewer neuromasts than WT 70

Figure 4.1: Schematic for how Sdc4 and Hs3sts regulate signaling within the primordium 78

Chapter 1: Introduction

1.1 The posterior lateral line of zebrafish

Aquatic vertebrates have a "distant-touch" sense mediated by the lateral line system. The lateral line is composed of a network of organs across the body surface, where their superficial location allows them to sense water flow in the animal's immediate environment. These organs are sensitive to pressure and vibration, allowing the animal to detect changes in local water currents. This sense informs the animal's spacial awareness and facilitates behaviors such as schooling, mating, prey detection, and predator avoidance [2]. For example, fish can use information gathered by their lateral lines to follow the wake of swimming prey [3] or orient themselves towards water currents [4].

The organs of the lateral line are mechanosensory neuromasts, which are distributed in a stereotypical pattern across the surface of the animal. Neuromasts are composed of peripheral support cells and central hair cells that function much like the hair cells of the mammalian inner ear. The hair cells extend a ciliary bundle through the epidermis, out into the surrounding water, shielded by a jelly-like cupula. Water currents displace ciliary bundles, and when each hair cell is displaced in a specific direction, it increases its firing rate to communicate information about the directional movement of water to the central nervous system.

In zebrafish (*Danio rerio*), the lateral line is subdivided into the head neuromasts that make up the anterior lateral line (ALL) and the trunk neuromasts of the posterior lateral line (PLL). The posterior lateral line primordium (PLLP) spearheads the early development of this system, establishing the first neuromasts along the horizontal myoseptum. The PLLP is a group of approximately 125 cells that forms just posterior to the otic vesicle. At

about 22 hours post fertilization (hpf), the cells of the PLLP detach from the lateral line placode and collectively migrate along the horizontal myoseptum just under the skin, finally reaching the tip of the tail at 48hpf (Figure 1.1.1). As migration progresses, trailing cells within the PLLP organize into rosette-shaped protoneuromasts that are then deposited from the trailing end. In general, about six neuromasts are deposited, plus a terminal cluster of two or three neuromasts, deposited where the PLLP fragments when migration terminates at the tail tip. While the PLLP establishes the first neuromasts of the lateral line, there will ultimately be many more. Additional neuromasts arise via three different mechanisms: 1) interneuromast cells, which are also deposited by the PLLP, are latent precursors that will later proliferate and form neuromasts [5]; 2) after the PLLP, two more primordia migrate and deposit neuromasts along the horizontal myoseptum and the dorsal midline, each primordium developing from different placodes and with their own innervating ganglia [6]; and 3) budding from existing neuromasts [7].

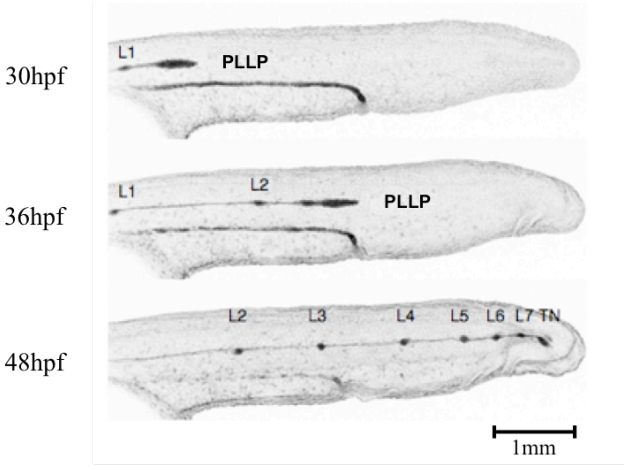

Figure 1.1.1: As the PLLP migrates, neuromasts are deposited from the trailing edge. The posterior lateral line primordium (PLLP) migrates along the horizontal myoseptum between 22 and 48hpf. As it progresses, neuromasts are periodically deposited (L1, L2, etc.), ultimately depositing 6 or 7 neuromasts, plus a terminal cluster. Migration slows at the PLLP reaches the tip of the tail. The PLLP terminates once it reaches the tail tip and fragments into a cluster of terminal neuromasts (TN). Adapted from Chitnis and Nogare, *Principles of Developmental Genetics*, 2015 [1].

1.2 Cell-cell signaling in the posterior lateral line primordium

Wnt and Fgf signaling

Within the PLLP, two signaling networks work in concert to pattern the cells of the leading and trailing domains (Figure 1.2.1A and B). The leading domain is characterized by relatively high levels of Wnt signaling activity, which maintains a population of mesenchymal-like cells [8]. Wnt tapers off towards the trailing end, where Fgf signaling organizes cells into epithelial rosettes that are eventually deposited as neuromasts [9, 10]. Fgf signaling induces cells to adopt a more columnar, epithelial morphology and promotes actin to associate with apical junctions, thereby inducing apical constriction. The domain of Wnt activity is essential for establishing the Fgf signaling center in the adjacent trailing domain. Initially, Wnt stimulates signaling throughout much of the PLLP, which then activates transcription of the ligands Fgf3 and Fgf10a (Figure 1.2.1C). Simultaneously, Wnt activates expression of *sef*, the FgfR1 inhibitor, and Fgf signaling cannot be activated where Wnt is strongest [11]. The Fgf ligands thus bind FgfR1 and activate downstream signaling in the most trailing cells of the PLLP, where Wnt signaling abates. In turn, Fgf signaling activates expression of the Wnt inhibitor *dikkopf* (*dkk1b*). The balance of the Wnt and Fgf signaling domains is further regulated by *dusp6*, an inhibitor of intracellular ERK signaling [12]. *Dusp6* is expressed in the leading two-thirds of the PLLP, dually activated by Wnt in leading cells and Fgf in more trailing cells, and inhibits Fgf-dependent incorporation of cells into protoneuromasts. Thus, this mutually inhibitory feedback system restricts Wnt activity to the leading domain and Fgf activity to the trailing domain. Broad Fgf signaling activity abates in the most trailing cells of the PLLP, as they are located furthest from the leading zone and, thus, from the source of Fgf3 and Fgf10a.

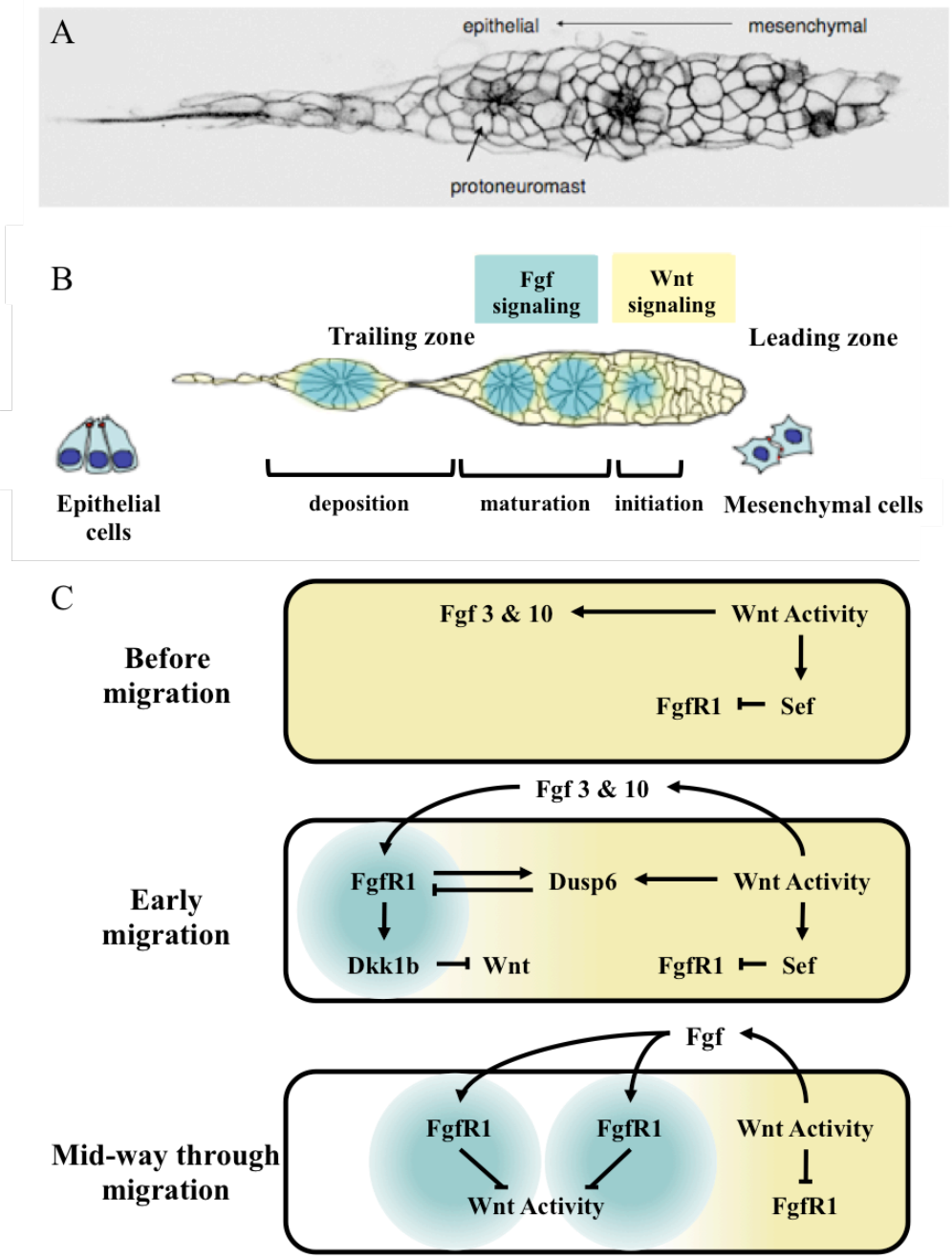

Figure 1.2.1: Wnt and Fgf work together signaling direct the mesenchymal to epithelial transition that forms protoneuromasts. (A) Cells in the leading domain are mesenchymal-like, while trailing cells are more epithelial in nature. The epithelial-like cells of the trailing domain organize into protoneuromasts. (B) Wnt signaling is dominant in the leading domain, where it maintains the population of mesenchymal-like cells. In more trailing cells, Fgf directs the progressive epithelialization of cells and organizes them into protoneuromasts. Initiation of protoneuromast formation occurs as cells group together and mature as proper rosette formations form, with a hair cell progenitor at the center and peripheral cells organized around it. Neuromasts are deposited from the trailing end. (C) Initially, Wnt signaling is dominant throughout the PLLP. Wnt activity initiates transcription of two Fgf ligands, which establish Fgf signaling in the trailing domain. The Wnt and Fgf systems are mutually inhibitory resulting in the establishment of distinct domains in the leading and trailing zones, respectively. Adapted from Chitnis and Nogare, *Principles of Developmental Genetics*, 2015 [1].

Perturbation of either Wnt or Fgf signaling results in defects in PLLP migration or rosette morphogenesis. Both overactivation and inhibition of the Wnt system cause defects in migration. When Wnt signaling is constitutively active, as in *apc* mutants or under treatment with the GSK-3 inhibitor BIO, and when it is suppressed, by treatment with Wnt inhibitor IWR or in *lef1* mutants, primordia stall before reaching the tip of the tail [8, 12-14]. Manipulation of the Wnt system likely causes migration defects because Wnt signaling activates expression of *cxcr4b*, *fgf3*, and *fgf10a* [8]. When Wnt activity increases or decreases, downstream transcriptional targets will be upregulated or downregulated, and if those targets play central roles in the collective cell migration of the PLLP, migration is likely to be impacted. Alternatively, complete inhibition of the Fgf signaling system, as in *Fgf3*:*Fgf10a* double mutants or SU5402-treated embryos, results in slow migration, inhibition of protoneuromast assembly, and ultimately stalling [8-10]. Partial inhibition of the Fgf system, through injection of an *fgf10a* morpholino, results in normal migration, but causes a significant delay in protoneuromast formation and deposition [12].

In this way, the Wnt and Fgf signaling systems are critical determinants of when and where protoneuromasts form, as well as migration of the system as a whole. Wnt activity tapers from leading to trailing end, while Fgf signaling starts at some distance from the leading edge and also diminishes toward the trailing end, as cells are further removed from the leading source of Fgf ligand. There is, however, limited Fgf signaling maintained in maturing neuromasts, as the central hair cell progenitor becomes a new source of Fgf10a (discussed below).

Chemokine signaling

Collective migration of the approximately 125 cells of the PLLP is steered by the chemokine signaling system. This system guides migration in a number of different cell types, including germ cells, leukocytes, neurons, and metastatic cancer cells [15]. The chemokine ligand Cxcl12a (formerly known as Sdf1a) initiates G protein-coupled signaling via interactions with the Cxcr4b chemokine receptor. This triggers an influx of calcium ions that promotes migratory behavior through regulation of protrusive activity and/or cell shape and adhesion [16, 17]. Meanwhile, binding of Cxcl12a to the Cxcr7b chemokine receptor does not initiate G protein-coupled signaling, and is therefore not generally thought to regulate cell migration [18].

The *cxcl12a* ligand is expressed in a uniform stripe along the horizontal myoseptum and two chemokine receptors are expressed in the PLLP [19-21] (Figure 1.2.2 A-E). Cells in the leading two-thirds of the primordium express the *cxcl12a* receptor *cxcr4b*, while the trailing cells express a different receptor, *cxcr7b*, and these receptors allow the PLLP to follow the trail of Cxcl12a. Disrupting Cxcl12a or either of its receptors inhibits migration of the PLLP [19, 21]. It is the polarized expression of these two receptors that allows the PLLP to dependably migrate from anterior to posterior, despite the uniform expression of *cxcl12a*. It is hypothesized that both Cxcr4b and Cxcr7b are internalized after binding their ligand, but only activated Cxcr4b is capable of initiating downstream signaling that induces migratory behavior [19, 22]. Meanwhile, after Cxcl12a binds to the Cxcr7b receptor, the complex is internalized, Cxcl12a is degraded, and Cxcr7b is recycled back to the cell surface, where it is available to bind new ligand [23]. The *cxcr7b*-expressing region

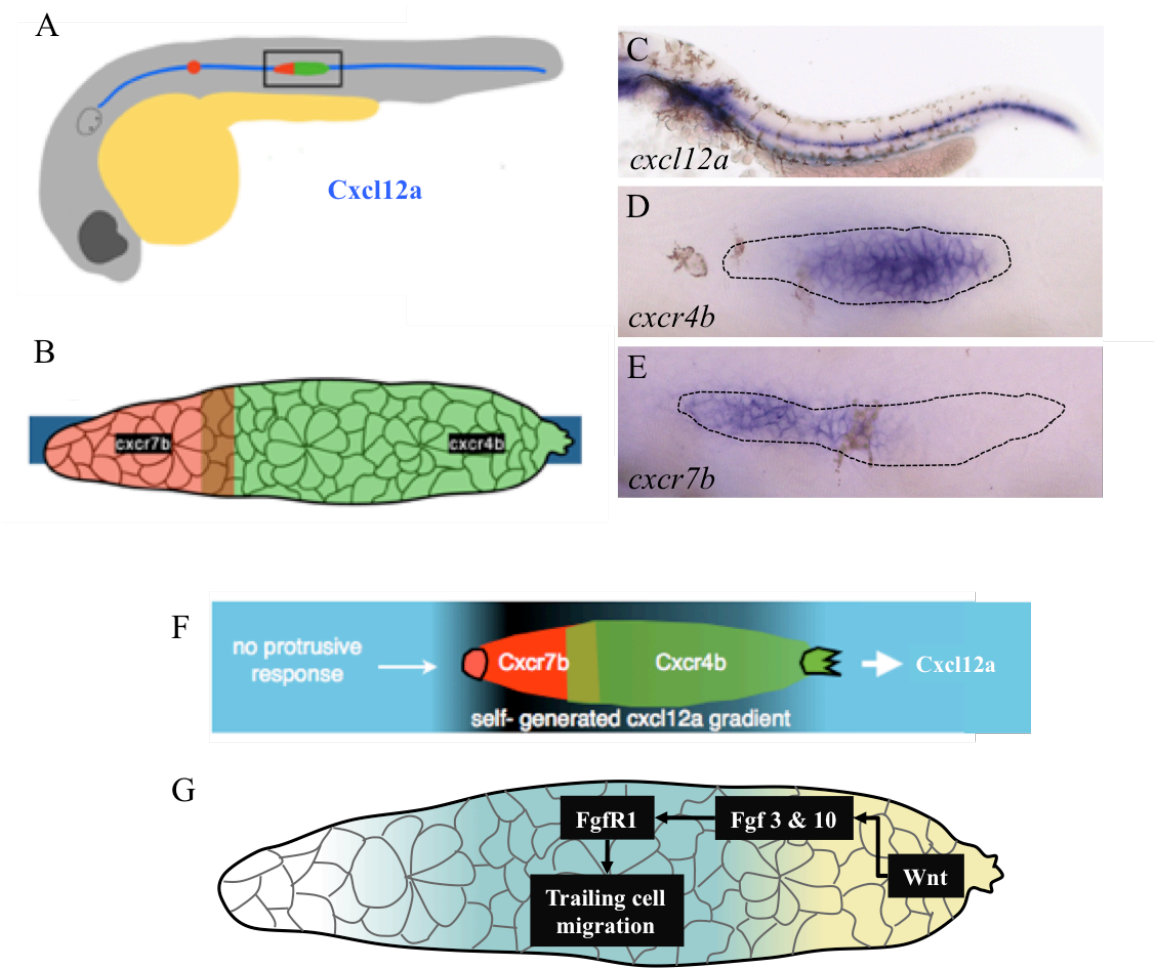

Figure 1.2.2: Chemokine signaling guides directional migration of the PLLP, while Fgf is a migrational cue for trailing cells. (A) Schematic showing a whole-embryo view of PLLP migration. A uniform stripe of Cxcl12a ligand is located along the horizontal myoseptum. The PLLP follows this stripe of ligand, migrating from posterior to anterior. (B) The PLLP expresses two chemokine receptors, Cxcr4b in the leading domain and Cxcr7b in the trailing domain. (C) *In situ* hybridization showing *cxcl12a* expression along the horizontal myoseptum. (D, E) *In situ* hybridization shows expression of *cxcr4b* and *cxcr7b* in the leading and trailing domains, respectively. (F) Schematic showing how the differential expression of Cxcr4b and Cxcr7b allow the PLLP to generate a local gradient of Cxcl12a along the length of the primordium. This allows the PLLP to react to the relatively high levels of Cxcl12a available to leading cells, and consistently guide the PLLP in one direction for the duration of migration. (G) Wnt activates Fgf3 and Fgf10 in leading cells. Fgf ligands are delivered from leading cells to trailing cells, where they activate FgfR1. In response to Fgf signaling, trailing cells migrate, following the leading zone. Adapted from Chitnis and Nogare, *Principles of Developmental Genetics*, 2015 [1].

therefore acts as a sink for Cxcl12a, contributing to a local gradient of chemokine ligand along the length of the PLLP [24, 25]. Under these conditions, there is a high level of Cxcl12a available at the leading edge for Cxcr4b to bind, and decreased levels of ligand available to the more trailing cells. This ensures that the PLLP migrates preferentially

towards the posterior end of the fish, as opposed to regressing anteriorly back to its starting point.

The chemokine signaling system guides PLLP migration primarily through the migratory behavior of the cells at the leading edge. However, fibroblast growth factor (Fgf) signaling is also important to this migration process, as suppression of Fgf activity causes the system to stall, halting migration [10]. Instead of responding directly to migration-inducing chemokines, the more trailing cells of the PLLP actually play follow-the-leader and migrate in response to the Fgf cues produced by cells in the leading domain [26] (Figure 1.2.3G). In primordia severed by laser ablation, trailing cells migrate and rejoin leading cells. Migration of the severed trailing portion occurs in response to the Fgf signal received from the leading portion, and this phenomenon occurs independent of chemokine signaling.

Notch signaling

In addition to its roles in rosettogenesis and migration, Fgf signaling is also responsible for the specification of a sensory hair cell progenitor at the center of each rosette. Fgf signaling activates expression of the proneural gene *atoh1a*, a basic helix-loop-helix transcription factor, which gives PLLP cells the potential to become sensory hair cells [9] (Figure 1.2.3). *Atoh1a* is expressed in a center-biased pattern, and in the most trailing protoneuromasts, its expression is restricted to the central cell of the rosette [27]. In the central cells of the rosettes, two Notch ligands, *deltaA* and *deltaD*, are activated by Fgf signaling and Atoh1a, respectively. Meanwhile, undifferentiated cells and support cells express *notch3* [28]. DeltaA and DeltaD can then activate Notch signaling in neighboring cells, which suppresses *atoh1a* expression in those cells [27]. When Notch signaling is lost,

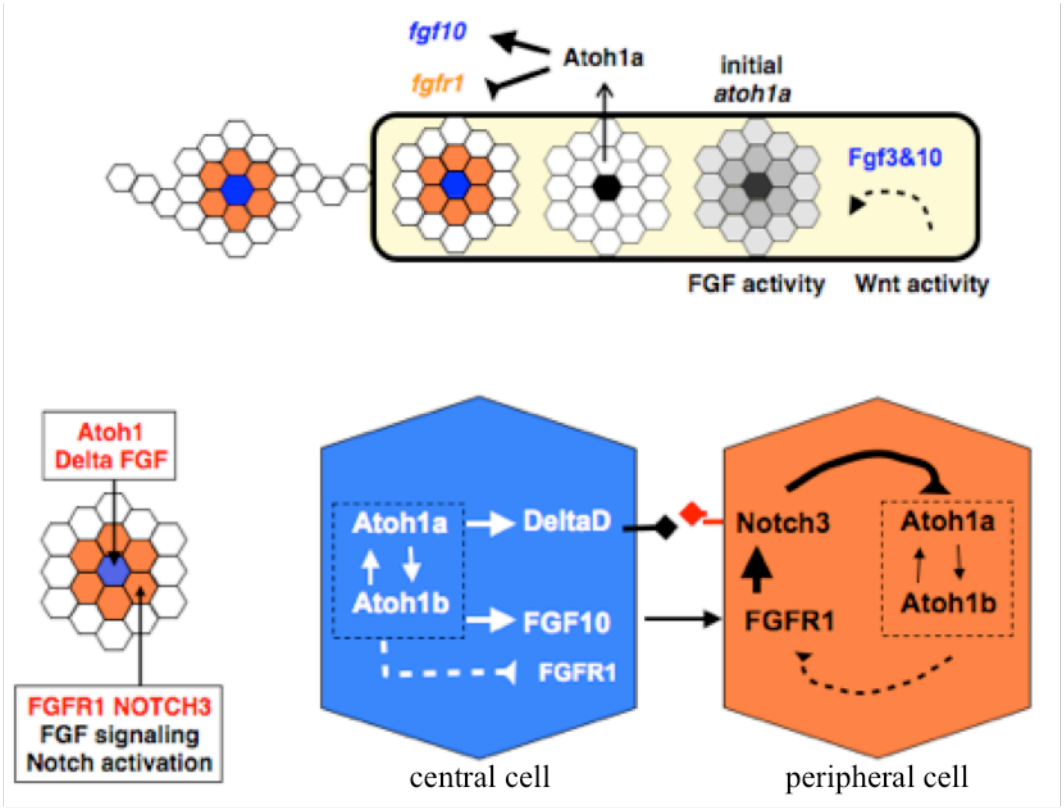

Figure 1.2.3: Notch and Fgf signaling specify the central cell of the rosette as a hair cell progenitor. (A) Wnt signaling in the leading domain activates expression of two Fgf ligands, Fgf3 and Fgf10. In turn, Fgf signaling activates center-biased expression of *atoh1a* in forming protoneuromasts. Atoh1a gives cells the potential to become sensory hair cells and becomes progressively more restricted to the central cell in the middle of each rosette. Atoh1a activates expression of *fgf10*, while also repressing *fgfr1*. Peripheral cells don't repress *fgfr1* and can respond to the Fgf10 ligand produced by the *atoh1a*-expressing cell. (B) Signaling schematic showing how Notch and Fgf signaling restrict *atoh1a* expression, ensuring that the central cell is specified as the hair cell progenitor. In the central cell (blue), a positive feedback loop between Atoh1a and Atoh1b ensures sustained expression of *atoh1a*. Atoh1a signaling also activates the Notch ligand DeltaD and Fgf10, while suppressing FgfR1. On neighboring peripheral cells (orange), DeltaD activates the Notch3 receptor, while Fgf10 (released by the central cell) activates FgfR1. Notch3 signaling suppresses Atoh1a, thereby allowing continued FgfR1 activity that supports *notch3* expression. Adapted from Chitnis and Nogare, *Principles of Developmental Genetics*, 2015 [1].

as in *mib1* mutants, *atoh1a* expression is unregulated and expanded, ultimately resulting in the loss of Fgf signaling, expansion of Wnt signaling, defective formation and maintenance of protoneuromasts, and stalling of PLLP migration. In the most trailing protoneuromast, Atoh1a also activates expression of its homolog, *atoh1b*, which, in turn, activates *atoh1a*. This positive feedback loop allows sustained expression of *atoh1a* specifically in the

central hair cell progenitor. Atoh1a, once established in the central hair cell progenitor, subsequently establishes a new Fgf signaling center, as it activates expression of *fgf10a* and inhibits *fgfr1*. Neighboring cells, inhibited from expressing *atoh1a* by Notch signaling, can freely express *fgfr1* and are capable of responding to the Fgf10a signal. Fgf signaling in these cells helps to maintain *fgfr1* and *notch3* expression, thereby suppressing the potential to be a sensory hair cell. Hence, a process of lateral inhibition ensures that the central cell is designated as the hair cell progenitor and neighboring cells are fated to be support cells.

Although terrestrial vertebrates do not have a distant-touch sense, the unique characteristics and accessibility of the zebrafish lateral line make it an extraordinarily tractable system in which to study several broadly applicable biological questions. The hair cells of the lateral line can regenerate after damage or death, and so this is an excellent system in which to studying the mechanisms driving damage and regeneration. Understanding the signaling networks and physical forces that regulate collective migration of the PLLP advances our general knowledge of collective cell migration, a process that is important in several different developmental contexts, as well as the metastasis of certain types of cancer. There are multiple signaling networks that pattern the PLLP and probing these networks contributes to our broader understanding of how these networks can coordinate cell fate decisions and morphogenesis during development. It is this last question of how intercellular signaling is regulated on which my project has focused. In particular, I am interested in how heparan sulfate proteoglycans (HSPGs) interact with signals among the cells of the PLLP, and how that interaction impacts morphogenesis of the PLL. By understanding the mechanisms that regulate HSPG

expression and function and how they, in turn, influence the dynamics of Wnt and Fgf signaling, we hope to develop a better understanding of the self-organization of the zebrafish posterior lateral line.

1.3 Structure of heparan sulfate proteoglycans

General structure and function

Heparan sulfate proteoglycans (HSPGs) are found on the cell surface, as well as distributed throughout the extracellular matrix, in most types of animal tissues. They emerged early in animal evolution, as they are present in nearly all animal species [29]. Due to the high variability of heparan sulfate (HS) structure and the structural specificity required by ligands, HSPGs are capable of regulating a wide variety molecular and cellular processes by expressing core proteins and modifying enzymes in a tissue-specific manner. Among their many functions, HSPGs are particularly well-studied in the context of cell-cell signaling, including the Wnt and Fgf pathways (reviewed in [30]). As a result of their binding interactions with signaling ligands and receptors, HSPGs have many demonstrated roles, including those in pattern formation, cell adhesion, and cell migration (reviewed in [31, 32]). HSPGs are so critical to these processes that in several model organisms disruption of heparan sulfate biosynthesis can cause death during development [33, 34] and is known to cause the disorder hereditary multiple osteochondromas in humans. Given the particular roles for HSPGs in the signaling networks and functions that are central in PLL development, I am interested how they regulate signaling within the PLLP and how that impacts pattern formation in this developing system.

HSPGs belong to a large family of proteoglycans, all of which are hybrid molecules composed of a core protein and covalently attached glycosaminoglycan (GAG) chains. GAG chains are linear polysaccharides modified by a series of enzymes during synthesis in the Golgi. There are four classes of GAGs: chondroitin sulfate, dermatan sulfate, heparan sulfate (HS), and keratan sulfate. Each class is differentiated by their saccharide subunit, level and type of sulfation, and epimerization. Among GAGs, HS is unique in that virtually all cell types express at least one HSPG core protein and the GAG chains of HSPGs have the most highly variable structure [35].

The core proteins of HSPGs are believed to have limited functions of their own, but are of central importance to the localization of the molecule. There are three major types of HSPG core proteins: 1) Syndecans are transmembrane proteins usually found embedded in the cell membrane; 2) Glypicans are also found on the cell surface, attached via a GPI anchor; and 3) Extracellular Matrix (ECM) proteins such as perlecan, agrin, and collagen XVIII (Figure 1.3.1). Although syndecans and glypicans are typically associated with the cell membrane, both proteins have cleavage sites that allow for shedding of these HSPGs from the cell surface. Many cells express multiple types of core proteins, but the HS chains on different core proteins of the same cell generally have the same sulfation patterns [36], suggesting that HS-modifying enzymes in the Golgi do not target specific core proteins, instead modifying all HSGAGs equally.

Core proteins in the zebrafish genome and their expression in the PLLP

The zebrafish genome contains three syndecan genes (*sdc2*, *sdc3*, and *sdc4*) [37], ten glypican genes (*gpc1a*, *gpc1b*, *gpc2*, *gpc3*, *gpc4*, *gpc5a*, *gpc5b*, *gpc5c*, *gpc6a*, and

gpc6b) [38], one perlecan (*hspg2*), one agrin (*agrn*), and one collagen XVIII (*col18a1*). Of these core proteins, six are specifically expressed in the PLLP. *Sdc3* is expressed throughout the primordium, with slightly higher expression in the central cells [39]. *Sdc4* is expressed in the trailing domain, with the strongest expression in the next-to-be-deposited protoneuromast and deposited neuromasts. *Gpc1b* is expressed in a few cells at the very leading edge of the PLLP and g*pc4* is expressed in the trailing two-thirds of the PLLP. *Agrn* and *gpc1a* also show specific expression in the PLLP, but the exact domain of expression within the PLLP has yet to be defined [38, 40]. Given their distinct expression patterns, it seems likely that each core protein has a specific function.

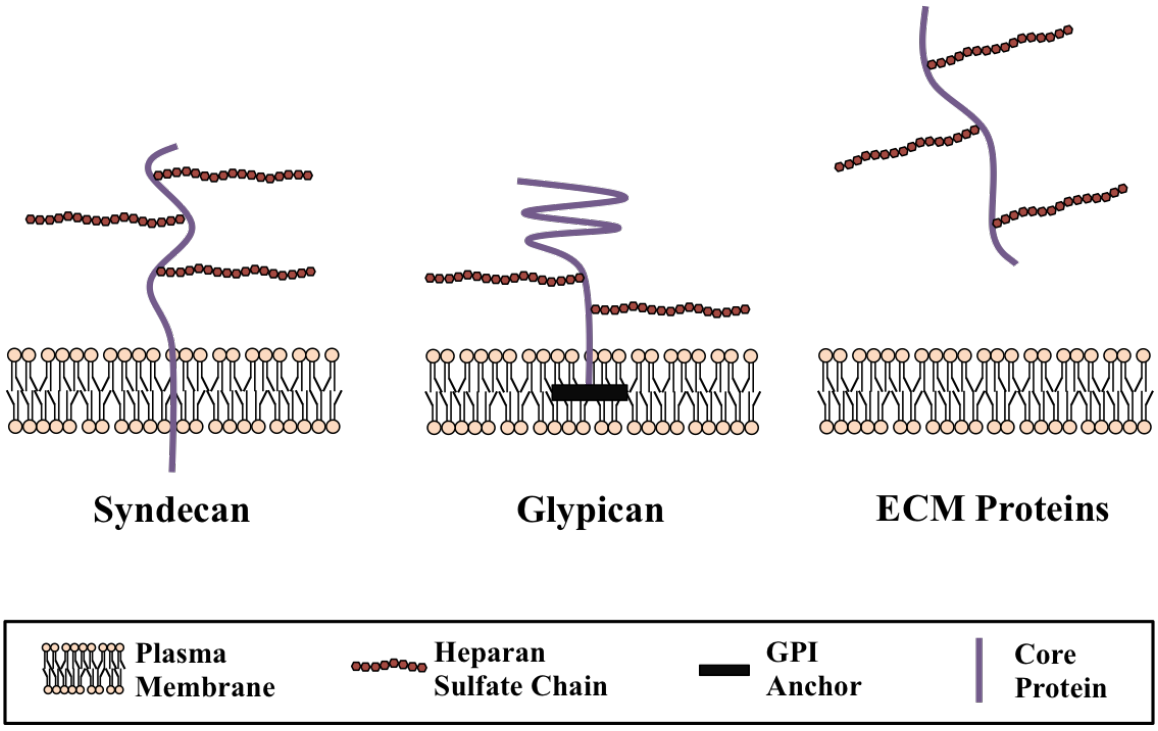

Figure 1.3.1: There are three classes of HSPG core proteins. Syndecan and Glypican are two HSPG core proteins that are associated with the cell membrane. Syndecans are transmembrane proteins, with a small intracellular domain and a large extracellular domain with several attached heparan sulfate chains. Glypicans are attached to the cell membrane via a GPI anchor and also have a large extracellular domain with multiple heparan sulfate chains. ECM proteins, which include perlecan, agrin, and collagen XVIII, exist in the extracellular space and associate with the ECM. The structure of each core protein is critical in determining its localization.

1.4 Biosynthesis of heparan sulfate glycosaminoglycan chains

The wide variety of HSPG functions is, in part, attributable to the variety of HSGAG chain structures, as these varied structures are each capable of specifically binding certain proteins whose function they modulate. The HSGAG chain backbone is composed of repeating disaccharide subunits of glucosamine and hexuronic acid (HexA). The hexuronic acid can be either D-glucuronic acid (GlcA) or its epimer L-iduronic acid (IdoA). Each subunit can be modified in a variety of ways. Glucosamine can be N-acetylated (GlcNAc), N-sulfated (GlcNS), or *O*-sulfated at positions 3 and 6. *O*-sulfation can also occur at position 2 of the hexuronic acid. Synthesis is a stepwise process, and a specific set of enzymes is responsible for each step of assembly and modification (Figure 1.4.1).

Initiation

There are three stages of HSGAG chain synthesis: initiation, polymerization, and modification. Initiation of all four types of GAG chains begins with the attachment of a tetrasaccharide linker to specific serine residues in the core protein. Attachment sites always consist of a Ser-Gly dipeptide, and heparan sulfate assembly is enhanced if repetitive Ser-Gly sequences and clusters of acidic amino acids flank the attachment site [41, 42]. Xylosyltransferase selects the attachment site and transfers a xylose, then galactosyltransferases add two D-galactose units, and, finally, glucuronosyltranferase I adds a GlcA. This completes the tetrasaccharide linker and the final addition of α4GlcNAc commits the process toward the synthesis of HS, as opposed to other GAG types.

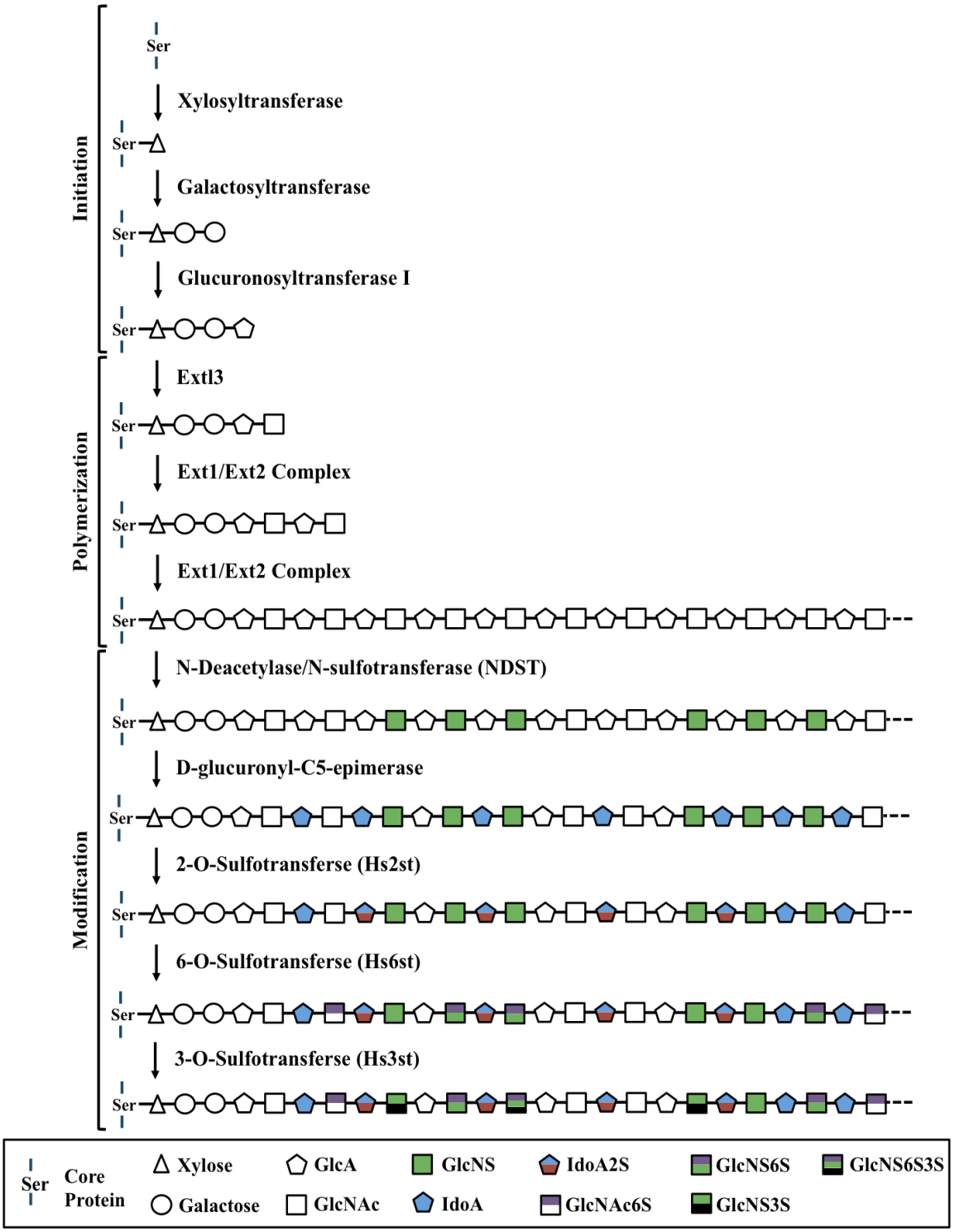

Figure 1.4.1: Heparan sulfate glycosaminoglycan chains are synthesized in a step-wise manner by a series of enzymes. During initiation, enzymes build a tetrasaccharide linker on specific serine residues in the core protein. During polymerization, exostosins add alternating glucosamine (GlcNAc) and glucuronic acid (GlcA) subunits. Five enzyme families perform specific modifications along the GAG chain. NDSTs deacetylate and subsequently sulfate some GlcNac subunits. A C5-epimerase epimerizes GlcA into Iduronic Acid (IdoA). Hs2sts sulfate some IdoA subunits. Hs6sts and Hs3sts sulfate some GlcNAc and GlcNS residues. Each enzyme preferentially modifies particular residues, but none of them uniformly modify all subunits of every HSGAG chain. Thus, each chain will have a unique structure and sequence of modifications.

Polymerization

During polymerization of HS, the Exostosin (Ext) family of glycosyltransferases add alternating GlcA and GlcNAc to the growing end of the polysaccharide, ultimately producing GAG chains of variable length. Zebrafish have four Ext genes, *ext1a*, *ext1b*, *ext1c* and *ext2*, and two Ext-like genes, *extl2* and *extl3*. Exts are type II transmembrane proteins with a small N-terminal cytoplasmic domain, a single-pass transmembrane segment, a stem region, and a large C-terminal enzymatic domain containing two active sites [43]. Within the enzymatic domain, the most C-terminal site is likely responsible for GlcNAc transferase activity, while the active site located more towards the N-terminal is the GlcA transferase site. [44]. Mammalian Ext1 and Ext2 function as a complex, and this complex has higher enzymatic activity than either Ext alone [45]. Polymerization by Exts is traditionally thought to proceed in the absence of chain modification, however some studies suggest that these two processes occur simultaneously. GlcA is preferentially transferred to an acceptor with deacetylated, sulfated glucosamine (GlcNS) at its terminus [46]. GlcNS is generated by the activity of N-deacetylase/N-sulfotransferase (NDST), one of the modification enzymes, on GlcNAc. Furthermore, the addition of 3'-phosphoadenyl 5'-phosphosulfate (PAPS), the sulfate donor from which sulfate groups are transferred to GAG subunits, stimulates polymerization of HS by Exts [47].

Modification

An epimerase and four classes of sulfotransferases perform modifications to the HSGAG chain. At each step, only some residues are modified, giving rise to the high diversity of HS structures and, therefore, the functional specificity and versatility of

HSPGs. First, NDSTs remove N-acetyl groups from some GlcNAc residues, nearly all of which are replaced with sulfate groups to produce GlcNS. In rare instances, deacetylated residues are left unsulfated, producing $GlcNH_2$ [48]. GlcNS residues tend to occur in clusters, suggesting that once sulfation begins, NDSTs preferentially target those regions containing the first sulfation sites. While mammals have four NDST genes, Zebrafish have five: *ndst1a*, *ndst1b*, *ndst2a*, *ndst2b*, and *ndst3* [49]. NDST structure is very similar to that of the glycosyltransferases: type II transmembrane protein with a large C-terminal domain containing catalytic sites for both N-deacetylation and N-sulfation [50, 51].

In the second step, D-glucuronyl-C5-epimerase (Glce) epimerizes GlcA to IdoA. Glce targets non-*O*-sulfated hexuronic acids located on the reducing side of non-*O*-sulfated GlcNS [52], thus ensuring that epimerization occurs after N-deacetylation/N-sulfation, but prior to *O*-sulfation. The zebrafish genome contains two of these epimerases, *glcea* and *glceb*, compared to just one in higher vertebrates [53]. The enzyme functions as a dimer with two catalytic sites in each of the C-terminal domains [54]. With epimerization, we begin to see how modification lends HS chains their specific functions, as epimerization serves to make HS chains more flexible and enables them to target specific ligands. Epimerization increases the flexibility of HS due to the fact that IdoA can adopt more conformations than either GlcA or GlcNAc [55], and in mouse embryonic fibroblasts, HS without IdoA was incapable of binding Fgf2 and glial-derived neurotrophic factor [56].

Third, uronosyl-2-*O*-sulfotransferase (Hs2st) sulfates position 2 on hexuronic acid residues. The enzyme preferably targets IdoA, stabilizing the epimer conformation, but the enzyme will also modify some GlcA subunits. The extent of 2-*O*-sulfation varies widely,

ranging from 50 to 90% of IdoA residues [57]. While other vertebrates have one Hs2st, zebrafish have two, *hs2st1a* and *hs2st1b*.

Fourth, some GlcNS and GlcNAc residues are sulfated at position 6 by glucosaminyl 6-*O*-sulfotransferase (Hs6st). While most other vertebrates have three Hs6sts, the zebrafish genome contains five Hs6st genes: *hs6st1a*, *hs6st1b*, *hs6st2*, *hs6st3a*, and *hs6st3b*. Each isoform of Hs6st appears to have its own specificity, but as a group these enzymes target IdoA-GlcNAc, HexA-GlcNS, and HexA-GlcNS3S for 6-*O*-sulfation [58]. Like NDST and Ext, Hs6st is a type II transmembrane protein with a C-terminal catalytic domain [59].

The last modification made to the HS chain is the sulfation of GlcNS and GlcNAc residues at position 3 by glucosaminyl 3-*O*-sulfotransferase (Hs3st). This is a relatively rare modification, accounting for less than 1% of sulfation events along a given GAG chain [60, 61]. Although this modification is made infrequently, most vertebrates express seven 3-*O*-sulfotransferases and zebrafish have eight Hs3st genes: *hs3st1*, *hs3st1l1*, *hs3st1l2*, *hs3st2*, *hs3st3b1a*, *hs3st3b1b*, *hs3st3l*, and *hs3st4*. Each *hs3st* has its own specific expression pattern and preferred target residues, suggesting regulatory and functional divergence [62].

1.5 Regulation of cell-cell signaling by heparan sulfate proteoglycans

Among their many functions, HSPGs have recently been shown to positively regulate Fgf signaling in the migrating PLLP. The Piotrowski lab used *ext2*/*extl3* double mutants, which are deficient in HSGAG chain synthesis, to examine the role of HS in the PLL [39]. They demonstrated that Fgf signal transduction relies upon functional HSPGs

and that HSPGs are critical for cell polarity in the PLLP. This is not an especially surprising discovery, given that HSPGs have long been known to regulate Fgf signaling in a number of different contexts. Several studies show that although Fgfs can bind the FgfR and activate downstream signaling, this interaction is more stable and prolonged in the presence of HSPGs [63-65]. FgfRs and paracrine Fgfs have HS-binding domains and generally have moderate-to-high affinity for HS [66, 67]. Small changes in the HS-binding domains allow Fgfs and FgfRs to selectively bind to specific HS chain sequences, meaning that different HSPGs elicit different downstream signaling responses [68]. For example, during branching morphogenesis in mouse lacrimal and salivary gland epithelium buds, Fgf7 and Fgf10 have different affinities for HS, and therefore induce different morphogenic effects. Fgf10 binds HS more strongly and promotes elongation, while Fgf7 binds HS less strongly and induces branching. By reducing the binding strength of Fgf10 to HS, it becomes a functional mimic of Fgf7 [69]. *Ext2* and *extl3* mutants were previously shown to exhibit defective pectoral fin development, very similar to the defect seen in *fgf10* mutants. Although Fgf10 protein is capable of rescuing this defect in *fgf10* mutants, this is not true in *ext2* or *extl3* mutants, indicating that HSPGs are required for Fgf10 signaling during limb development in zebrafish. Meanwhile, Fgf4 is perfectly capable of activating downstream signaling in *ext2* and *extl3* mutants, indicating that the requirement for HS in the limb bud is specific to Fgf10 [70]. Overall, HSPGs are widely known to regulate Fgf signaling in a number of ways, including the restriction or facilitation of ligand diffusion, transportation of ligands to target cells, presentation of ligands to receptors, and stabilization of the ligand-receptor complex as co-receptors [66, 71].

Although HSPGs' signaling function is most well-studied in the context of Fgf signaling, they are known to regulate other signaling pathways, as well. In cell culture using mouse L cells, the presence of intact HSPGs stabilizes Wnt3a signaling [72]. Multiple *Drosophila* mutants with defective HSPG synthesis strongly resemble the Wnt mutant *wingless* phenotype and exhibit defective Wnt signaling [73-76]. In Gpc3 knockout mice, the non-canonical Wnt/JNK signaling pathway is inhibited, while the canonical Wnt/β-catenin signaling pathway is ectopically activated [77]. In *Xenopus*, Sdc4 has also been implicated in non-canonical Wnt signaling during convergent extension, as a binding partner of the Wnt receptor Frizzeled7 [78]. Notum is a secreted α/β-hydrolase that cleaves membrane-anchored glypicans from the cell surface. In both *Drosophila* and zebrafish Notum mutants, Wnt/β-catenin signaling is unrestricted, suggesting that glypicans shape the Wnt morphogen gradient [79, 80].

Recently, several studies have demonstrated the HSPGs may also regulate Notch signaling. In adults, skeletal muscle growth and repair depend on muscle cell progenitors that are maintained in a stem cell niche. Sdc3 and Notch are both components of this niche and without Sdc3, the cell cycle arrests in S phase. Sdc3 and Notch actually exist as a complex on the stem cell membrane and the Sdc3 mutant phenotype is rescued by ectopic expression of a constitutively active Notch intracellular domain [81]. In smooth muscle cells, Notch2 and Notch3 signaling activate *sdc2* expression, and Sdc2 subsequently interacts with Notch3 to activate downstream signaling [82]. While HSPG core proteins appear to be important for Notch signaling in some contexts, the fine modifications on the GAG chains may be of less importance for Notch signaling, as 3-*O*-sulfation does not appear to be critical to Notch signaling in *Drosophila*. Both *Drosophila* 3-*O*-

sulfotransferases, Hs3st-A and Hs3st-B, are involved in the regulation of intestinal stem cell proliferation and midgut homeostasis maintenance, but neither mutations in *hs3st-b*, nor RNAi knockdown of *hs3st-a*, induce defects in Notch signaling [83]. HSPGs' potential to regulate Wnt, Fgf and, and Notch signaling is particularly interesting, given the importance of these three signaling pathways in patterning the PLLP. The questions that instigated the work presented in this dissertation center around which PLLP signaling pathways require HSPGs and how HSPGs impact the functions of those signaling networks.

One focus of this dissertation is Sdc4, which is very specifically expressed in the trailing domain of the PLLP. Sdc4 is a core protein that is known to interact with various growth factors and activate downstream signaling, including the Fgf signaling pathway. While the HS chains attached to the extracellular portion of the protein bind a variety of signaling ligands and receptors, the small intracellular domain has been shown to facilitate downstream signaling. Of particular interest to the study of PLLP signaling, Sdc4 has been shown to regulate both Fgf signaling (reviewed in [84]) and chemokine signaling ([85-88]).

Another focus of this dissertation is Hs3st, the enzyme that makes the final modification to the HSGAG chain. Two Hs3st enzymes are specifically expressed in the leading zone of the PLLP. Although few studies have focused on particular functions for 3-*O*-sulfated HS, a number of binding partners have been identified (reviewed in [89]). Most notably, a recent study showed that 3-*O*-sulfation is critical in a binding interaction with FgfR and promotes signaling by Fgf10 [90].

1.6 Aims of this thesis

Morphogenesis of the PLLP is dependent on the interplay between the Wnt and Fgf signaling pathways and the work in this thesis aims to increase our understanding of how these pathways are regulated to produce the zebrafish lateral line. Specifically, I am interested in how specific elements of HSPGs contribute to the regulation of cell signaling, the downstream functions of signaling pathways, and, ultimately, morphogenesis of the PLL. It was previously known that HSPGs are generally significant for PLL development and through the use of mutants and morphants, I have more specifically defined the functions of Sdc4, an HSPG core protein, and 3-*O*-sulfation, a unique HSPG modification. I initially focused on these two factors because the relevant proteins are specifically expressed in the PLLP. My work shows that both Sdc4 and 3-*O*-sulfated HSPGs are integrated into the signaling network of the PLLP, as each is regulated by PLLP signaling factors and each is also responsible for regulating that same signaling network. It is hoped that these studies provide additional insight into PLL development and, more generally, an improved comprehension of the regulation of intercellular signaling.

In chapter 2, I present work examining the roles of Sdc4 in Fgf signaling, especially migration of the PLLP. I show that Sdc4 is involved in protoneuromast formation and collective cell migration through promotion of Fgf signaling. Meanwhile, Fgf signaling regulates *sdc4* by suppressing its expression, thereby establishing a negative feedback loop to moderate its own function. Lastly, I also demonstrate that Sdc3 can also support Fgf-mediated functions, in addition to Sdc4.

In chapter 3, I explore the regulation and function of 3-*O*-sulfation, a very specific modification made to the HSGAG chain. I show that Wnt signaling mediates

transcriptional activation of two 3-*O*-sulfotransferases, thereby promoting this particular type of sulfation. Despite the fact that Fgf activity and 3-*O*-sulfated HS occupy distinct domains within the PLLP, 3-*O*-sulfation regulates protoneuromast formation via Fgf signaling. The co-expression of 3-*O*-sulfotransferases and Fgf ligands in the leading domain suggests that 3-*O*-sulfation of HSPGs is involved in the delivery of the Fgf signal to trailing cells.

Ultimately, Sdc4 and 3-*O*-sulfated HSPGs regulate PLL development via complementary roles in Fgf signaling. Wnt signaling promotes 3-*O*-sulfation of HSPGs, which, in turn, supports the production and/or delivery of Fgf ligands from leading cells in the PLLP. Meanwhile, Sdc4 assists with the reception of the Fgf signal in trailing cells and exists in a negative feedback loop with Fgf activity. Thus, this HSPG modification and core protein have specific functions in regulating cell signaling in the context of the zebrafish lateral line.

Chapter 2: Syndecan4 mediates cell differentiation and migration via Fgf signaling in the zebrafish lateral line primordium

2.1 Introduction

A number of signaling pathways regulate development of the zebrafish lateral line. Within the primordium, Wnt and Fgf signaling are critical to the formation of protoneuromasts and cell migration. Meanwhile, chemokine signaling guides the collective cell migration of the entire primordium. HSPGs, expressed throughout nearly all animal tissues, have been shown to regulate cell signaling pathways and their downstream functions in development. Although the full extent of how HSPGs regulate signaling is still being studied, the core protein Sdc4 has been shown to regulate both Fgf signaling and chemokine signaling. Furthermore, Sdc4 is expressed in the trailing cells of the primordium, suggesting that it may play some function within the PLLP.

Syndecan4 structure, signaling capabilities, and function

Syndecans all contain a PDZ-binding domain in their cytoplasmic tails that binds a number of ligands containing the PDZ motif. Sdc4 is unique among syndecans in that its cytoplasmic tail also has a seven-residue motif that binds phosphatidylinositol 4,5-bisphosphate (PIP_2) [91, 92]. The PDZ-binding domain is thought to facilitate the inclusion of syndecans into larger complexes, while PIP_2 is hydrolyzed by phospholipase C_γ to produce two second messengers: 1) inositol 1,4,5-triphosphate, involved in the release of Ca^{2+} from the smooth endoplasmic reticulum; and 2) diacylglycerol, which activates protein kinase C alpha (PKCα). PKCα is involved in numerous signaling pathways and

cellular functions, including proliferation, differentiation and motility [93]. The PDZ- and PIP_2-binding domains appear to regulate much of the downstream signaling effects of Sdc4.

Activation of Sdc4 has been shown to promote cell migration. The Rho GTPase family, which includes RhoG, Rac1, and RhoA, are involved in remodeling of the actin cytoskeleton [94]. When no external ligand is bound to Sdc4, Sdc4 binds synectin via the PDZ-binding domain and this interaction suppresses cell migration by inhibiting the activity of Rho GTPases [95, 96]. The binding of several external ligands, including Fgf2 and the ECM component fibronectin, causes Sdc4 molecules to cluster into lipid rafts [97, 98]. This clustering activates PKCα, releases the Rho GTPases to be activated, and ultimately promotes cell motility [99]. Sdc4 is also known to facilitate focal adhesion formation, a critical process during cell migration, in cooperation with integrin via interaction with fibronectin in the ECM [100, 101].

Syndecan4 as a regulator of Fgf signaling

Sdc4 has a well-documented history of regulating Fgf signaling, especially Fgf2. Both in cell culture and *in vivo*, the presence of Sdc4 enhances Fgf2 signaling and downstream responses such as migration and proliferation [102, 103]. This activation of Fgf signaling requires both the HS chains and the cytoplasmic tail of Sdc4. In *sdc4*$^{-/-}$ mouse muscle progenitor cells, Sdc3 cannot compensate for the loss of Sdc4, leading to near-total loss of Fgf2-induced ERK1/2 activation and a decrease in cell migration [104]. In rat endothelial cells, both the PIP_2- and PDZ-binding domains are critical to Fgf2 signaling, but not for other growth factor signaling, suggesting that Sdc4 can selectively regulate Fgf

signaling through its cytoplasmic tail [105]. The interaction of Fgf2 and Sdc4 also determines the duration and intensity of Fgf-induced MAPK signaling [71]. In the absence of Fgf2, Sdc4 suppresses RhoG. When Fgf2 is introduced, an FgfR1-Sdc4-Fgf2 signaling complex is formed, releasing RhoG, which induces membrane ruffling and internalization of the complex via macropinocytosis. This internalization results in the formation of an active signaling vesicle that stimulates ERK1/2 signaling. Even with a dominant-negative FgfR, Fgf2 can transiently activate ERK1/2 signaling and cell migration in cells expressing Sdc4, activities that were inhibited by the removal of HSGAG chains [106]. In addition to promoting the intensity of Fgf signaling at the cell surface, Sdc4 can also regulate the range of the Fgf signal when the Sdc4 ectodomain is shed from the cell surface. In *xenopus*, the serine protease xHtrA1 cleaves Sdc4 to produce a soluble Fgf-ectodomain complex that promotes long-range signaling of Fgf4 [107]. The role of proteases and ectodomain shedding remains unexplored in in the PLLP.

Syndecan4 as a regulator of chemokine signaling

In addition to its roles in Fgf signaling, Sdc4 has also been implicated in Cxcl12a/Cxcr4 signaling in tumor cells. Sdc4, but not Sdc1 or Sdc2, forms a complex with Cxcl12a and Cxcr4 in HeLa cells, peripheral lymphocytes, and macrophages [88]. Sdc4 can independently bind both Cxcr4 and Cxcl12a, but while Cxcl12a binds to Sdc4 in a HSGAG chain-dependent manner, the binding of Cxcr4 to Sdc4 is independent of the HSGAG chains [87]. This suggests that the Cxcl12a ligand binds to the extracellular HSGAG chains of Sdc4 and the receptor Cxcr4 associates directly with the core protein. Cxcl12a-activated p44/p42 MAPK and JNK/SAP kinase signaling requires Sdc4, but the

Cxcl12a-dependent Ca^{2+} mobilization is independent of Sdc4, indicating that Sdc4 is selectively required for particular functions of Cxcl12a signaling [87]. Cxcl12a/Cxcr4 signaling also induces shedding of the Sdc4 ectodomain in HeLa cells, suggesting that Sdc4 plays an additional role in chemokine signaling away from the originating cell [85]. When Sdc4 is suppressed by RNAi, Cxcl12a-induced HeLa cell invasion is strongly reduced [86]. Thus, Sdc4 mediates some downstream chemokine signaling and cell chemotaxis as a co-receptor for Cxcl12a.

Sdc4 is specifically expressed in the trailing domain of the PLLP [39], but its role in PLLP morphogenesis was unknown. We set out to study whether Sdc4 had a role in any of these signaling pathways and their downstream impacts on lateral line development. We find that *sdc4* is expressed in the trailing domain, where it is suppressed by Fgf signaling. Using morpholino-mediated knockdown and mutants generated by the CRISPR/Cas9 system, we show that the loss of Sdc4 interferes with the polarized Wnt-Fgf signaling system. The absence of Sdc4 weakens Fgf signaling activity, allowing the domain of Wnt signaling to expand. This, in turn, impacts the processes downstream of Fgf signaling, interfering with protoneuromast formation and PLLP migration. Additionally, another Syndecan, Sdc3, may be able to compensate for the loss of Sdc4. These results indicate that activation of the Fgf receptor, protoneuromast formation, and PLLP migration all depend, in part, on the function of Sdc4 and that Sdc3 can also help support Fgf-mediated processes.

2.2 Results

Sdc4 is expressed in the trailing domain of the PLLP and suppressed by Fgf signaling

To determine where *sdc4* is expressed in the PLL, *in situ* hybridization was performed in 31hpf zebrafish embryos, when the primordium is about mid-way through migration. As previously described, *Sdc4* is expressed in the trailing domain of the PLLP [39], as well as in deposited neuromasts (Figure 2.2.1A and B). Although *sdc4* is expressed in the trailing zone where Fgf signaling is generally more active (as indicated by *pea3* expression), *sdc4* is strongest in the most trailing cells with less *pea3* expression (Figure 2.2.1C). The domain of *sdc4* expression remains relatively stable during the course of migration, although the intensity of expression diminishes somewhat over time (Figure 2.2.1D-F).

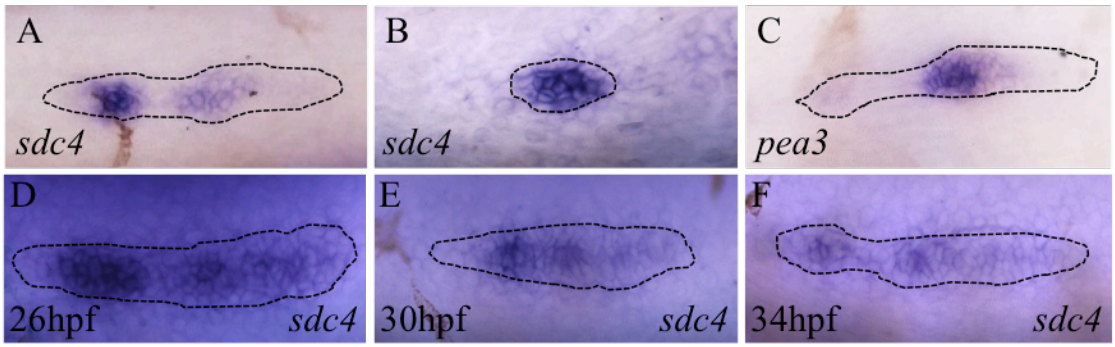

Figure 2.2.2: Sdc4 is expressed in the trailing domain of the primordium. (A) *In situ* hybridization for sdc4 shows expression in the trailing zone, especially in depositing neuromasts (arrowhead) (*n*=17). (B) Expression persists in deposited neuromasts (*n*=17). (C) *Pea3*, a marker of Fgf signaling activity, is also expressed in the trailing domain, although it is weaker in the most trailing cells (*n*=13). (D-F) A time course shows that the expression domain of sdc4 is relatively stable over eight hours, but the intensity of expression does decrease somewhat as migration progresses (26hpf *n*=20, 30hpf *n*=20, 34hpf *n*=20). All embryos used for *in situ* hybridization were derived from the transgenic line tg[cldnb:lynGFP], in which GFP is expressed in the PLLP. The dotted lines mark the outline of the PLLP, as delineated by a GFP antibody.

The domain of *sdc4* expression suggests several possibilities for how it is regulated. Given its exclusion from the leading domain, it is possible that the Wnt and BMP signaling systems, both of which are active in the leading domain, suppress its expression.

Furthermore, given expression of *sdc4* in the trailing domain, within the domain of Fgf activity, it is possible that Fgf signaling activates expression of this HSPG. To investigate these possibilities, we used chemical inhibitors to manipulate these signaling pathways.

To investigate the possibility of Wnt as a leading zone suppressor, we used IWR to suppress Wnt signaling and BIO to activate Wnt signaling. IWR suppresses Wnt signaling by stabilizing Axin in the β-catenin destruction complex, thereby enabling the degradation of β-catenin, which mediates the canonical transcriptional response to Wnt signaling. BIO activates Wnt signaling through a complimentary mechanism, as it inhibits GSK-3 in the β-catenin destruction complex, allowing for a build-up of β-catenin and downstream transcriptional activation of Wnt targets. *Lef1* expression demonstrates the efficacy of these two inhibitors (Figure 2.2.2E-G). Consistent with Wnt signaling also inhibiting *sdc4* expression, IWR increased and BIO somewhat suppressed *sdc4* expression (Figure 2.2.2A-

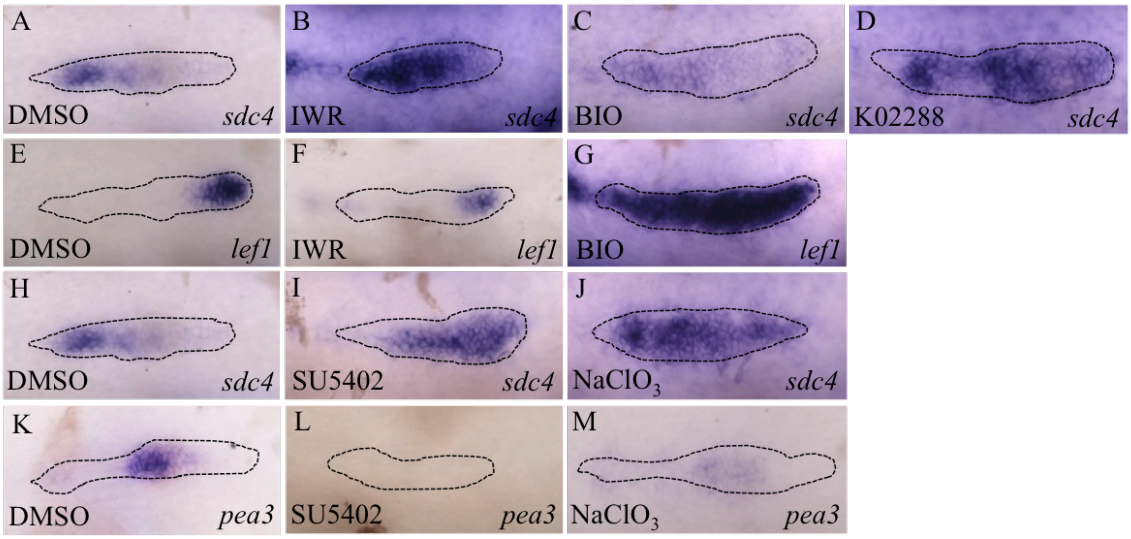

Figure 3.2.2: Fgf signaling suppresses sdc4 expression. (A) DMSO controls show expression of *sdc4* in trailing cells (*n*=17). (B) Suppression of Wnt signaling via IWR treatment also expands sdc4 expression (*n*=17). (C) BIO, which activates ectopic Wnt activity, has a small impact of sdc4 expression, subtly repressing it (*n*=20). (D) Treatment with K02288, an inhibitor of BMP signaling, also expands sdc4 expression (*n*=18). (E,F,G) *Lef1* in situ hybridization demonstrates the efficacy of IWR and BIO in regulating Wnt activity. IWR suppresses *lef1* expression, while it expands under BIO treatment (DMSO *n*=16, IWR *n*=11, BIO *n*=16) (H,I,J) Inhibition of Fgf signaling through SU5402 or NaClO3 treatment expands sdc4 expression, as compared to DMSO controls (DMSO *n*=17, SU5402 *n*=21, $NaClO_3$ *n*=19). (K,L,M) *Pea3* expression show that SU5402 and $NaClO_3$ treatments both suppress Fgf signaling (DMSO *n*=13, SU5402 *n*=12, $NaClO_3$ *n*=7).

C). Wnt activation also determines expression of *bmp2b* in the leading zone, so we asked if BMP signaling regulates *sdc4* expression. Inhibition of BMP signaling with signaling inhibitor K02288 also increased *sdc4* expression (Figure 2.2.2D), showing that this signaling pathway also has the potential to prevent *sdc4* expression. These results indicate that Wnt signaling suppresses *sdc4* expression in leading cells.

To determine if Fgf promotes expression of *sdc4* in trailing cells, we inhibited Fgf signaling through treatment with the chemical inhibitors SU5402 and sodium chlorate ($NaClO_3$), both of which suppress Fgf signaling as measured by *pea3* expression (Figure 2.2.2K-M). SU5402 suppresses Fgf signaling by directly inhibiting the FgfR, while $NaClO_3$ indirectly inhibits Fgf by suppressing HSPG sulfation [39]. $NaClO_3$ prevents the formation of the sulfation donor 3'-phosphoadenosin 5'-phosphosulfate (PAPS). The loss of PAPS prevents 2-*O*- and 6-*O*-sulfation [108], and sulfation is reduced by 55% [39]. This decrease in sulfation fundamentally changes HSPG structure, and diminishes their ability to bind targets. Fgfs and FgfRs are both HSPG binding partners, and this large-scale disruption in sulfation decreases the efficacy of Fgf signaling. Contrary to our hypothesis, both of these Fgf inhibitors expand *sdc4* expression (Figure 2.2.2H-J). These observations raised the possibility that Fgf signaling actually suppresses *sdc4* in nascent protoneuromasts located closer to the leading end, where Fgf signaling is more active, and that its expression is therefore only permitted in the most trailing protoneuromasts that are preparing for deposition, where Fgf signaling is lower (Figure 2.2.1A and C). It should also be noted that SU5402 and $NaClO_3$ both inhibit Fgf signaling and permit more Wnt activity in the trailing zone, where Fgf signaling normally helps suppress Wnt signaling. However,

this indirect expansion in the domain of Wnt activity was not associated with reduced *sdc4* expression, suggesting that Wnt is probably not a direct suppressor of *sdc4* expression.

While the effects of IWR and BIO suggest that Wnt suppresses *sdc4* expression, inhibition of Fgf signaling, which is associated with an expansion of the domain of Wnt activity, caused an expansion of *sdc4* expression, rather than a reduction. This seemingly paradoxical observation suggested that changes in Fgf, Wnt, and BMP signaling might, in part, indirectly influence *sdc4* signaling. Although IWR, BIO, $NaClO_3$, and K02288 inhibit a variety of signaling pathways, they all slow or stall migration of the PLLP. Perhaps the inhibition of migration causes an upregulation in *sdc4* expression. Consistent with this hypothesis, we observed an expansion of *sdc4* expression in *cxcl12a* morphants, in which PLLP migration is arrested at the migration starting point (Figure 2.2.3A-C).

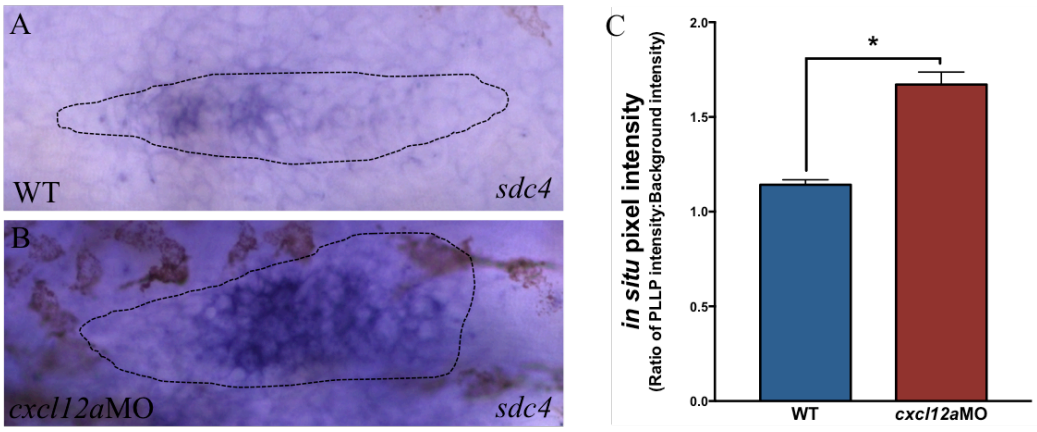

Figure 2.2.3: Intensity of *sdc4* expression is increased in *cxcl12a* morphants. (A,B) Representative images show the increase in expression in *cxcl12a* morphants, compared to WT controls. (C) Quantification of *sdc4* expression in WT and *cxcl12a* morphants is significantly different (WT n=15, *cxcl12a*MO n=15). Expression intensity is normalized to background expression intensity, and is shown as a ratio of average PLLP pixel intensity to average background pixel intensity. *$p < 0.01$. Bars represent mean ± SEM.

Knockdown of *sdc4* interferes with protoneuromast formation and slows PLLP migration

Given the PLLP-specific expression of *sdc4* in soon-to-be-deposited protoneuromasts, and the established importance for HSPGs in the PLLP [39], we examined the phenotype caused by morpholino knockdown of *sdc4*. A previously verified translation-blocking antisense morpholino [109], was used to target *sdc4*. We observed cell death in *sdc4* morphant PLLP during time-lapse imaging, whereas WT PLLP experience little or no cell death. Cell death is a known p53-dependent off-target effect of some morpholinos, and so in these preliminary studies examining the function of *sdc4*, we co-injected a *p53* morpholino to examine changes that were less likely to be determined by p53-dependent cell death. *Sdc4* morphants have significantly fewer neuromasts and the primordium dissipates after depositing L4/L5, failing to migrate to the tip of the tail or deposit a terminal cluster (Figure 2.2.4A-C). In morphants, the first pair of neuromasts (L1/L2) is spaced further apart than wild-type, the next two pairs (L2/L3 and L3/L4) are

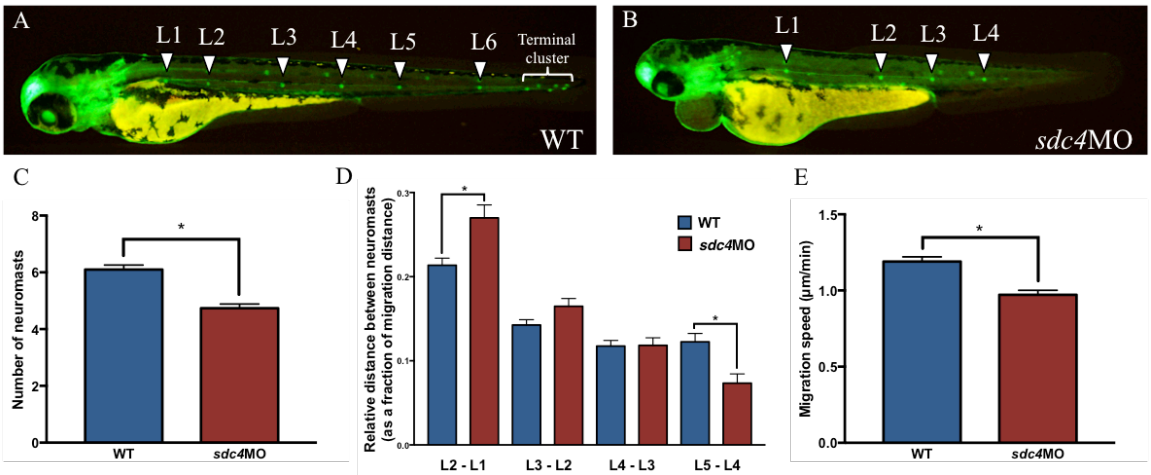

Figure 2.2.4: Sdc4 morphants have fewer neuromasts. (A,B,C) Sdc4MO have significantly fewer neuromasts than uninjected embryos. The primordium dissipates after depositing L4/L5, failing to migrate to the tip of the tail or deposit a terminal cluster (WT *n*=20, *sdc4*MO=19). (D) Early neuromasts (L1 and L2) are spaced further apart, but become progressively more closely spaced. (E) Close spacing is due to a slow rate of migration, as confirmed by time-lapse microscopy (WT *n*=4, *sdc4*MO=5). **p* < 0.01. Bars represent mean ± SEM.

normally spaced, and the final pair (L4/L5) is spaced significantly closer together than wild-type (Figure 2.2.4D). Migration speed is reduced in sdc4 morphants, as measured in time-lapse movies that span from 28hpf to 48hpf (Figure 2.2.4E and Supplementary Movie 1). The slow decline in the spacing between each subsequent pair of neuromasts is the result of slower migration. These results indicate that Sdc4 is important for normal migration of the PLLP.

The increased space between L1 and L2 suggested that protoneuromast formation may also be compromised in morphants. To determine if this was true, frames from time-lapse movies were analyzed for neuromast number at five hourly intervals from 29hpf to 33hpf. wild-type primordia generally had three protoneuromasts, while *sdc4* morphants tended to have only two protoneuromasts (Figure 2.2.5A-C). Furthermore, NM1 and NM2 were located further from the leading edge of the PLLP in morphants, relative to the length

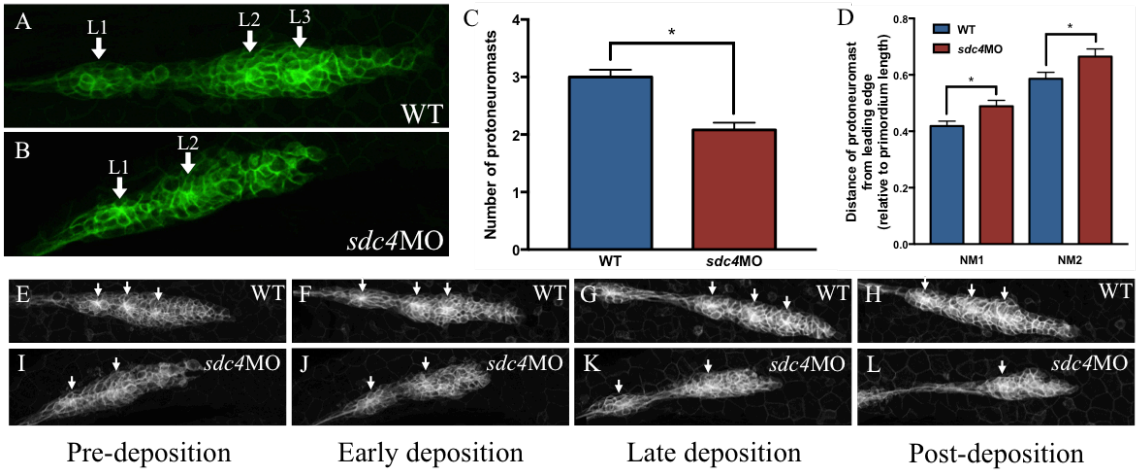

Figure 2.2.5: Sdc4 morphant primordia have fewer forming protoneuromasts. Frames from time-lapse movies were analyzed for neuromast number at five hourly intervals (29hpf-33hpf). (A,B,C) WT primordia have 3 protoneuromasts, while *sdc4*MO have only 2 protoneuromasts. Images show protoneuromasts (NM) in WT and *sdc4*MO, numbered and marked by arrows. Although *sdc4*MO primordia are shorter than WT primordia, they still had fewer neuromasts per unit of distance. (D) Each protoneuromast (generically marked as NM1 and NM2 because measurements were made over the course of five hours) is located further from the leading edge of the PLLP in morphants, relative to the length of the primordium. (E,F,G,H) WT primordia show very clear protoneuromasts before, during, and after deposition; cells are arranged in the stereotypical rosette formation with clear apical constriction of the cells at the rosette center. (I,J,K,L) Although *sdc4*MO form and deposit protoneuromasts, their rosettes do not appear to be as clearly defined as in WT. Arrows mark neuromast centers. WT n=20, *sdc4*MO=25. *$p < 0.05$. Bars represent mean ± SEM.

of the primordium (Figure 2.2.5D). Although *sdc4* morphant primordia are shorter than wild-type primordia, they still had fewer neuromasts when data was normalized to PLLP length. In addition to having fewer protoneuromasts at any given time, *sdc4* morphant protoneuromasts are poorly formed. Wild-type primordia show very clear protoneuromasts before, during, and after deposition; cells are arranged in the stereotypical rosette formation with clear apical constriction of the cells at the rosette center (Figure 2.2.5E-H). Although morphants form and deposit protoneuromasts, their rosettes do not appear to be as clearly defined as wild-type rosettes, as determined in a transgenic line, which marks the boundaries of PLLP cells with GFP (*tg[cldnb:lynGFP]*; Figure 2.2.5I-L).

Sdc4 morphants exhibit weak Fgf signaling

As knockdown of *sdc4* hampered the timely and orderly formation of protoneuromasts, we examined *pea3* expression in *sdc4* morphants to determine if Fgf signaling, required for neuromast morphogenesis, is impaired. In morphants, *pea3* expression is less intense and the relative length of the expression domain is shorter (Figure 2.2.6A-C). This indicates that Fgf signaling is weakened by the absence of Sdc4. Meanwhile, expression of *lef1*, a marker of Wnt activity, is expanded in the leading domain (Figure 2.2.6D-F). Since Fgf signaling normally represses Wnt activity, it may be that Wnt expands due to attenuated Fgf signaling caused by *sdc4* knockdown.

Ectopic expression of *sdc4* causes dorsalization of zebrafish embryos

To this point, our results suggest that Sdc4 is required for Fgf signaling during PLLP migration and neuromast formation. In order to further investigate the function of

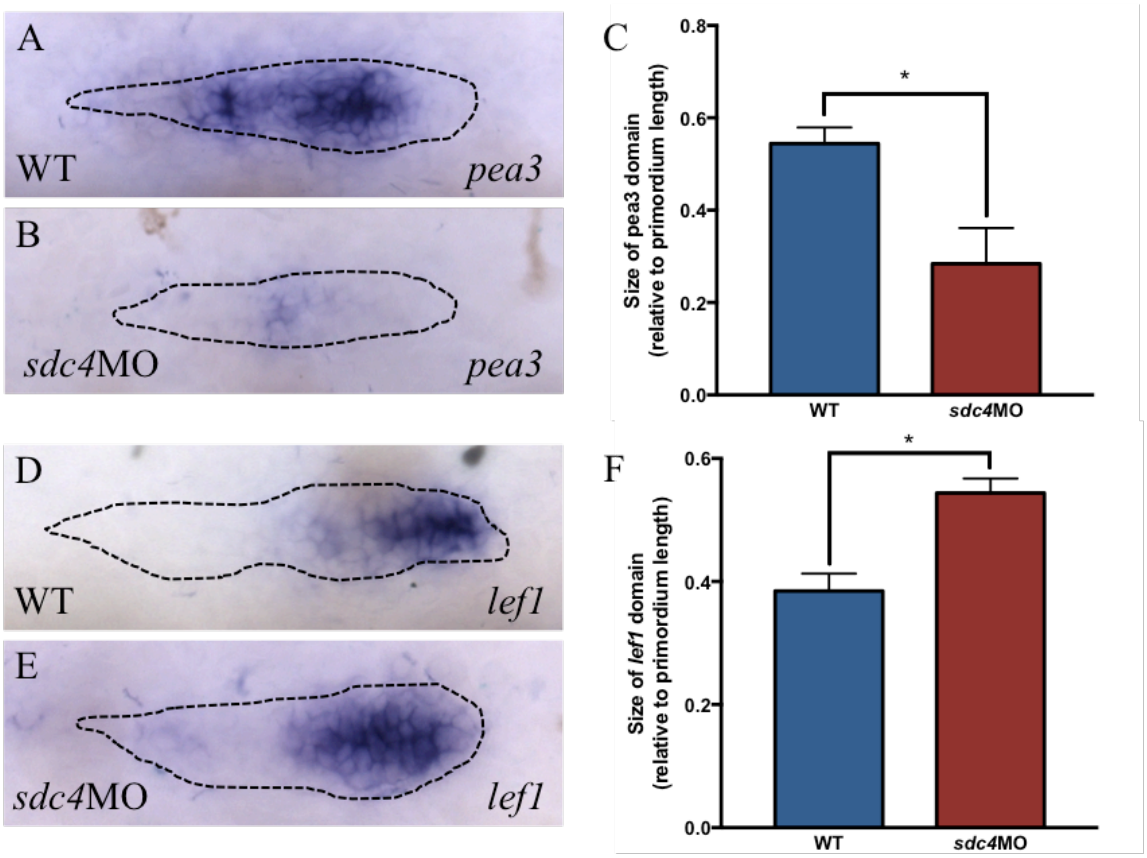

Figure 2.2.6: *Sdc4* morphants exhibit weak Fgf signaling. (A,B) Pea3 expression is weaker in sdc4 morphants (WT *n*=14, *n*=9). (C) The relative length of the *pea3* domain is significantly reduced in *sdc4*MO. (D,E,F) *Sdc4*MO also have an expanded *lef1* expression domain that is significantly longer, indicating that Wnt signaling is expanded (WT *n* = 12, *sdc4*MO=12). $^{*}p < 0.01$. Bars represent mean ± SEM.

Sdc4, we ectopically expressed *sdc4* by injecting *sdc4* mRNA at the one-cell stage. At shield stage, embryos injected with 25pg of *sdc4* mRNA showed increased expression of *spry4*, a target of Fgf signaling (Figure 2.2.7A and B). By the time body axis formation was complete, embryos injected with *sdc4* mRNA have defects in dorsoventral axis patterning, where dorsal structures have developed at the expense of ventral structures (Figure 2.2.7C-G). This defect where the development of dorsal structures is favored over the development of ventral structures is known as dorsalization. Dorsalized embryos also exhibit some defects in anterior-posterior patterning. Imaged at 48hpf, even embryos injected with the low dose of 10pg of mRNA could be dorsalized, with about 17% of

embryos exhibiting a dorsalized phenotype. At 25pg and 50pg doses, 50% of embryos were dorsalized. Generally, the higher the dosage, the more severe the dorsalization. At dosages of 150pg and 300pg of *sdc4* mRNA, all injected embryos were dorsalized (data not shown). During dorsoventral patterning, Fgf signaling allows for the development of dorsal structures, and ectopic activation of Fgf signaling can cause dorsalization [110, 111]. Therefore, dorsalization of *sdc4* mRNA-injected embryos is consistent with our hypothesis that Sdc4 facilitates Fgf signaling in zebrafish.

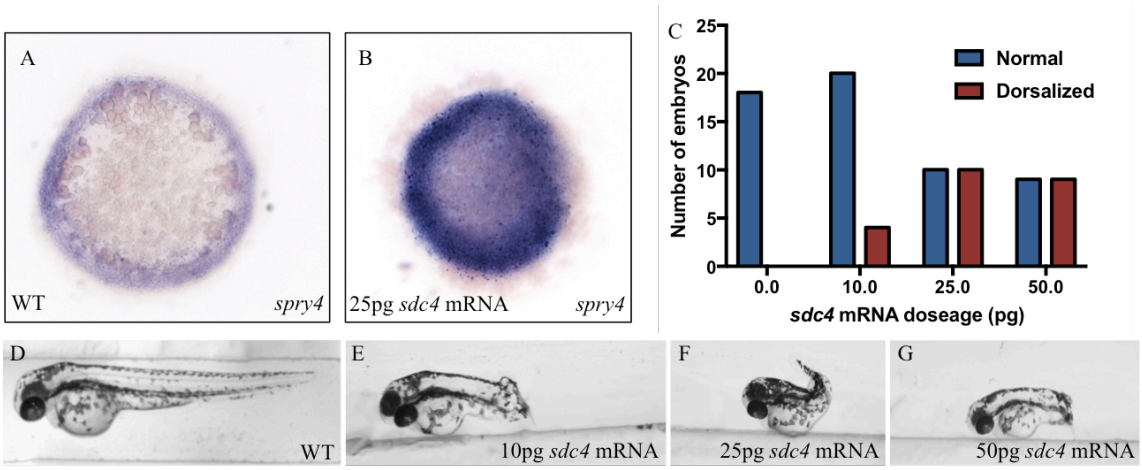

Figure 2.2.7: Overexpression of sdc4 causes ectopic activation of Fgf signaling. (A) Expression of *spry4*, a target of Fgf signaling, is limited to the marginal zone at 50% epiboly (*n*=12). (B) *Spry4* expression is increased in embryos injected with *sdc4* mRNA (*n*=15). (C) Distribution of normal and dorsalized embryos in *sdc4* mRNA-injected embryos (WT *n*=18, 10pg *n*=24, 25pg *n*=20, 50pg *n*=18). (D) Example of a WT embryos with a normal dorsoventral axis. (E,F,G) Examples of embryos, dorsalized to varying degrees, all injected with *sdc4* mRNA.

Our results thus far indicate a role for Sdc4 in Fgf signaling, which is consistent with an extensive literature documenting the variety of functions Sdc4 plays in the Fgf signaling pathway. However, our results are based on morpholinos, which are known to have a number of off-target effects that can create false phenotypes [112, 113]. With regards to the lateral line specifically, we have found that morpholinos can cause expanded *lef1* expression, reduced *pea3* expression, and increased spacing between neuromasts as a result of their off-target effects, completely independent of the gene knockdown they

perform. In order to demonstrate the validity of our morpholino-based findings, we generated targeted mutations in the extracellular domain of *sdc4* using the CRISPR/Cas9 system [114].

Sdc4 **mutants have a normal pattern of neuromasts despite changes in signaling**

Sdc4 mutants appear to have a normal number of neuromasts and the relative distance between neuromasts is similar to wild-type siblings (Figure 2.2.8 A- D). However, despite a normal pattern of neuromast deposition, the PLLP in *sdc4* mutants does show some changes in Wnt and Fgf signaling. Expression of *lef1* and *pea3* was observed at three time points over eight hours during PLLP migration. At 26hpf, the intensity of *lef1* expression is similar between wild-types and mutants, but at 30hpf, *lef1* expression is more intense in mutants (Figure 2.2.8E-J and Q). This indicates that Wnt signaling starts of relatively normal in *sdc4* mutants, but it fails to regress at the same rate as it does in wild-type embryos. Meanwhile, expression of *pea3* appears normal at 26hpf, but by 30 and 34hpf, its expression is significantly less intense in mutants (Figure 2.2.8K-P and R). This indicates that Fgf signaling, like Wnt signaling, is initially functioning at normal levels; as migration progresses, Fgf fails to maintain as high a level of activity as in wild-type. These results indicate that *sdc4* is necessary for normal Wnt and Fgf signaling, but that the PLLP signaling network can still compensate for this loss, migrate, and establish a normal pattern of deposited neuromasts.

Because *sdc4* morphants exhibit a slow speed of PLLP migration, we wanted to know if Sdc4 regulated PLLP migration through a role in chemokine signaling, in addition to its regulation of Fgf signaling. In cell culture experiments, Sdc4 has been shown to

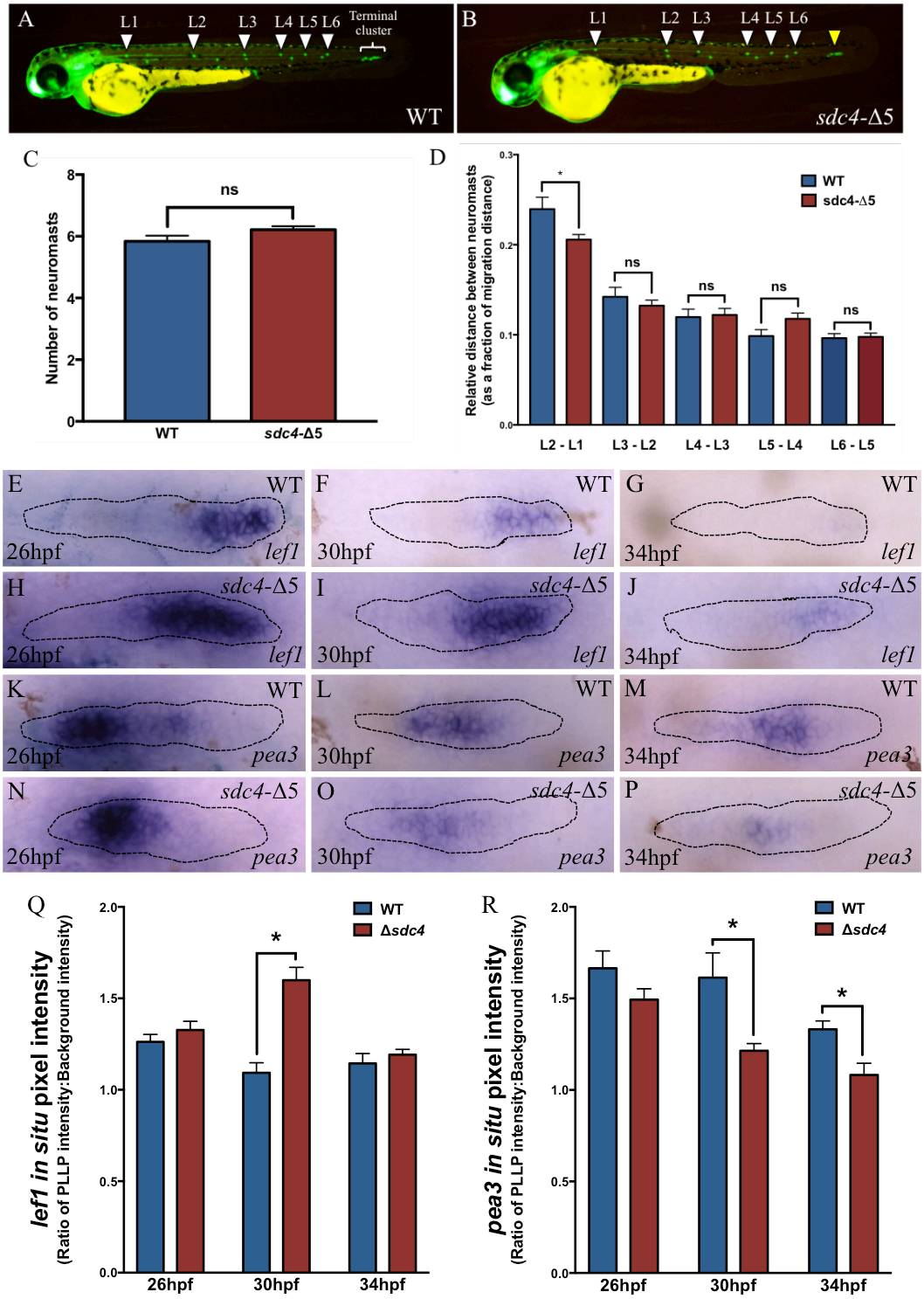

Figure 2.2.8: *Sdc4* mutants have a normal pattern of neuromast deposition, despite changes in Wnt and Fgf signaling. (A,B,C,D) The neuromast deposition pattern in *sdc4* mutants is largely normal, with a normal number of neuromasts that are generally properly spaced (WT n=19, Δ*sdc4* n=14). (E,F,G,H,I,J, Q) *In situ* hybridization for *lef1* in WT and mutants at 26hpf, 30hpf, and 34hpf (WT 26hpf n=15, WT 30hpf n=15, WT 34hpf n=15, Δ*sdc4* 26hpf n=14, Δ*sdc4* 30hpf n=19, Δ*sdc4* 34hpf n=27). (K,L,M,N,O,P,R) *In situ* hybridization for *pea3* in WT and mutants at 26hpf, 30hpf, and 34hpf(WT 26hpf n=14, WT 30hpf n=13, WT 34hpf n=15, Δ*sdc4* 26hpf n=22, Δ*sdc4* 30hpf n=20, Δ*sdc4* 34hpf n=12). Expression intensity is normalized to background expression intensity, and is shown as a ratio of average PLLP pixel intensity to average background pixel intensity. *$p < 0.05$. Bars represent mean ± SEM.

associate with both Cxcr4b and Cxcl12a, and to be critical to certain downstream signaling pathways activated by Cxcl12a [86-88]. To determine if chemokine signaling might be altered in *sdc4* mutants, we looked at expression of *cxcr4b* and *cxcr7b*, the two chemokine ligand receptors expressed within the PLLP. Both genes show marked upregulation in *sdc4* mutant PLLP (Figure 2.2.9A, B, D, E), with significantly greater intensity of expression, as compared to wild-type (Figure 2.2.9 C and F). The upregulation of *cxcr4b* in mutants may well be due to the ectopic activation of Wnt signaling, as Wnt signaling has been proposed to facilitate expression of this chemokine receptor [8]. It is uncertain what

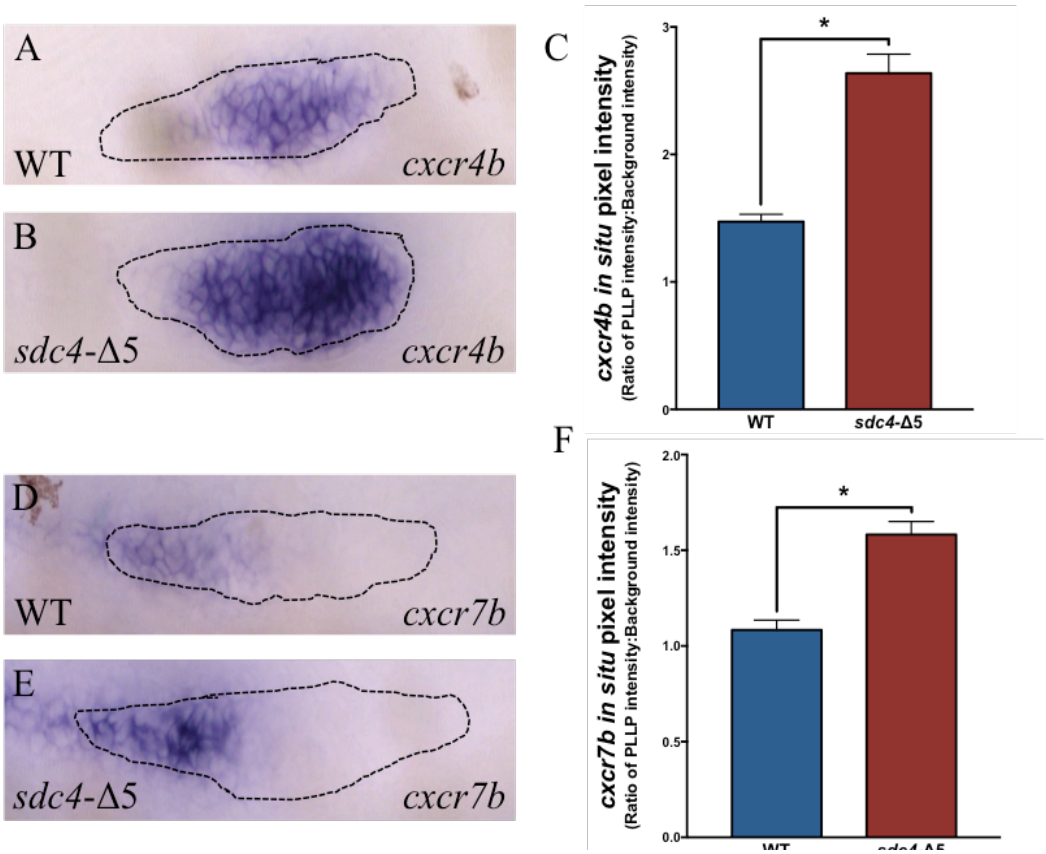

Figure 2.2.9: *Sdc4* mutants have increased expression of chemokine receptors. (A,B) Representative images show increased expression of *cxcr4b* in *sdc4* mutants. (C) Analysis of *in situ* hybridization staining intensity shows significantly increased expression in mutants (WT n=20, Δ*sdc4* n=15). (D,E) Representative images show increased expression of *cxcr7b* in *sdc4* mutants. (F) Analysis of *in situ* hybridization staining intensity shows significantly increased expression in mutants (WT n=20, Δ*sdc4* n=12). Expression intensity is normalized to background expression intensity, and is shown as a ratio of average PLLP pixel intensity to average background pixel intensity. *$p < 0.01$. Bars represent mean ± SEM.

signaling network is responsible for the upregulation of its expression in *sdc4* mutants. Both Cxcr4b and Cxcr7b are necessary to maintain consistent migration of the PLLP from anterior to posterior, and the loss of either receptor results in a failure of directed migration [20, 21]. Perhaps the increase in *cxcr7b* is the result of a compensatory mechanism that is responding to the Wnt-induced increase in *cxcr4b*, allowing a similar upregulation in the expression of both receptors. Although the expression of the two receptors is changed, the balance between *cxcr4b* and *cxcr7b* is maintained, preserving the local *cxcl12a* gradient they create along the length of the PLLP.

Inhibiting Fgf signaling within the PLLP in *sdc4* mutants suggests a role for Sdc4 in migration

Although *sdc4* mutants show no obvious neuromast or PLLP migration phenotype, CRISPR mutants have been shown to compensate for mutations deleterious to their signaling network [115]. We hypothesized that despite such compensation, the genetic regulatory network might not be as robust and thus be much more susceptible to manipulations that perturb the system. In order to reveal any vulnerabilities specific to the *sdc4* mutants, we wanted to simultaneously compromise the function of the signaling systems that normally work in concert with Sdc4. Since our morpholino studies and previous work by other researchers indicate a role for Sdc4 in Fgf signaling, we hypothesized that in the context of *sdc4* loss, mild inhibition of the Fgf signaling network within the PLLP may cause stronger defects in *sdc4* mutants than in wild-type siblings.

Morpholino-induced knockdown of *fgf10*, one of the two Fgfs expressed in the PLLP, delays the establishment of FgfR signaling within the PLLP and subsequent

protoneuromast formation and deposition [12]. This phenotype is usually seen after injecting a 4ng dose of *fgf10*MO into wild-type embryos. In order to draw out the vulnerabilities of the *sdc4* mutants without causing too strong a defect in wild-type embryos, we used a low dose of the *fgf10* morpholino (1ng) that causes little or no phenotype in wild-type embryos. Interestingly, in *sdc4* mutants injected with a low dose of *fgf10* morpholino, the PLLP has completed a significantly smaller fraction of its migration to the tip of the tail at 48hpf, a time by which most wild-type PLLP have almost completed this journey (Figure 2.2.10A, B, and E). By 72hpf, PLLP migration to the tail tip is completed in all embryos; however, *sdc4* mutants injected with *fgf10* morpholino have deposited an additional neuromast compared to wild-type siblings also injected with the *fgf10* morpholino (Figure 2.2.10C, D, and F). The difference in migration distance at 48hpf suggested that *fgf10* knockdown in *sdc4* mutants causes slow PLLP migration, allowing time for the deposition of an extra neuromast prior to termination, as is observed at 72hpf. Indeed, measurement of migration speed in time-lapse movies demonstrates that *sdc4* mutant PLLP migrate significantly slower than their wild-type siblings, when both are injected with the *fgf10* morpholino (Figure 2.2.10G and Supplementary Movie 2).

Using an alternate strategy that also targets Fgf signaling, we looked for differences in PLLP behavior in *sdc4* mutants following exposure to $NaClO_3$. $NaClO_3$ inhibits formation of the sulfation donor 3'-phosphoadenosine 5'-phosphosulfate (PAPS), thereby inhibiting three major types of sulfation (N-sulfation, 2-*O*-sulfation, and 6-*O*-sulfation) that are usually performed on the HS chain during biosynthesis and altering the ability of HS to bind to target signaling molecules [108]. When wild-type embryos are treated with

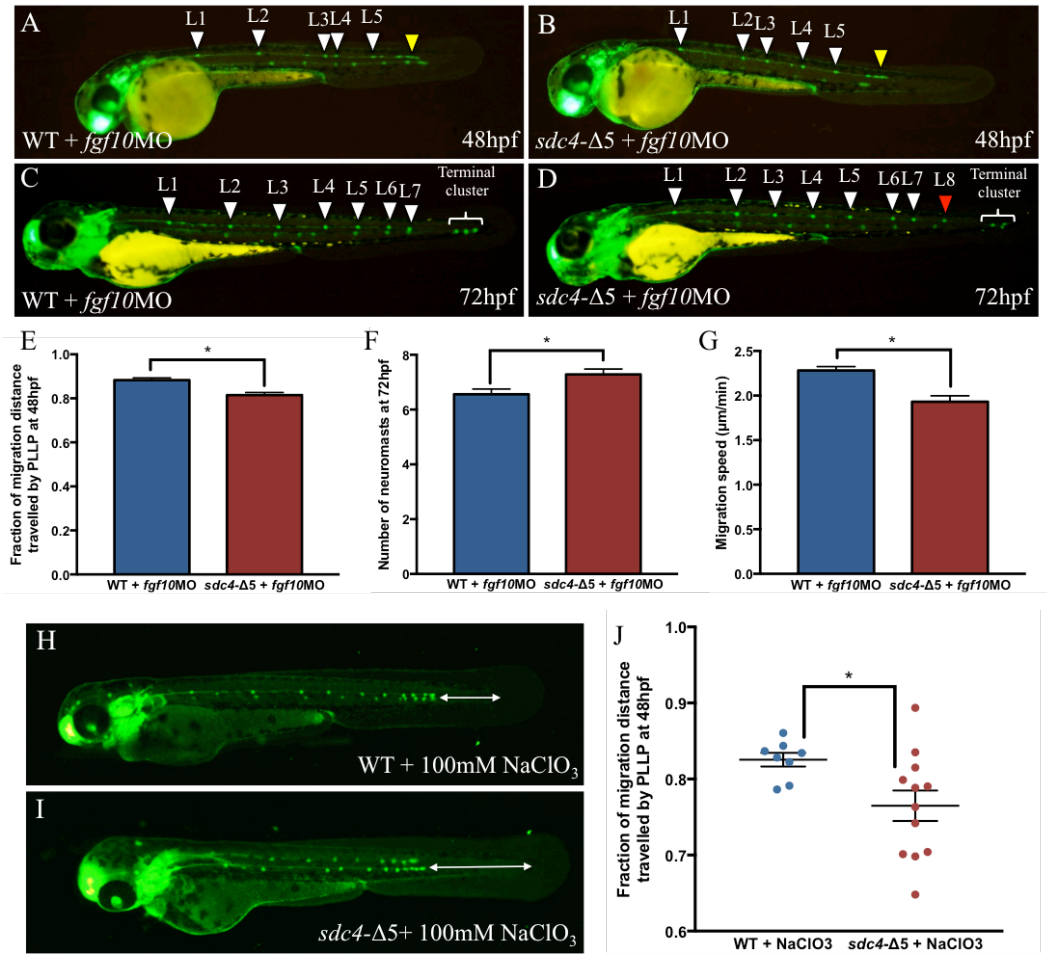

Figure 2.2.10: Inhibition of Fgf signaling in *sdc4* mutants causes migration defects. (A,B,E) The PLLP in WT embryos injected with a low dose of *fgf10*MO (1ng) have migrated significantly further than the PLLP in *sdc4* mutant siblings also injected with *fgf10*MO (migrating PLLP marked by yellow arrow; WT *n*=14, Δ*sdc4* *n*=14). (C,D,F) At 72hpf, PLLP migration finished and *sdc4* mutants have one extra deposited neuromast (marked by a red arrow), as comopared to WT siblings (WT *n*=21, Δ*sdc4* *n*=25). (G) The difference in migration distance and extra neuromast are due to significantly slower migration speed, as confirmed by measurement of the migration speed in time-lapse movies (WT *n*=6, Δ*sdc4* *n*=5). (H,I,J) Treatment with a low dose of $NaClO_3$ (100mM) specifically causes stalling and termination earlier in *sdc4* mutants, as compared to WT siblings (arrows mark distance left to migrate; WT *n*=8, Δ*sdc4* *n*=12). **p* < 0.05. Bars represent mean ± SEM.

200mM of $NaClO_3$, the PLLP stalls and Fgf signaling within the PLLP is compromised [39]. When *sdc4* mutants are treated with a low dose of $NaClO_3$ (100mM), the PLLP stalls and terminates earlier in *sdc4* mutants, as compared to wild-type siblings treated with the same dose (Figure 2.2.10H- J).

Sdc3 works with Sdc4 to support neuromast formation and PLLP migration

The migration defects seen in *sdc4* morphants and in *sdc4* mutants with disturbed PLLP signaling support the hypothesis that Sdc4 plays some role in regulating migration of the PLLP. Since *sdc4* mutants show no migration defects without signaling manipulation, it seems that Fgf signaling and other PLLP HSPGs, either together or independently, work to compensate for the loss of Sdc4. A search of the literature suggested that Syndecan3 (Sdc3), another syndecan homolog, makes a particularly attractive candidate. *Sdc3* is expressed throughout the PLLP [39] and the protein has a relatively similar structure to that of Sdc4. Although Sdc3 cannot always compensate for the loss of Sdc4 [104], there is some evidence that Sdc3, like Sdc4, also has a role in Fgf signaling [116, 117].

Sdc3 morphants do exhibit some of the same defects as *sdc4* morphants. They have fewer neuromasts and also have increased spacing between pairs of neuromasts, but have no apparent defect in migration (Figure 2.2.11A- D). To test the idea that Sdc3 compensates for the loss of Sdc4 in *sdc4* mutants, we injected a low dose of a *sdc3* morpholino into *sdc4* mutants. Mutants with *sdc3* knocked down do, in fact, show similar defects as Fgf-suppressed *sdc4* mutants. At 48hpf, they are significantly delayed along the path of migration due to a slower rate of migration speed (Figure 2.2.11 E-H and Supplementary Movie 3). These findings therefore indicate that Sdc3 does compensate for the absence of Sdc4 in mutants and support the hypothesis that Sdc3, like Sdc4, can facilitate Fgf signaling when necessary.

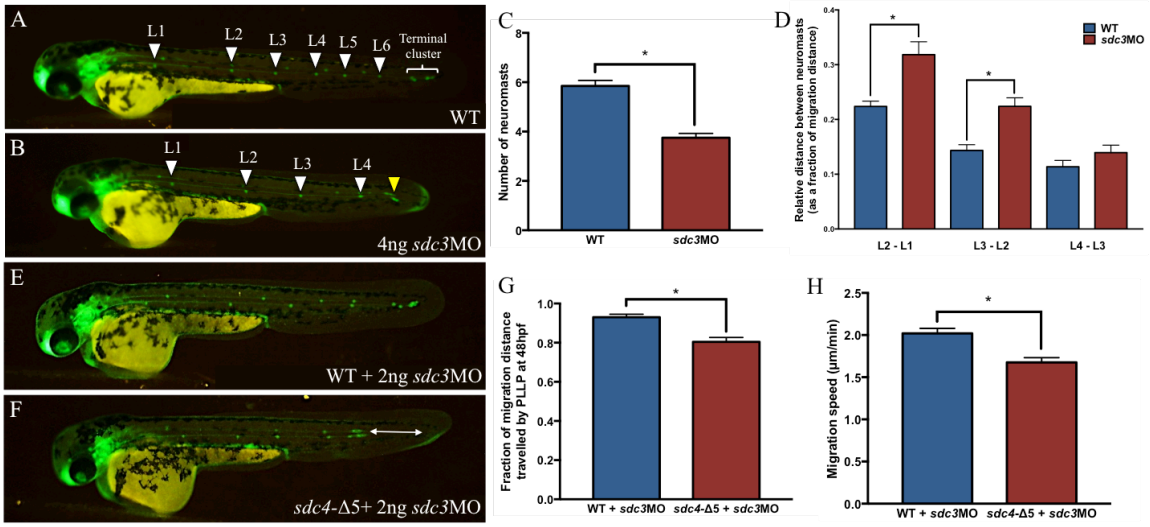

Figure 2.2.11: Knockdown of sdc3 causes migration defects in *sdc4* mutants. (A,B,C,D) *Sdc3* morphants have fewer neuromasts that are more spaced out, compared to WT (yellow arrow marks the still-migrating PLLP; WT *n*=20, *sdc3*MO *n*=20). (E,F,G) In *sdc4* mutants injected with a low dose of the sdc3 morpholino, the PLLP has not migrated as far as WT siblings also injected with the *sdc3* morpholino (arrow marks distance left to migrate; WT *n*=16, Δ*sdc4 n*=19). (H) *Sdc4* mutants injected with the *sdc3* morpholino have a slow rate of PLLP migration (WT *n*=8, Δ*sdc4 n*=16.) **p* < 0.05. Bars represent mean ± SEM.

2.3 Discussion

The interplay of Wnt and Fgf signaling is critical to morphogenesis of the zebrafish lateral line, as these signaling pathways help direct the central processes of collective cell migration and protoneuromast formation. However, the mechanisms that regulate these signaling pathways and control PLL morphogenesis are not fully understood. HSPGs regulate cell signaling, including Wnt and Fgf, in a wide variety of contexts and are expressed throughout animal tissues. One particular HSPG core protein, Sdc4, is very specifically expressed within the PLLP. We began this study with the intent of understanding how Sdc4 might regulate PLLP signaling and morphogenesis of the PLL.

We have shown that Sdc4 is an integral member of the signaling pathways that pattern the PLLP. Our results suggest that Sdc4 promotes Fgf signaling, as the loss of Sdc4

in morphants and mutants weakens Fgf signaling output, and leaves embryos vulnerable to changes in protoneuromast formation and PLLP migration speed. Meanwhile, Fgf signaling negatively regulates *sdc4* expression, thereby establishing a negative feedback loop to moderate its own function. Thus, we identify Sdc4 as a player in the known functions of Fgf signaling in the PLLP.

We found that *sdc4* is expressed in the trailing domain, where we traditionally consider Fgf signaling to be the dominant signaling network. A closer inspection of *sdc4* expression revealed that the strongest *sdc4* expression is in the next-to-be-deposited cells of the PLLP and in deposited neuromasts. In these regions, Fgf signaling activity actually tapers off, so although both Fgf activity and Sdc4 are present in trailing cells, they do not occupy identical regions within the trailing domain.

In order to determine what regulates expression of *sdc4*, we artificially manipulated signaling networks to see how this impacted *sdc4*. We find that Wnt signaling represses it, excluding Sdc4 from the leading zone. In trailing cells, Fgf signaling also represses *sdc4* expression, indicating a negative feedback loop where Sdc4 promotes Fgf activity that then suppresses *sdc4*. Though our results show that *sdc4* expression is suppressed by Fgf signaling, this finding contradicts an earlier Sdc4 regulation study in the PLLP. In a paper published last year, Venero Galanternik, *et al*. (2015) showed that SU5402 treatment suppresses *sdc4* expression [39]. The reasons for this discrepancy remain unclear at this time.

Interestingly, our *sdc4* regulation experiments yielded some contradictory results that led us to formulate additional hypotheses for how Sdc4 is regulated. We ectopically activated Wnt signaling using BIO treatment, which moderately repressed *sdc4* expression.

We also artificially suppressed Fgf signaling through SU5402 treatment, which dramatically expanded *sdc4* expression. However, SU5402 has a dual impact on PLLP signaling: while it inhibits Fgf signaling, it allows for the expansion of Wnt signaling, which is normally repressed in trailing cells by Fgf activity. Thus, despite the fact that BIO and SU5402 both ectopically activate Wnt signaling throughout the primordium, the former suppresses *sdc4* expression, while the latter expands it. One important difference between these two manipulations, however, is that while exposure to BIO increases Wnt signaling, it also increases Fgf expression and this, in turn, is associated with an increase in Fgf signaling. On the other hand, the increase in Wnt signaling associated with exposure to SU5402 is associated with reduced Fgf signaling. Ultimately, whether *sdc4* is increased may depend less on whether Wnt activity is increased, and more on whether Fgf signaling is decreased. While reduced Fgf signaling correlates with increased *sdc4* expression, its expression was also increased following exposure to K02288, a chemical expected to inhibit BMP signaling. This raised the possibility that *sdc4* expression was also negatively regulated by BMP signaling. While this remains a possibility, there was something in common with all the chemical treatments that were associated with increased *sdc4* expression: all these manipulations were associated with slower or stalled migration of the PLLP. As *sdc4* is normally expressed in trailing cells that are beginning to slow down or have been deposited, we hypothesized that progressive loss of migratory behavior may itself be associated with increased *sdc4* expression. To begin exploring this idea, we looked at *sdc4* expression in *cxcl12a* morphants, in which the PLLP does not migrate along the horizontal myoseptum and is stalled at the migration start point. *Sdc4* expression is increased in these morphants, in support of our hypothesis (Figure 2.2.3A-C). A potential

role for migratory behavior in suppressing *sdc4* expression, though interesting, remains speculative at this time, and many more experiments would need to be done to test this hypothesis. For example, we need to determine if other manipulations that stall migration, without obvious effects on the Wnt, Fgf, BMP, and chemokine signaling pathways, also result in increased *sdc4* expression. Another prediction of this hypothesis is that *sdc4* expression may be broader in the PLLP early in its development, before its migratory behavior is initiated. Identification of the signaling network(s) that activate Sdc4 activity would help to promote our understanding of the role Sdc4 plays in PLL development, and provide clues as to its function in other contexts.

Our investigation into the role of Sdc4 in PLL development centered around the phenotypes resulting from the loss of Sdc4 activity. Preliminary experiments used a morpholino to knock down *sdc4*. These experiments suggested that Sdc4 regulates Fgf signaling activity and is specifically involved in collective cell migration and protoneuromast formation, both of which are functions of Fgf signaling. Still, morpholinos are known to cause a number of off-target effects, which can include expanded Wnt signaling and apoptosis, both of which we observed in *sdc4* morphants. We therefore generated *sdc4* mutants using the CRISPR/Cas9 system, intending to confirm our conclusion that Sdc4 regulates Fgf signaling. *Sdc4* mutants, generated by CRISPR, display a decrease in Fgf signaling and an expansion of Wnt signaling, indicating that the signaling changes we observed in morphants were due, at least in part, to the loss of Sdc4 and not the off-target effects of morpholinos. However, the PLLP migrates at a normal speed in mutants and lays down a normal pattern of neuromasts. There are several reasons that could explain why the phenotype in *sdc4* mutants is weaker than the one observed in morphants.

First, studies show that compensatory networks can make up for the loss of certain genes in CRISPR/Cas9-generated mutants, whereas the same compensatory networks are not activated when morpholinos target the same genes [115]. Indeed, the increased expression of *lef1*, *cxcr4b*, and *cxcr7b* in *sdc4* mutants may represent changes in the network that reflect such compensatory behavior. We tested the hypothesis that some factor compensates for the loss of Sdc4 and found this to be true. *Sdc4* mutants are more vulnerable to manipulation of Fgf signaling than are wild-type embryos, and exhibit migration defects as a result of partial Fgf inhibition. Another potential reason for the weak phenotype in *sdc4* mutants is that other HSPG(s) could be the compensating factor(s) supporting Fgf signaling. After all, individual syndecan mouse mutants are also macroscopically indistinguishable from wild-type mice [118, 119]. In addition to Sdc4, several other HSPG core proteins are expressed in the PLLP, including another syndecan, Sdc3 [39]. *Sdc3* is broadly expressed throughout the PLLP, thus overlapping *sdc4* expression, and all syndecans possess a generally similar structure. Although there is not an extensive literature on Sdc3, there is some evidence that Sdc3 can regulate Fgf signaling [117]. These characteristics make Sdc3 an ideal candidate for an HSPG that can compensate for the loss of Sdc4. As *sdc3* knockdown in *sdc4* mutants causes slow PLLP migration (a phenotype the *sdc3* morpholino is not capable of causing alone), it seems likely that these two syndecans are both capable of supporting Fgf signaling.

To further qualify the role of Sdc4 signaling in PLL development, we wanted to overexpress *sdc4*. We did this through injection of *sdc4* mRNA; unfortunately, the resulting changes in dorsoventral axis patterning made specific evaluation of the lateral line difficult. Still, the exaggerated expression of Fgf-responsive genes and ultimate

dorsalization of the embryo in response to *sdc4* overexpression supports our model that Sdc4 supports Fgf signaling in the trailing cells of the PLLP. More PLLP-specific *sdc4* overexpression could be achieved by PLLP-specific promoter-driven *sdc4* expression to circumvent the problems created by dorsoventral patterning.

Our conclusion that Sdc4 facilitates Fgf signaling and its downstream functional roles fits well with the previously known signaling functions of Sdc4. Many studies of Sdc4 have demonstrated that it can support Fgf signaling, both as a co-receptor to FgfR and as an independent receptor (reviewed in [120]). Sdc4 stabilizes the binding of Fgf ligand to FgfR, resulting in more sustained MAPK/ERK signaling [63-65], and allowing for activation of intracellular signaling with lower absolute concentration of the Fgf ligand [121]. Even in the absence of a functional FgfR, Fgf can still transiently activate ERK1/2 signaling, using Sdc4 as its receptor and activator of intracellular signaling [106]. Given this context, and the knowledge that *sdc4* expression is strongest in the most trailing cells of the PLLP that are furthest from the population of Fgf-producing cells in the leading domain, perhaps Sdc4 helps sustain neuromast maturation in this area where Fgf ligands, secreted in response to Wnt signaling in leading cells, are less available.

Fgf signaling has three defined functions within the migrating PLLP. First, Fgf organizes cells into protoneuromasts, through the epithelialization of cells and the organization of those cells into neuromasts [9, 10]. Second, within each protoneuromast, Fgf signaling initiates center-biased *atoh1a* expression which specifies that cell to become the sensory hair cell progenitor [9, 27]. Lastly, Fgf ligands act as migrational cues to trailing cells; while the leading cells guide directional PLLP migration via chemokine signaling, trailing cells are induced to migrate and follow the leading cells by Fgf signals [26]. Our

results demonstrate that Sdc4 regulates at least two of these Fgf-mediated processes; namely, protoneuromast formation and cell migration. The PLLP in *sdc4* morphants contains fewer protoneuromasts, while both morphants and Fgf-inhibited mutants all display slower rates of PLLP migration.

Our conclusion that Sdc4 supports cell migration is consistent with previous findings that Sdc4 is involved in the regulation of directional migration of neural crest cells [109]. Although we conclude that Sdc4 supports PLLP migration via Fgf signaling, it is worth noting that Sdc4 also has a documented role in chemokine signaling, which is also critical to PLLP migration. Sdc4 is a binding partner for both Cxcl12a and Cxcr4, critical to some downstream signaling of Cxcr4 [87, 88]. While it is theoretically possible the Sdc4 and Cxcr4 interact in the PLLP to mediate migration, this seems unlikely given their respective expression domains. *Cxcr4b* is expressed in the leading two thirds of the PLLP [23], while the strongest *sdc4* expression is in the most trailing cells. Although their domains of expression may overlap, the somewhat disparate expression patterns of *cxcr4b* and *sdc4* suggest that Sdc4 is not a key co-receptor for Cxcl12a in this system. Given the expression of *sdc3* throughout the PLLP, it is possible that Sdc3 interacts with the chemokine signaling system. However, our results suggest that Sdc3 only plays a role in migration in the absence of Sdc4.

We conclude that Sdc4 promotes Fgf signaling in the formation of protoneuromasts, but we have not explored any possible functions of Sdc4 in mature neuromasts. We know that *sdc4* is strongly expressed in deposited neuromasts, even many hours after deposition. The neuromasts deposited in *sdc4* morphants appear to be stable, when observed in time-lapse movies (Supplementary Movie 1), but perhaps the neuromasts

in morphants or mutants experience defects in the longer term that we have not comprehensively analyzed. One avenue worth exploring is the differentiation of the central cell into sensory hair cells. The central cell becomes a new source of Fgf10a, activated by Atoh1a, which then binds to FgfR1 on neighboring peripheral cells and helps to ensure their fate as support cells [27]. If Sdc4 helps mediate this interaction in maturing neuromasts, then weak Fgf signaling in peripheral cells might push would-be support cells towards a sensory hair cell fate. It would be of interest to examine the neuromasts of morphants and/or mutants to see if they have a normal number of hair cells in future studies.

Another unexplored line of inquiry is the regeneration of hair cells. Lateral line neuromasts are fully capable of regenerating hair cells even if all existing hair cells die (reviewed in [122]). While Notch and Wnt signaling typically work together to organize the regeneration of hair cells in the PLL, targets of Fgf signaling are downregulated in the neuromast immediately following hair cell death [123]. We also know that Fgf signaling is critical to hair cell specification during development [27] and there is some evidence that Fgfs to have a functional role in hair cell regeneration in the avian ear [124]. A similar hypothesis has been proposed for the lateral line, positing that Fgf is involved in the regeneration of lateral line hair cells [122, 125], but whether Fgf signaling actually does assist Notch and Wnt in this process is still unknown. If Fgf is indeed involved in hair cell regeneration, then this would also implicate Sdc4. One preliminary experiment could be to subject *sdc4* mutants to stimuli that would promote hair cell apoptosis and assess if they regenerate the proper number of hair cells in the same time frame as wild-type embryos.

Our study illustrates how one HSPG core protein, Sdc4, is regulated by signaling networks within the PLLP, and how it, in turn, influences lateral line development through

its own regulation of those signaling networks. Repressed by both Wnt and Fgf signaling in the leading and middle cells of the primordium, Sdc4 is present in the most trailing cells, where it promotes Fgf signaling and the downstream processes of cell migration and protoneuromast maturation. These findings contribute to our understanding of how the PLL develops, as well as our broader knowledge of how HSPGs regulate intercellular signaling.

2.4 Appendix

Three movies of PLLP migration made by time-lapse imaging are referenced in this chapter. The full-length movies, the titles of which are listed below, are available in the supplemental files for this dissertation.

1) Supplemental Movie 1 – WT and Sdc4MO PLLP migration.avi
2) Supplemental Movie 2 – WT and Sdc4 mutant with 1ng Fgf10MO.avi
3) Supplemental Movie 3 – WT and Sdc4 mutant with 2ng Sdc3MO.avi

Chapter 3: 3-*O*-sulfated heparan sulfate supports Fgf signaling in the zebrafish lateral line

3.1 Introduction

The structure of HS chains is highly variable because they are decorated with a wide assortment of modifications. The degree to which a chain is modified, and the pattern of those modifications, is thought to determine the specificity of any given HSPG, allowing them to bind specific targets. Thus, as a group, HSPGs are capable of binding to many different types of signaling ligands and cell surface proteins, while individual HSPGs can have very specific targets and functions. While the previous chapter examined the role of one type of HSPG core protein and its impact on PLL development, now we focus in on 3-*O*-sulfation, a unique type of modification made to HSPGs. Recent research into signaling regulation within the PLLP demonstrates that, taken as a whole, the sulfation modifications made to HSPGs are critical to Fgf signaling and protoneuromast formation [39], but we wanted to investigate the specific role(s) of 3-*O*-sulfation. This modification has been shown to promote Fgf signaling during development [90] and two of the enzymes that generate this modification are specifically expressed within the PLLP [62].

After the core HSPG protein is synthesized, it is transported to the Golgi apparatus, where a series of enzymes build the HS chains onto the core protein and modify them in a step-wise manner. Briefly, a tetrasaccharide linker is attached to specific serine residues in the core protein, glycosyltransferases attach alternating glucosamine and glucuronic acid subunits, and then certain subunits are epimerized and/or sulfated. The last step in this process is 3-*O*-sulfation of some glucosamine subunits by heparan sulfate 3-*O*-sulfotransferases (Hs3sts).

Rarity and types of 3-*O*-sulfation

Of all the modifications made to the HSGAG chain, 3-*O*-sulfation is the rarest, although its prevalence is understudied and varies based on the source of HS. In bovine aortic endothelial cells, 1% of disaccharides are 3-*O*-sulfated [126]. The level of 3-*O*-sulfated disaccharides rises to 5% in mouse Reichert's basement membrane cells, but the same study showed that basement membrane cells isolated from Engelbreth-Holm-Swarm tumors had 0% 3-*O*-sulfation [127]. HS in human follicular fluid contain 6% 3-*O*-sulfated glucosamine residues [128]. In general, 3-*O*-sulfation is believed to account for less than 1% of sulfation events on HS [60, 61]. And yet, vertebrates have more homologous genes for Hs3st than for any other enzyme in the HSGAG biosynthesis pathway. The zebrafish genome contains eight Hs3st genes and each one has a unique expression pattern and set of binding partners, suggesting regulatory and functional divergence [62].

Although all eight Hs3st isoforms add a 3-*O*-sulfate to glucosamine residues, these modifications come in two different flavors. The first subgroup of isoforms (Hs3st1-like), which includes Hs3st1 and Hs3st1l1, generates 'AT-type' 3-*O*-sulfation, so-called due to the ability of antithrombin to bind to this type of modification [129]. These enzymes are intraluminal and lack the typical transmembrane domain of other HSGAG synthesis enzymes. AT-type sulfation generally occurs on HexA-GlcNS or HexA-GlcNS6S residues that lack 2-*O*-sulfation [130, 131]. The second subgroup (Hs3st3-like isoforms), which includes Hs3st2, Hs3st3b1a, Hs3st3b1b, Hs3st3l, and Hs3st4, produce 'gD-type' 3-*O*-sulfation, to which the glycoprotein gD of type I herpes simplex virus (HSV-1) preferentially binds [132]. Unlike the AT-type subgroup, gD-type Hs3sts are type II transmembrane domains with a short cytoplasmic domain at the N-terminal, a hydrophobic

α helix that crosses the Golgi membrane, a so-called SPLAG domain (enriched in Ser, Pro, Leu, Ala, and Gly residues) that may serve as a flexible connecting arm, and a large C-terminal catalytic domain [133]. This subgroup of Hs3sts is known to target GlcA2S-GlcNS, IdoA2S-GlcNS, and IdoA2S-$GlcNH_2$ residues [134]. Unique among Hs3sts, Hs3st1l2 is capable of generating both AT- and gD-type binding sites [135]. Two of the Hs3st3-like isoforms, *hs3st3b1a* and *hs3st3b1b*, are specifically expressed in the PLLP [62]. The specific roles of each type of 3-*O*-sulfation are understudied, but Hs3st3-like sulfation has been shown to promote Fgf10 signaling in epithelial progenitor cells of the mouse fetal salivary gland [90].

Specific roles for 3-*O*-sulfation

The modifications made to the GAG chain are frequently essential to the functional roles of HSPGs. Most ligands bind to highly sulfated regions, or at the borders between modified and unmodified stretches of the GAG chain [136]. Some ligands recognize certain structural motifs as their specific binding sites and therefore require a specific pattern of sulfation to bind HS. In 3T3 fibroblasts, three different Fgf ligands were shown to have distinct sulfation requirements in order to bind HS and promote downstream activity [137]. Fgf2 required 2-*O*-sulfation, Fgf1 required both 2- and 6-*O*-sulfation, and Fgf4 required unsulfated GAG sequences. Another study showed that N-sulfation and, to a lesser extent, *O*-sulfation, were critical for formation of the ternary complex between HS, Fgf1, and FgfR1 [138].

Although many proteins have been identified as HSPG binding partners, few studies have specifically examined the effect of 3-*O*-sulfation on binding. But despite their relative rarity, 3-*O*-sulfation sites can also be a critical component of a ligand binding site

on HS. As previously mentioned, antithrombin and gD preferentially bind to certain 3-*O*-sulfated sites. Antithrombin is an anticoagulant whose catalytic activity is greatly enhanced when bound to HS. It was the first binding partner to be identified for 3-*O*-HS, when 3-*O*-sulfate was identified as a critical component of the antithrombin-binding sequence on HS [139, 140]. During HSV-1 infection, gD-type 3-*O*-sulfation is critical to viral entry into target cells. It has been shown that gD selectively binds to Hs3st3b1a-modified HS, thereby facilitating virion fusion with the cell and promoting HSV-1 infection [141].

In addition to antithrombin and gD, several other ligands also show specificity for 3-*O*-sulfated HS and, in some cases, these ligands have been shown to have a preference for AT-type or gD-type sites. In epithelial KIT+ progenitor cells isolated from mouse fetal salivary glands, FgfR2b preferentially interacts with gD-type 3-*O*-sulfation, and Hs3st3-modified HS enhances formation of the ternary complex between HS, Fgf10, and FgfR2b [90]. Clearance of circulating HS is mediated by liver sinusoidal endothelial cells by stabilin. In cell culture, cells expressing stabilin take up AT-type Hs3st1-modified HS more efficiently than non-3-*O*-sulfated HS, and this uptake is inhibited in the presence of antithrombin [142]. Cylophilin B binds to cell-surface HS on peripheral blood T lymphocytes and triggers migration and adhesion of these cells. This binding interaction is lost, as is downstream activation of ERK1/2, when gD-type 3-*O*-sulfation is downregulated by siRNA knockdown of human *hs3st3b* [143]. Although a specific binding partner hasn't been identified, two Hs3sts regulate left-right patterning by Kupffer's vesicle in zebrafish. AT-type Hs3st1l2 regulates cilia length via Fgf signaling, while gD-type Hs3st3l functions in cilia motility by activating Kinesin 3b expression and dynein assembly. Morpholino knockdown of either one disrupts proper patterning [144]. Within the PLLP, two gD-type

3-*O*-sulfotransferases, *hs3st3b1a* and *hs3st3b1b*, are very specifically expressed [62]. Given that HSPGs frequently play a role in signaling pathways that are critical to PLLP patterning and migration, and that gD-type 3-*O*-sulfation can be critical for ligand binding, Hs3st3b1a and Hs3st3b1b are a particular focus of this chapter.

In this study, we focus on the role of Hs3st3b1a and Hs3st3b1b in the PLLP. We find that *hs3st3b1a* and *hs3st3b1b* expression is activated in the leading zone by Wnt signaling. However, despite their presence in leading cells, these two enzymes facilitate Fgf signaling, which is active in the trailing domain. Loss of Hs3st3s in morphants results in decreased *pea3* expression, fewer forming protoneuromasts, and fewer deposited neuromasts. Double *hs3st3b1a*/*hs3st3b1b* mutants generated using the CRISPR/Cas9 system show similar defects, with fewer deposited neuromasts. We posit that Hs3st3s, present in the same cells that produce Fgf3 and Fgf10, regulate the delivery of Fgf ligands to trailing cells, where they activate their receptor.

3.2 Results

Wnt signaling activates expression of two Hs3st3 enzymes in the leading domain.

Previous research showed expression of both *hs3st3b1a* and *hs3st3b1b* in the PLLP [62]. To more specifically define the expression domains of these two genes, and how they change over time, we performed *in situ* hybridization over an 18-hour time course during the period of PLLP migration. Expression of both *hs3st3b1a* and *hs3st3b1b* is polarized from the start, restricted to the leading domain at 22hpf, just before PLLP migration begins (Figure 3.2.1H and O). At this stage of PLLP development, Wnt activity is still quite broad, as indicated by the expression of *lef1*, a marker of Wnt activity (Figure 3.2.1A). Although

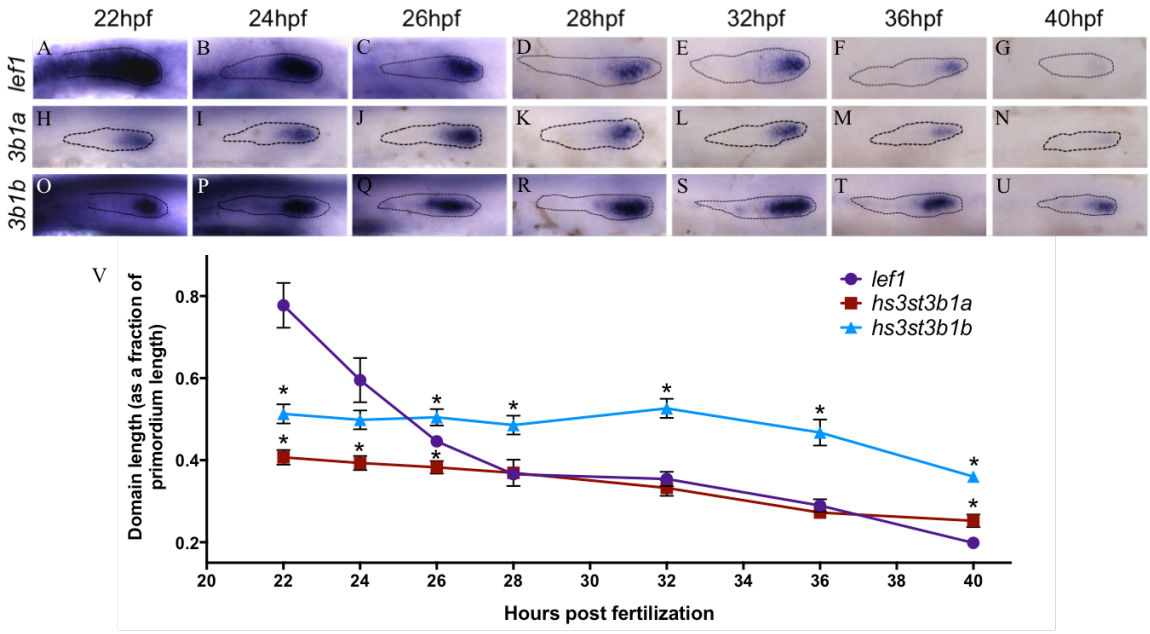

Figure 3.2.1: Hs3st3b1a and hs3st3b1b are expressed in the leading domain. (A-G) *Lef1* expression, while initially broad, recedes over time and becomes progressively more restricted to leading cells (22hpf n=12, 24hpf n=12, 26hpf n=12, 28hpf n=10, 32hpf n=10, 36hpf n=10, 40hpf n=9). (H-N) Polarized from the start of expression, *hs3st3b1a* expression also recedes during the course of migration (22hpf n=20, 24hpf n=15, 26hpf n=20, 28hpf n=11, 32hpf n=16, 36hpf n=19, 40hpf n=17). (O-U) Expression of *hs3st3b1b* is polarized and becomes more restricted to leading cells over time, but more slowly than *lef1* or *hs3st3b1a* (22hpf n=19, 24hpf n=17, 26hpf n=19, 28hpf n=20, 32hpf n=19, 36hpf n=18, 40hpf n=20). (V) Quantification of expression domain size, as a fraction of primordium length, for *lef1*, *hs3st3b1a*, and *hs3st3b1b* throughout an 18-hour time course. *The length of the expression domain is significantly different than the length of the *lef1*expression domain, when $p < 0.05$. Plot points represent mean ± SEM.

Wnt activity does become polarized and *lef1* expression becomes restricted to the leading domain, this process has not completed by 22hpf. Thus, the polarized expression of these two 3-*O*-sulfotransferases precedes the visible polarization of *lef1* expression. As time and PLLP migration progress, the expression domains of *lef1*, *hs3st3b1a*, and *hs3st3b1b* all recede, becoming more and more restricted to the leading cells (Figure 3.2.1A-U). *Lef1* expression recedes most quickly, while the two sulfotransferases persist until late in migration, and *hs3st3b1b* persists the longest (Figure 3.2.1.V).

Due to the fact that *hs3st3b1a* and *hs3st3b1b* are expressed in the leading domain, we hypothesized that they may be regulated by Wnt signaling. To elucidate which signaling networks regulates expression of these two enzymes, we treated embryos with a panel of

chemical inhibitors and performed *in situ* hybridization for both *hs3st3*s. These experiments were performed simultaneously with *in situ* hybridization for *lef1* and *pea3*, the expression of which demonstrates the efficacy of these inhibitors (Figure 3.2.2K-Q). The chemical inhibitor BIO prevents destruction of β-catenin through inhibition of GSK-3, allowing the buildup of β-catenin and resultant ectopic activation of Wnt signaling, while a different inhibitor, IWR, stabilizes this destruction complex through inhibition of Axin, effectively inhibiting Wnt signaling. Treatment with BIO increases the intensity of both *hs3st3*s, whereas treatment with IWR, a Wnt inhibitor, suppresses expression of both *hs3st3*s (Figure 3.2.2A-C, F-H). SU5402 is an Fgf inhibitor that also causes a subsequent increase in Wnt signaling. Fgf normally suppresses Wnt signaling, and so the absence of Fgf activity in SU5402-treated embryos allows for the expansion of Wnt signaling. Treatment with SU5402 increases expression of *hs3st3b1a* while actually decreasing the expression level of *hs3st3b1b*, suggesting differential roles for Fgf signaling in the regulation of these two genes (Figure 3.2.2A, D, F, and I). Because ectopic activation of Wnt induced by BIO also causes the expansion of Wnt-activated expression of *fgf3* and *fgf10*, simultaneous treatment with BIO and SU5402 more thoroughly suppresses Fgf activity and ectopically activates Wnt more than either treatment alone. This double inhibitor treatment causes an increase in the expression of both *hs3st3b1a* and *hs3st3b1b* (Figure3.2.2A, E, F, and J). These results indicate that Wnt signaling positively regulates expression of *hs3st3b1a* and *hs3st3b1b*. However, the role of Fgf signaling is slightly more complex. Expression of *hs3st3b1b* under BIO treatment is expanded, and although it does expand under BIO+SU5402 treatment, the expansion is not quite so dramatic. Because Wnt signaling initiates transcription of *fgf3* and *fgf10*, in addition to upregulating Wnt activity,

Fgf activity also increases. Thus, the difference in *hs3st3b1b* expression under these two treatment conditions, plus the decrease in expression with SU5402 alone, suggests that Fgf and Wnt signaling are co-activators of *hs3st3b1b*. Meanwhile, similar expansions of *hs3st3b1a* occur under BIO, SU5402, and BIO+SU5402 treatments, indicating that *hs3st3b1a* only requires Wnt signaling for activation.

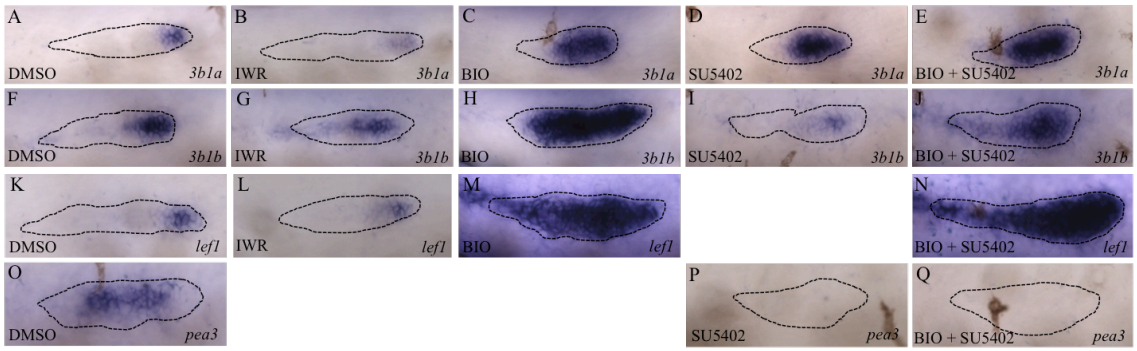

Figure 3.2.2: Wnt activates expression of *hs3st3b1a* and *hs3st3b1b*. (A-E) *Hs3st3b1a* expression in DMSO, IWR, BIO, SU5402, and combined BIO+SU5402 treatment conditions (DMSO *n*=18, IWR *n*=17, BIO *n*=21, SU5402 *n*=23, BIO+SU5402 *n*=20). (F-J) *Hs3st3b1b* expression in DMSO, IWR, BIO, SU5402, and combined BIO+SU5402 treatment conditions (DMSO *n*=19, IWR *n*=21, BIO *n*=16, SU5402 *n*=20, BIO+SU5402 *n*=18). (K-N) *Lef1* expression in DMSO, IWR, BIO, and combined BIO+SU5402 treatment conditions (DMSO *n*=14, IWR *n*=18, BIO *n*=17, BIO+SU5402 *n*=17). (O-Q) *Pea3* expression in DMSO, SU5402, and combined BIO+SU5402 treatment conditions (DMSO *n*=17, SU5402 *n*=11, BIO+SU5402 *n*=10).

Although Wnt signaling activates expression of both of these 3-*O*-sulfotransferases, their expression does not precisely mirror that of *lef1*, a classic marker of Wnt activity. Unlike Lef1, the expression of Hs3st3s is polarized from the start, and the rate at which they recede is different. This suggests that other factors regulate expression of *hs3st3b1a* and *hs3st3b1b*. We have already established that Fgf signaling is likely a co-activator of *hs3st3b1b*, but perhaps there is some other co-activator that regulates expression of one or both of these genes. It is also possible that *hs3st3* genes and *lef1* have differential sensitivity to Wnt activation and that *hs3st3*s require a very high level of Wnt activity which is only present in the leading domain. Alternatively, there may be a repressor that negatively regulates expression of *hs3st3*s and prevents their expression from the trailing domain.

Even when embryos are treated with BIO or BIO+SU5402, expression of *hs3st3b1a* and *hs3st3b1b* is excluded from the most trailing cells of the primordium, despite the fact that *lef1* expression and Wnt activity has expanded throughout the PLLP and even into the trail of depositing cells behind the PLLP. Fgf signaling is prominent in the trailing domain and would seem to be an obvious candidate for the repressor role, but given our results thus far, this signaling network activates *hs3st3b1b* and has no obvious role in the regulation of *hs3st3b1a*.

Knockdown of *hs3st3*s results in fewer neuromasts.

In order to determine the role of Hs3st3 activity in the PLLP, we used morpholinos to knock down *hs3st3* activity. We knocked down *hs3st3b1a* and *hs3st3b1b* individually and simultaneously, and measured the number of neuromasts, as well as the spacing between pairs of neuromasts (Figure 3.2.3A-F). Morphants typically have two fewer neuromasts than their wild-type siblings; *hs3st3b1a* morphants and *hs3st3b1a*/*hs3st3b1b* double morphants have two fewer neuromasts, while *hs3st3b1b* morphants have one fewer neuromast than wild-type embryos. *Hs3st3b1a* morphants and *hs3st3b1a*/*hs3st3b1b* double morphants also have increased spacing between most pairs of neuromasts, while spacing changes in *hs3st3b1b* morphants is subtler. Two morpholinos, both splice-blocking and translation-blocking, were used against the *hs3st3* homologs and all resulted in similar phenotypes. Given that double morphants strongly resemble single *hs3st3b1a* morphants, and *hs3st3b1b* had a less severe phenotype, in future analyses, we focused on *hs3st3b1a* single morphants. At high dosages, morpholinos can have toxic effects, so the use of a

single *hs3st3* morpholino was intended to decrease these toxic and off-target effects. A more detailed analysis of *hs3st3b1a* morphants can be found in Figure 3.2.4. Of particular interest is that *hs3st3b1a* morphants have no change in migration speed (Figure 3.2.4F and Supplementary Movie 4). More complete inhibition of HSPG sulfation, through treatment with $NaClO_3$, results in slowing and eventual stalling of PLLP migration, as well as the formation of ectopic filopodia, demonstrating that sulfation is generally critical to HSPG function in the PLLP [39]. It seems that when just 3-*O*-sulfation is inhibited, through morpholino-mediated knockdown of the 3-*O*-sulfotransferases, PLLP migration is not

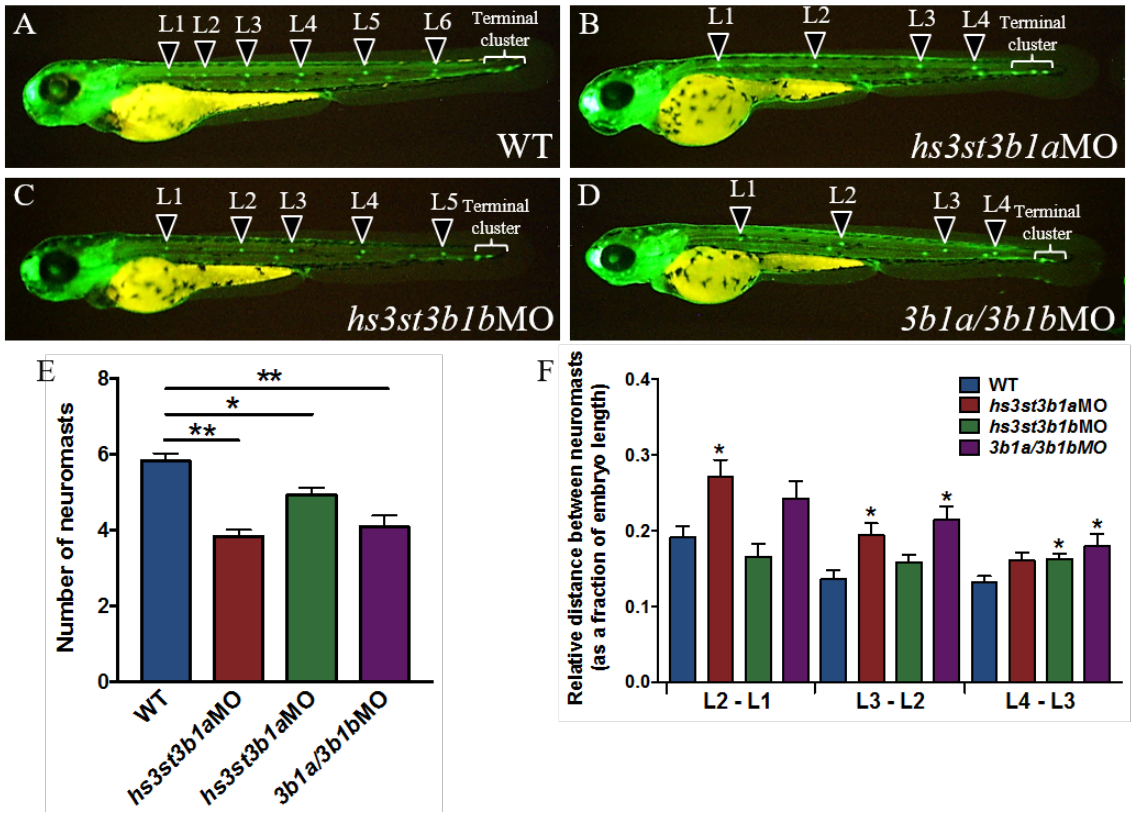

Figure 3.2.3: *Hs3st3* morphants have fewer deposited neuromasts. (A) WT embryos typically have six neuromasts, as well as a terminal cluster of neuromasts at the tip of the tail (n=20). (B) *Hs3st3b1a* morphants have four neuromasts deposited along the trunk (n=20). (C) *Hs3st3b1b* morphants have about five trunk neuromasts (n=20). (D) Double *hs3st3b1a*/*hs3st3b1b* morphants have four neuromasts (n=20). (E) All *hs3st3* morphants have fewer neuromasts than WT, but *hs3st3b1a* morphants and *hs3st3b1a*/*hs3st3b1b* double morphants have the fewest (**$p < 0.0001$, *$p < 0.01$). (F) *Hs3st3b1a* morphants and *hs3st3b1a*/*hs3st3b1b* double morphants have increased spacing between pairs of neuromasts, while *hs3st3b1b* morphants only have increased spacing between the last pair of neuromasts (*$p < 0.05$). Bars represent mean ± SEM.

impacted. The more limited phenotype we see in morphants suggests that this rare type of HSPG sulfation has a much more modest role in regulating PLLP signaling.

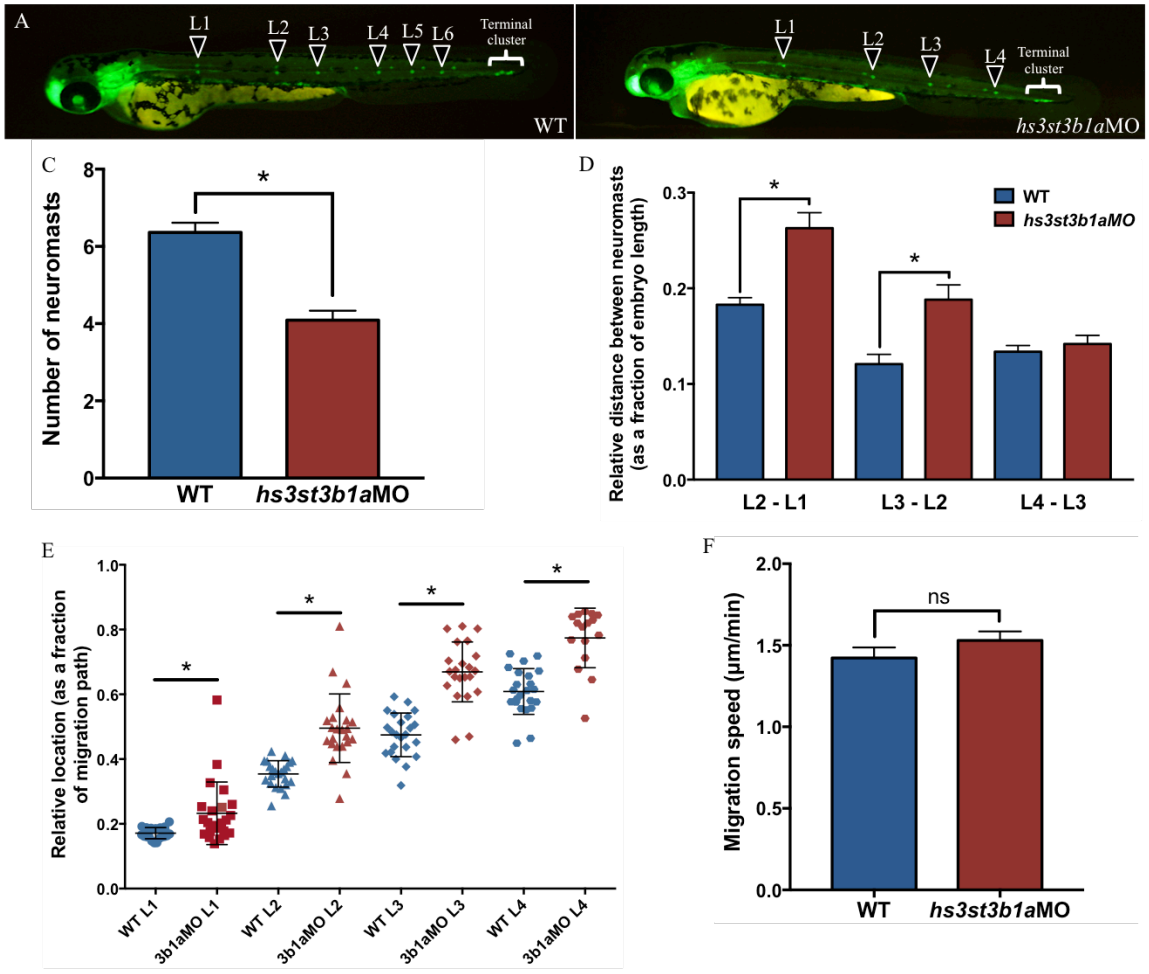

Figure 3.2.4: *Hs3st3b1a* morphants have fewer neuromasts and their deposition appears to be delayed. (A-C) Morpholino-knockdown of *hs3st3b1a* causes a decrease in the number of deposited neuromasts (WT *n*=22, *hs3st3b1a*MO *n*=22). (D,E) Due to increased spacing between pairs of neuromasts, each neuromast is deposited significantly later along the path of migration, compared to WT. (F) *Hs3st3b1a* morphants have a normal speed of PLLP migration (WT *n*=3, *hs3st3b1a*MO=8). *$p < 0.01$. Bars represent mean ± SEM.

Increased spacing between neuromasts and fewer deposited neuromasts in *hs3st3b1a* morphants suggested that protoneuromast formation may be compromised in morphants. To test this, we looked to see if morphants have fewer protoneuromasts by analyzing time-lapse movies. Time-lapse frames were analyzed for protoneuromast number at seven intervals between 27hpf and 33hpf. Wild-type primordia generally had 3-4 protoneuromasts, while *hs3st3b1a* morphants tended to have 2-3 protoneuromasts

(Figure 3.2.5A-C). Although morphant primordia are shorter than wild-type primordia, they still had proportionally fewer protoneuromasts when PLLP length was taken into account. Additionally, the protoneuromasts within morphant primordia were located significantly further from the leading edge of the PLLP, relative to the length of the primordium (Figure 3.2.5D). Taken together, these results indicated the protoneuromast formation is delayed in *hs3st3b1a* morphants. Given that Fgf signaling is responsible for organizing trailing cells into protoneuromasts, the impaired formation of protoneuromasts suggested that Fgf signaling may be compromised in *hs3st3b1a* morphants.

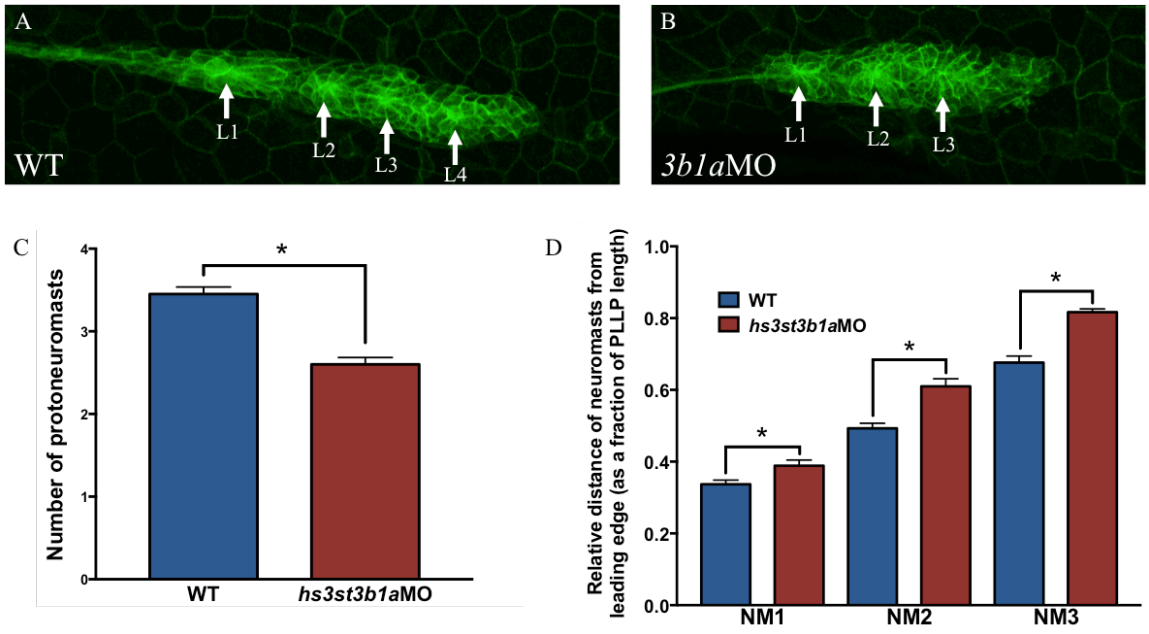

Figure 3.2.5: *Hs3st3b1a* morphants have fewer protoneuromasts. Frames from time-lapse movies were analyzed for neuromast number at seven hourly intervals (27hpf-33hpf). (A-C) WT primordia have 3-4 protoneuromasts, while *hs3st3b1a*MO have only 2-3 protoneuromasts. Images show protoneuromasts in WT and *hs3st3b1a*MO, numbered and marked by arrows. Although *hs3st3b1a*MO primordia are shorter than WT primordia, they still had fewer neuromasts per unit of distance (WT n=42, *hs3st3b1a*MO n=35). (D) Each protoneuromast (generically marked as NM1, NM2, and NM3 because measurements were made over the course of seven hours) is located further from the leading edge of the PLLP in morphants, relative to the length of the primordium. Arrows mark neuromast centers. *$p < 0.01$. Bars represent mean ± SEM.

Knockdown of *hs3st3b1a* decreases the size of the Fgf signaling domain.

In order to determine the impact of *hs3st3b1a* knockdown on PLLP signaling, we performed *in situ* hybridization for *lef1* and *pea3* in *hs2st3b1a* morphants at 31hpf. *Lef1* expression appears to be relatively normal in morphants, indicating that 3-*O*-sulfation has little role in Wnt signaling (Figure 3.2.6A and B). Meanwhile, the *pea3* expression domain is significantly shorter in length in morphants (Figure 3.2.6C-E), signifying that the Fgf signaling domain is decreased in size. The Fgf signaling domain is also located further from the leading edge of the PLLP (Figure 3.2.6F). This impairment in Fgf signaling is therefore the most likely cause for the delay in protoneuromast formation.

The first Fgf signaling center (as indicated by *pea3* expression) begins to establish at the most trailing end of the PLLP between 20 and 22hpf. Migration typically begins after 2-3 protoneuromasts associated with Fgf signaling centers have begun to form and the Wnt system (defined by the domain of *lef1* expression) becomes restricted to a smaller leading zone. As time continues and PLLP migration proceeds, subsequent Fgf signaling centers form, moving progressively closer to the leading domain. As Fgf signaling suppresses Wnt signaling, this process also restricts *lef1* expression to the leading domain more and more. Although primordia migrate normally in *hs3st3b1a* morphants, the system fails to expand the Fgf signaling domain to the same extent as is seen in wild-type primordia. Thus, the distance of the *pea3* expression domain and forming protoneuromasts from the leading edge in *hs3st3b1a* morphants suggests that the establishment of Fgf signaling is not as robust in these embryos.

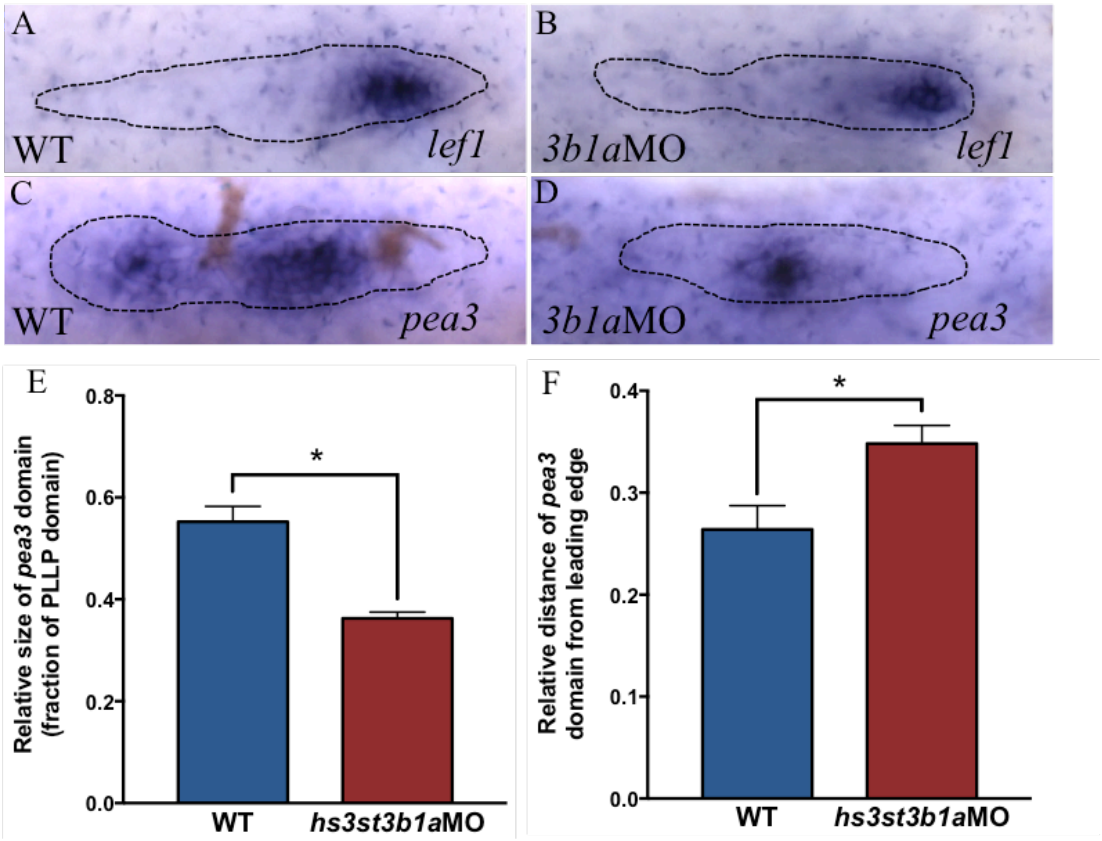

Figure 3.2.6: *Hs3st3b1a* morphants have decreased Fgf signaling. (A,B) *In situ* hybridization for *lef1* marks the domain of Wnt activity. The *lef1* expression domain is unchanged in *hs3st3b1a* morphants (WT *n*=15, *hs3st3b1a*MO *n*=12). (C,D) *Pea3* expression marks the domain of active Fgf signaling (WT *n*=13, *hs3st3b1a*MO *n*=12). (E) The length of the *pea3* domain, normalized to the length of the PLLP, is significantly shorter in *hs3st3b1a* morphants. (F) The *pea3* domain is located significantly further from the leading edge in *hs3st3b1a* morphants. *$p < 0.01$. Bars represent mean ± SEM.

The PLLP is a dynamic system, and so a static picture of the system at any given time point can be misleading as to the reality of how it functions. To more thoroughly explore establishment of Fgf signaling in *hs3st3b1a* morphants, we performed *in situ* hybridization for *pea3* at four time points over 12 hours during migration of the PLLP. In wild-type primordia, *pea3* expression is fairly consistent, demonstrating that the Fgf system is fairly steady between 24 and 36hpf (Figure 3.2.7A-D). However, although *pea3* expression is clear in *hs3st3b1a* morphants at 24hpf, *pea3* expression wanes over time and by the latter two time points, its domain is much shorter in length than in wild-type embryos (Figure 3.2.7E-I). Furthermore, despite having a normal-sized *pea3* domain in the early

time points, at every time point, that domain is located further from the leading edge than in wild-type embryos (Figure 3.2.7J). Thus, although the *pea3* expression domain in *hs3st3b1a* morphants seems to be normal in size early in PLLP migration, it is never as close to the leading edge as is normal and its size cannot be sustained for the duration of the PLLP's journey. These results support our contention that the strength of the Fgf signaling system depends upon 3-*O*-sulfated HSPGs.

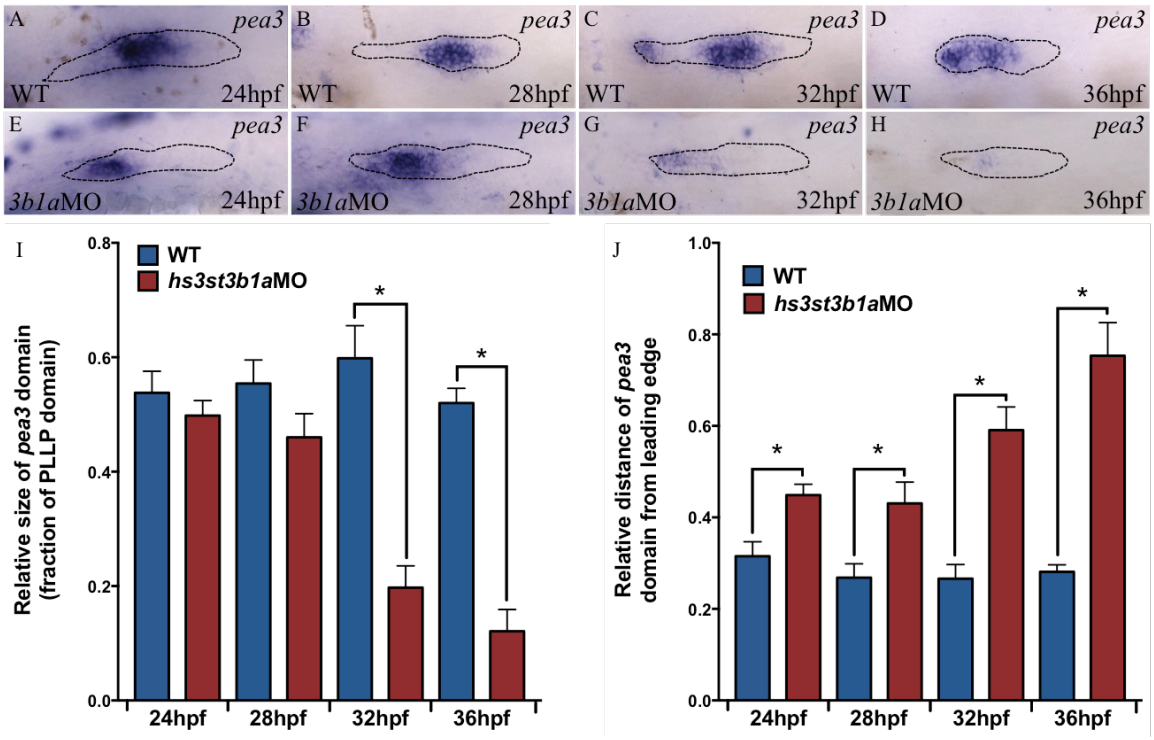

Figure 3.2.7: *Hs3st3b1a* morphants have decreased Fgf signaling. (A,B,C,D) *In situ* hybridization for *pea3* in WT embryos at 24, 28, 32, and 36hpf (24hpf *n*=12, 28hpf *n*=11, 32hpf *n*=8, 36hpf *n*=13). (E,F,G,H) *In situ* hybridization for *pea3* in *hs3st3b1a* morphants at 24, 28, 32, and 36hpf (24hpf *n*=10, 28hpf *n*=14, 32hpf *n*=17, 36hpf *n*=10). (I) The length of the *pea3* domain, normalized to the length of the PLLP, at 24, 28, 32, and 36hpf. The domain is significantly smaller at 32 and 36hpf. (J) The distance of the *pea3* domain from the leading edge, normalized to the length of the PLLP, at 24, 28, 32, and 36hpf. The domain is significantly further from the leading edge at all time points. *$p < 0.05$. Bars represent mean ± SEM.

Overexpression of *hs3st3*s causes dorsalization of zebrafish embryos.

Having established that knockdown of *hs3st3b1a* impairs Fgf signaling and Fgf-mediated protoneuromast formation, we wanted to know what impact overexpression of

hs3st3b1a and *hs3st3b1b* would have on development. Embryos were injected with either *hs3st3b1a* or *hs3st3b1b* mRNA individually, or co-injected with both mRNAs. Ectopic expression of *hs3st3*s causes dorsalization in all three cases (Figure 3.2.8A-D). The severity of dorsalization and overall number of dorsalized embryos is dose-dependent, increasing with the concentration of mRNA injected. Co-injection of both *hs3st3*s results in a dorsalized phenotype in nearly 100% of injected embryos.

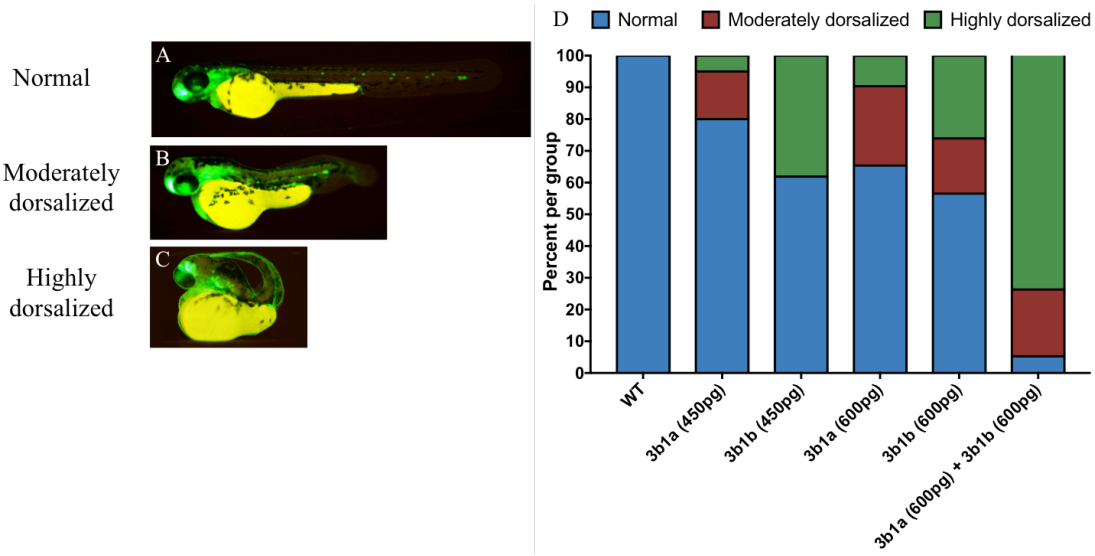

Figure 3.2.8: Overexpression of *hs3st3* mRNA causes dorsalization. (A-C) Examples of normal, moderately dorsalized, and highly dorsalized embryos. (D) Graph shows the degree of dorsalization in injected embryos. Embryos were injected with either 450pg or 600pg of each *hs3st3* mRNA, or co-injected with both *hs3st3* mRNAs (WT *n*=23, 3b1a(450pg) *n*=20, 3b1b(450pg) *n*=21, 3b1a(600pg) *n*=52, 3b1b(600pg) *n*=23, 3b1a(600pg)+3b1b(600pg) *n*=19).

During dorsoventral patterning, BMP signaling promotes the development of ventral structures,[110] while Fgf inhibits BMP activity on the dorsal side of the embryo, thereby allowing for the development of dorsal structures [111]. An excess of BMP signaling favors development of ventral structures, while an excess of Fgf signaling allows for the development of dorsal structures at the expense of ventral structures. Thus, the fact that *hs3st3* mRNA induces dorsalization indicates a role for 3-*O*-sulfation in positively regulating Fgf signaling.

Both our morpholino-knockdown and mRNA overexpression experiments indicate a role for Hs3st3s in Fgf signaling, which would be consistent with previously published research on the role of 3-*O*-sulfation. However, morpholinos are known to have a number of off-target effects that can create false phenotypes. This is particularly problematic for the phenotype we observe in *hs3st3b1a* morphants, as we have previously found that reduced *pea3* expression and increased spacing between neuromasts can be the result of off-target effects. Therefore, we sought to confirm our results using mutants. Targeted mutations in the flexible SPLAG domain of *hs3st3b1a* and *hs3st3b1b* were induced using the CRISPR/Cas9 system.

***Hs3st3b1a*/*hs3st3b1b* mutants have fewer neuromasts than wild-types.**

Single mutants in *hs3st3b1a* and *hs3st3b1b* appear to have no abnormal phenotype, exhibiting a normal number of neuromasts. However, *hs3st3b1a*/*hs3st3b1b* double mutants have fewer neuromasts than wild-type embryos (Figure 3.2.9A-C). The decrease in the number of neuromasts is primarily due to the delay in deposition of L2, and a somewhat smaller delay in the deposition of L4 (Figure 3.2.9D). The increased spacing between L1-L2 and L3-L4 causes all subsequent neuromasts to be deposited significantly later along the migration path than they are in wild-type embryos (Figure 3.2.9E). This phenotype reflects the morphant phenotype, where we observe a similar increase in interneuromast spacing and decrease in neuromast number.

The decrease in the number of neuromasts observed in *hs3st* mutants may correlate with compromised Fgf signaling and protoneuromast formation. However, experiments to test this hypothesis are still in progress, as these mutants have a low success rate in producing fertilized eggs.

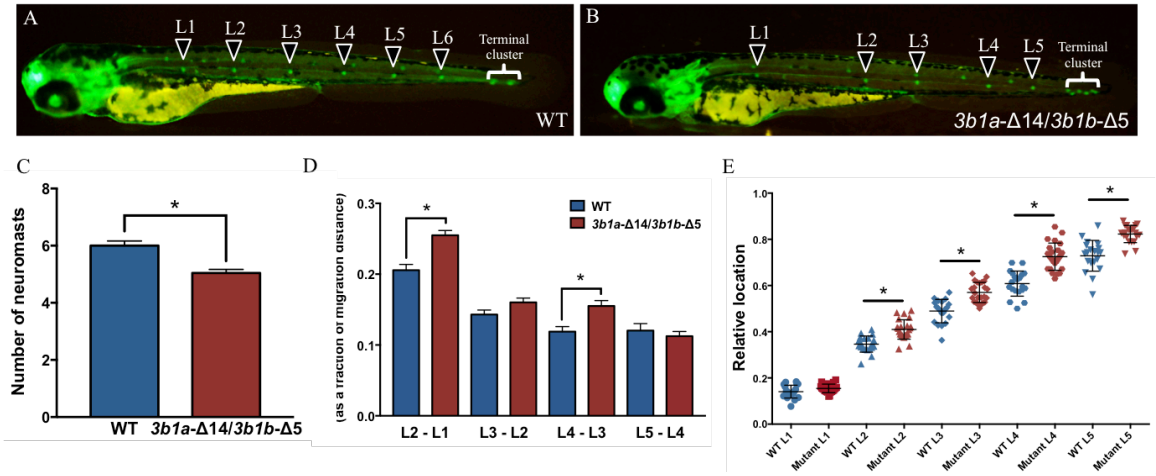

Figure 3.2.9: *Hs3st3b1a*/*hs3st3b1b* double mutants have fewer neuromasts than WT. (A-C) WT embryos typically have 6 neuromasts, while *hs3st3* mutants have five (WT *n*=20, Δ*hs3st3b1a*/Δ*hs3st3b1b* *n*=24). (D) The first pair of neuromasts (L1 and L2) and the third pair (L3 and L4) have spaced further apart from each other in mutants, than the corresponding neuromasts in WT. (E) The increased spacing between some pairs of neuromasts results in a significant delay in the deposition of every neuromast after L1 along the path of migration. **p* < 0.01. Bars represent mean ± SEM.

3.3 Discussion

Morphogenesis of the zebrafish lateral line is critically dependent on a coordinated signaling network controlled by Wnt and Fgf. This system regulates collective cell migration and protoneuromast formation, and disturbances to the network can interfere with one or both of these processes. Thus, Wnt and Fgf signaling must be carefully controlled, but the regulatory mechanisms responsible for coordinating the integration of this network are not fully understood. One signaling regulation mechanism that has not been thoroughly explored is the role of HSPGs. HSPGs are ubiquitously expressed and can regulate a wide variety of distinct signaling pathways, due to their highly variable structure.

Variations in this structure allow HSPGs to specifically target a diverse set of ligands. 3-*O*-sulfation is a particular component of this structure, a rare modification made to the heparan sulfate chain just prior to the completion of biosynthesis. Although this sulfation event is rare, some signaling ligands are known to require 3-*O*-sulfated sites in their HSPG binding interaction. Two of the eight enzymes that perform this type of sulfation in zebrafish are specifically expressed in the PLLP. We began this study with the intent of understanding how these two genes are regulated and the functional significance of 3-*O*-sulfation in lateral line signaling and morphogenesis.

We have shown that these two Hs3st3 enzymes are integrated into the signaling pathways that pattern the PLLP. Our results suggest that Wnt signaling activates both *hs3st3b1a* and *hs3st3b1b* expression, while Fgf signaling is a co-activator for *hs3st3b1b*. The loss of Hs3st3s in morphants and mutants alters neuromast deposition pattern, an Fgf-directed activity, and morphants exhibit decreased Fgf signaling output. Thus, although they are expressed in the leading domain, 3-*O*-sulfated HSPGs regulate the activity of Fgf signaling in the trailing domain.

While a previous study showed tissue-specific expression of Hs3st3s in the PLLP [62], we have further defined the expression of *hs3st3b1a* and *hs3st3b1b*. Expression of both enzymes is polarized to the leading domain from the start of their expression. Their respective domains recede as migration progresses, although *hs3st3b1a* recedes slightly faster than *hs3st3b1b*. This pattern of expression mirrors that of the Wnt target *lef1*, which is also expressed in the leading domain and also becomes progressively more restricted to the leading cells. The similarity between the expression patterns of *lef1* and the *hs3st3*s suggested that transcription of these two genes might be activated by Wnt signaling. Our

results are consistent with this hypothesis, as activation and repression of Wnt signaling correlate with increased and decreased *hs3st3* expression, respectively. Expression of both *hs3st3*s remains excluded from the most trailing cells, even when Wnt induces signaling activity throughout the whole of the PLLP. We thought that Fgf signaling might be responsible for repressing *hs3st3* in trailing cells, and so artificially suppressed Fgf activity. However, our results show that Fgf has no role in regulating *hs3st3b1a*, while Fgf and Wnt are co-activators of *hs3st3b1b*.

To investigate the function of *hs3st3*s, we initially used morpholinos to knock down the function of these genes. These experiments revealed a decrease in the number of protoneuromasts forming within the PLLP, and a subsequent change in the neuromast deposition pattern. As Fgf signaling governs protoneuromast formation, these results indicated a role for 3-*O*-sulfated HSPGs in facilitating Fgf signaling, which is supported by reduced Fgf signaling output in morphants. However, morpholinos have a number of off-target effects, including apoptosis, a phenomenon we did observe in these morphants. We therefore sought to confirm a role for *hs3st3*s in Fgf signaling using mutants generated by CRISPR/Cas9. *Hs3st3b1a*/*Hs3st3b1b* double mutants recapitulate the morphant phenotype of fewer deposited neuromasts, hinting that these 3-*O*-sulfated HSPGs are indeed important for Fgf-mediated protoneuromasts formation. Unfortunately, we have not yet had the chance to further explore any defects in Fgf signaling exhibited by these mutants, as they have extremely low mating success.

Overexpression experiments for *hs3st3b1a* and *hs3st3b1b* resulted in dorsalization of the embryo. Although further experiments are necessary to confirm that this effect is

due to ectopic activation of Fgf signaling, this result is consistent with our model that Hs3st3s support Fgf signaling in the cells of the PLLP.

A handful of ligands have been identified that specifically bind to 3-*O*-sulfated HSPGs. One factor that determines ligand binding is the type of 3-*O*-sulfation, for the eight enzymes that perform this modification fall into two subgroups, each of which preferentially sulfate different substrates, ultimately producing unique 3-*O*-sulfation patterns. The 3-*O*-sulfotransferases that generate Hs3st1-like, or AT-type, activity produce a pattern that binds antithrombin (AT) [140], among other ligands. The other group of 3-*O*-sulfotransferases perform Hs3st3-like, or gD-type, activity, producing a product capable of binding a separate group of ligands, including glycoprotein D (gD), a component of the viral envelope of herpes simplex virus (HSV) [132]. Hs3st3b1a and Hs3st3b1b fall into the latter category. One known function of Hs3st3-like activity is particularly interesting in the framework of our study. In the KIT+ epithelial progenitor cells of mouse fetal salivary glands, 3-*O*-sulfated HSPGs (3-*O*-HS) stabilize the binding of Fgf10 to FgfR2b, and promote Fgf-induced progenitor expansion during development of the salivary glands [90]. In this context, Hs3st3-generated 3-*O*-HS binds FgfR2b, and are involved in a positive feedback loop in which 3-*O*-HS/FgfR2b/Fgf10 signaling enhances the expression of 3-*O*-HS. The loss of 3-*O*-HS reduces Fgf10/FgfR2b-dependent growth, but the introduction of 3-*O*-HS rescues this phenotype. This established function of Hs3st3-type 3-*O*-sulfation is consistent with our hypothesis that the enzymatic activity of Hs3st3b1a and Hs3st3b1b has a downstream impact on Fgf signaling.

Within the migrating PLLP, Fgf has several known functions. First, Fgf is responsible for directing protoneuromast formation by promoting the epithelialization of

cells and inducing the apical constriction that generates rosettes [9, 10]. Second, Fgf signaling initiates center-biased *atoh1a* expression in the protoneuromasts, helping to establish the central cell of each rosette as a sensory hair cell progenitor [9, 27]. Finally, Fgf released by the leading cells acts as a migrational cue for trailing cells, which migrate and follow the leader cells in response to that cue [26]. Our results indicate that Hs3st3s influence the first of these Fgf-mediated processes, assisting in the formation of protoneuromasts. We also find that Hs3st3s do not regulate Fgf-mediated cell migration, as PLLP migration appears to be unchanged in morphants. Perhaps 3-*O*-sulfated HSPGs are only involved in limited functions of Fgf signaling due to the fact that this is just one type of modification on the heparan sulfate chain, and a rare one at that. Hence, we might expect the influence of Hs3st3s on signaling to be subtle, as opposed to the more wide-ranging effects of more common HSPG characteristics.

Since Hs3st3s are not themselves HSPGS, but enzymes involved in the biosynthesis of heparan sulfate chains, there must be some HSPG substrate also synthesized in leading cells on which Hs3st3's perform 3-*O*-sulfation. There are several HSPGs that could fill this substrate role, and future work could identify Hs3st3 target(s) to more completely define how HSPGs regulate PLLP signaling. Two candidates are Sdc3 and Glypican1b, which are both present in leading cells [39].

Despite their presence in the leading cells of the PLLP, our results indicated a role for these enzymes in promoting Fgf signaling, which is typically active in the trailing domain. However, the two Fgf ligands which activate Fgf signaling in those trailing cells, Fgf3 and Fgf10, are actually produced by leading cells and then delivered to trailing cells. This suggests the possibility that 3-*O*-sulfation is somehow involved in the effective

maturation and/or delivery of Fgf signals to trailing cells. Recent work in our lab indicates that some Fgf ligand delivery occurs via filopodia-like structures that extend from leading cells and deposit vesicles which are then taken up by trailing cells. The disparate locations of *hs3st3* expression and Fgf signaling activity suggests that 3-*O*-sulfated HSPGs might be involved in this delivery system. HSPGs can facilitate cargo delivery between cells [145]; In fact, HSV hijacks this cargo delivery system in order to bind and invade target cells, and its mechanism of cell entry requires Hs3st3-modified HS [141]. HSPGs can also transport cargo along filopodia, a process exemplified by a phenomenon known as viral surfing, in which HSV virions exploit the cargo transport mechanism to facilitate infection [146]. It is possible that HSPGs have a parallel mechanism in the PLLP, with Fgf-packed vesicles as the cargo transported along filopodia and received by the trailing cells. If HSPGs do function in the delivery of Fgf signals via filopodia-deposited vesicles, given their expression patterns, it seems likely that Hs3st3b1a and Hs3st3b1b are important for the delivery of the ligand. Further study is required to support this hypothesis; most importantly, cell autonomy experiments must be performed, showing that Hs3st3s are required in Fgf-source cells in order to activate the FgfR and downstream signaling in neighboring cells.

Our study illustrates how one type of HSPG modification, 3-*O*-sulfation, is integrated into the signaling networks of the PLLP. The two enzymes that perform this modification are activated by Wnt signaling in the leading domain, but the HSPGs they sulfate appear to regulate Fgf signaling in more trailing cells, where 3-*O*-sulfated HSPGs regulate protoneuromast formation. These findings contribute to our understanding of how

the PLL develops, and identify a new function for a rare and understudied HSPG modification.

3.4 Appendix

One movie of PLLP migration made by time-lapse imaging is referenced in this chapter. The full-length movie, the title of which is listed below, is available in the supplemental files for this dissertation.

1) Supplemental Movie 4 – WT and 3b1aMO PLLP migration.avi

Chapter 4: Concluding remarks and future directions

The polarized system of Wnt and Fgf signaling in the cells of the migrating primordium governs morphogenesis of the zebrafish lateral line. Wnt maintains a relatively mesenchymal population of cells in the leading domain, while Fgf signaling organizes cells into epithelial rosettes in the trailing domain and induces migration of those trailing cells. The interplay between the Wnt and Fgf systems is a critical determinant of protoneuromast formation, neuromast deposition, and collective cell migration. However, the mechanisms that regulate these two interconnected networks are not fully understood. As HSPGs are widespread regulators of many intercellular signaling pathways, and are almost universally distributed in animal tissues, this class of molecules make ideal candidates for regulation of signaling within the PLLP. I began the work presented in this dissertation knowing that two classes of HSPG-related proteins are specifically expressed within the cells of the PLLP, but their functions had not been identified. The first was Sdc4, a type of HSPG core protein that is embedded in the cell membrane. The second class consisted of two 3-*O*-sulfotransferases, Hs3st3b1a and Hs3st3b1b, that both generate a rare, but sometimes critical, modification on heparan sulfate chains.

The work presented in this dissertation investigated particular functions of HSPGs in the development of the zebrafish lateral line. Previous research established the general importance of HSPGs in Fgf signaling during PLL development [39]. Our research has more specifically defined the functions of Sdc4 and 3-*O*-sulfated HSPGs and their roles in mediating protoneuromasts formation and cell migration via Fgf signaling.

My analysis of the expression patterns of Sdc4 and Hs3st3s revealed that these two proteins occupy distinct domains within the PLLP (Figure 4.1). *Sdc4* is expressed in the

most trailing cells, while *hs3st3*s are expressed in the leading domain. Wnt and Fgf signaling both regulate the expression of these HSPG-related genes. In the case of *sdc4*, Wnt and Fgf signaling both repress its expression, thereby restricting it to the most trailing cells, where these signaling networks are less active or not active at all. Meanwhile, Wnt activates expression of both *hs3st3b1a* and *hs3st3b1b* in leading cells, and Fgf signaling is a co-activator of *hs3st3b1b*.

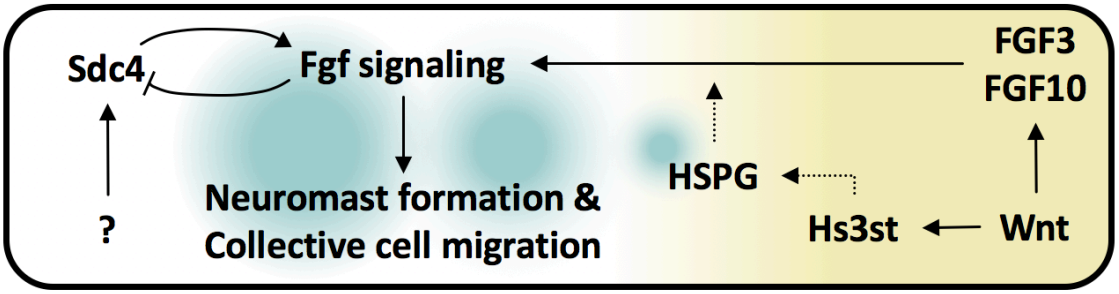

Figure 4.1: Schematic for how Sdc4 and Hs3sts regulate signaling within the primordium. Wnt signaling (yellow) activates expression of two *hs3st* isoforms and two Fgf ligands in the leading domain. These Hs3sts modify HS chains on unidentified HSPG(s). These 3-*O*-sulfated HSPGs may play a role in the delivery of Fgf3 and Fgf10 ligands from leading cells to trailing cells. Meanwhile, in the trailing domain, Fgf signaling (light green) is focused in developing protoneuromasts, promoting protoneuromast formation and collective cell migration. Expression of *sdc4* is promoted by an unknown factor and repressed by both Fgf and Wnt signaling. Sdc4 is involved in reception of the Fgf signal in trailing cells. Sdc4 and Hs3sts are therefore on opposite ends of the Fgf signaling pathway, and promote the downstream Fgf-mediated processes of neuromast formation and collective cell migration.

Although these proteins occupy disparate domains, they have complementary roles in the regulation of Fgf signaling and its downstream functions. Fgf ligands are produced by leading cells, where their transcription is dependent on Wnt activity. Since Wnt also represses FgfR, Fgf ligands establish robust Fgf signaling centers in the trailing domain, where they direct rosettogenesis, sensory hair cell specification, and trailing cell migration. Within this Fgf signaling framework, I have identified specific roles for Sdc4 and Hs3sts. *Hs3st3*s are co-expressed in the leading cells that also produce *fgf3* and *fgf10*, and I hypothesize that they act to ensure delivery of these two ligands to their receptors on

trailing cells. On the trailing cells, the receiving end of Fgf signaling, Sdc4 promotes Fgf signaling in response to those Fgf ligands. Based on the results of experiments utilizing both mutants and morphants for these genes, I find that both Hs3st3 and Sdc4 promote protoneuromast formation, and Sdc4 has an additional role in cell migration. Thus, Wnt-activated Hs3st3s are another way in which the leading cells regulate the Fgf signaling network that patterns the trailing cells, while Sdc4 provides a mechanism by which Fgf signaling can attenuate or facilitate its own function.

The findings presented here are consistent with known functions of Hs3st3-modified HSPGs and Sdc4, as presented in the literature. 3-*O*-sulfated HSPGs have been shown to specifically promote Fgf signaling and its downstream effects. The role of Sdc4 in Fgf signaling is well established, as it can act as both a co-receptor to FgfR and as an independent receptor for Fgf ligands.

Future studies will focus on several aspects that could not be fully explored in the context of this dissertation. One particularly interesting line of study is the role of Sdc4 in deposited neuromasts. Although we identified notable expression of *sdc4* in deposited neuromasts, its function(s) there remain unknown. There are several aspects of hair cell formation and maintenance in which Sdc4 could play a role. If Sdc4 is involved in Fgf signaling in deposited neuromasts, then it may help determine cell fate in the support cells that surround the central hair cells. Fgf signaling in these peripheral cells helps ensure their fate as support cells and prevents them from adopting a hair cell fate [27].

It would also be worthwhile to investigate whether Sdc4 is involved in the regeneration of hair cells. While the hair cells of the zebrafish PLL and the hair cells of the mammalian inner ear are functionally similar, zebrafish hair cells can regenerate and

mammalian hair cells cannot (reviewed in [122]). Notch and Wnt signaling are known to direct the regeneration of PLL hair cells, and there are some studies that suggests Fgf signaling could be involved in this regeneration process as well [27, 122-125]. If Sdc4 regulates any of these three pathways in the neuromasts, it is possible that it is also a regulator of hair cell regeneration.

One final aspect of hair cell development to which Sdc4 may contribute is the planar cell polarity pathway that orients hair cells. The orientation of a hair cell determines which water current direction it is capable of detecting. Mature neuromasts have a number of hair cells at their center, and all of the hair cells within a neuromast will align themselves in parallel but opposing directions, with each pair of hair cells oriented in opposite directions. The orientation of these hair cells is determined by the trajectory of PLLP migration, as hair cells align along the migration axis [147]. Planar cell polarity (PCP) signaling underlies this process of hair cell orientation [148]. PCP signaling is dependent on a group of signaling proteins that included the Wnt receptor Frizzled (Fzd), Fzd's cytosolic target Disheveled (Dvl), and another membrane receptor called Vangl2 (reviewed in [149]). Previous studies have shown that Sdc4 is actually required for PCP signaling in other developmental contexts. During convergent extension in *Xenopus*, Sdc4 binds to Dvl and is required for Fzd-mediated PCP signaling [78]. Furthermore, Sdc4 and Vangl2 interact genetically and regulate neural tube closure via PCP signaling [150]. Perhaps Sdc4 plays a similar role in PCP-directed sensory hair cell orientation.

In the future, we would also like to pursue more direct studies of 3-*O*-sulfated HSPGs and Sdc4 on opposite ends of the delivery mechanism that transports Fgf ligands from leading cells to trailing cells may provide exciting insights into how signals can travel

between cells, outside the traditional mechanism of ligand diffusion. Based on recent studies performed in our lab, we know that leading cells extend long filopodia-like processes towards trailing cells. These processes deposit membrane-bound vesicles that are then taken up by trailing cells, where they are rapidly transported from the basal surface to the apical surface. We hypothesize that these vesicles contain Fgf signaling ligands, and that this is a mechanism by which leading cells signal trailing cells via the Fgf signaling pathway. We also have evidence that HSPGs are involved in this vesicle-delivery system, as the loss of HS chain sulfation (and therefore the crippling of HSPG function) ultimately causes a loss of these filopodia-like processes and the vesicles they deposit. HSPGs are known to facilitate cargo delivery between cells [145], and we posit that 3-*O*-sulfated HSPGs and Sdc4 could be involved in the delivery of these vesicles. Herpes Simplex Virus (HSV) is known to hijack this cargo delivery system in order to bind and invade target cells – and this mechanism of cell infection requires Hs3st3-modified HS and Sdc [141, 151]. HSPGs can also transport cargo along filopodia, a process exemplified by a phenomenon known as viral surfing, in which HSV virions exploit the cargo transport mechanism to facilitate infection [146]. We think that Sdc4 and Hs3st3s may have a parallel function in the PLLP, enabling the transport of Fgf-packed vesicles along PLLP filopodia, deposition of those vesicles, vesicle uptake by trailing cells, and/or response to the cargo contained within those vesicles.

In order to have any impact on signaling, Hs3st3s must perform 3-*O*-sulfation on an HSPG core protein. There are at least five core proteins expressed in the cells of the primordium, but not all are expressed in the leading cells where Hs3st3s are available to modify the HS chains. The most attractive candidates for 3-*O*-sulfation are Gpc1a,

expressed in the very most leading cells, and Sdc3, expressed throughout the primordium [39]. Future studies will specifically confirm which HSPG core proteins are modified by Hs3st3s.

Experiments described in this thesis using mutants, morphants, and gene expression studies have provided us with clues as to the roles of specific HSPGs and HS chain modifications in regulating Wnt and Fgf signaling. I hope this work will help us better understand morphogenesis of the PLL and the more general principles underlying HSPG mediation of intercellular signaling.

Chapter 5: Materials and Methods

5.1 Solutions

Hybridization buffer: 50% Formamide (Ambion), 5x SSC, ph 7.0 (Quality Biological), 500 µg/mL yeast tRNA (Sigma-Aldrich), 50µg/mL Heparin (Sigma-Aldrich), 0.1% Tween 20 (Fisher) in sterile H_2O. Stored at -20°C.

50% Formamide/2x SSCT: 50% Formamide (Ambion), 2x SSC (Quality Biological), 0.1% Tween 20 (Fisher) in sterile H_2O. Stored at RT.

2x SSCT: 2x SSC (Quality Biological), 0.1% Tween 20 (Fisher) in sterile H_2O. Stored at RT.

0.2x SSCT: 0.2x SSC (Quality Biological), 0.1% Tween 20 (Fisher) in sterile H_2O. Stored at RT.

Blocking solution: 1% blocking reagent (Roche) in PBST. Stored at 4°C.

NTMT: 100mM Tris, pH 9.5, 50mM $MgCl_2$ (Quality Biological), 100mM NaCl (Quality Biological), 0.1% Tween 20 (Fisher).

PBST: 1% phosphate buffered saline (PBS, Amresco), 0.001% Tween 20 (Fisher). Stored at RT

Genomic digestion buffer: 10mM Tris, ph 8.0 (Quality Biological), 10mM EDTA (Quality Biological), 200mM NaCl (Quality Biological), 0.5% SDS (Quality Biological), 200µg/mL proteinase K (Abcam).

5.2 Zebrafish

Zebrafish were maintained under standard conditions and staged according to Kimmel *et al*. (1995) [152]. The *tg[cldnb:lynGFP]* transgenic strain was described previously [20].

5.3 CRISPR mutants and genotyping

Mutant lines were generating using the CRISPR/Cas9 system.[114] CRISPR targets were identified using CHOPCHOP (https://chopchop.rc.fas.harvard.edu/), which also designed genotyping primers. gRNA templates were generated as previously described [153]. Briefly, a targeting oligo (T7 promoter, 20-nucleotide target sequence and a 20-nucleotide sequence that overlapped to a generic gRNA template) was annealed with an 80-nucleotide chimeric gRNA core sequence. The annealed oligos were then filled in using PfuUltra II Fusion DNA Polymerase (Agilent) under the following conditions: 98°C for 2 minutes; 50°C for 10 minutes, 72°C for 10 minutes. 2µL of gRNA template was then used to transcribe gRNA by *in vitro* transcription using the HiScribe T7 Yield RNA Synthesis kit (New England BioLabs). To induce target mutations, embryos from the *tg[cldnb:lynGFP]* line were co-injected with 250pg of gRNA and 250ng of Cas9 protein (PNA Bio). Indels were detected via PCR and confirmed by sequencing. Table 5.7.1 lists

oligos used for gRNA synthesis. All oligos and PCR primers were obtained from Eurofins MWG Operon.

Table 5.3.1: gRNA oligos

Target gene	Sequence (brackets indicate mutation target)
sdc4	5'-TAATACGACTCACTATAG[GGTACCTCTGAAAAACAAGG]GTTTTAGAGC TAGAAATAGC-3'
hs3st3b1a	5′-TAATACGACTCACTATAG[GGGATAGCAGGTGCCGTGAA] GTTTTAGAGCTAGAAATAGC-3′
hs3st3b1b	5′-TAATACGACTCACTATAG[GGACAATAGTAATCGAGCGA] GTTTTAGAGCTAGAAATAGC-3′
chimeric gRNA core sequence	5′-AAAAGCACCGACTCGGTGCCACTTTTTCAAGTTGATAACGGACTAGCCTTATTT TAACTTGCTATTTCTAGCTCTAAAAC-3′

For genotyping, DNA was extracted from embryos or fin clips through digestion in genomic digestion buffer at 55°C overnight. DNA digestion was diluted 1:25 prior to PCR. Table 5.7.2 lists the primers used for genotyping. PCR samples were genotyped using an Applied Biosystems 3130xl Genetic Analyzer.

Table 5.3.2: PCR Primers

Target Gene	Direction	Sequence
sdc4	Forward	5'-TGTAAAACGACGGCCAGTTGTGTCTCTCAGCTGTGACCTT-3'
	Reverse	5'-GTGTCTTATCCTCATCGTCAGTCTGGTTT-3'
hs3st3b1a	Forward	5'-TGTAAAACGACGGCCAGTAGGGACCTGCTAAACAACGA-3'
	Reverse	5'-GTGTCTTTTATTATCGCTTGGGGCAAC-3'
hs3st3b1b	Forward	5'-TGTAAAACGACGGCCAGTATGCTGCTCCTCTGGGTCTA-3'
	Reverse	5'-GTGTCTTGTCTGGACAGGAGCTTGGAC-3'

5.4 Morpholinos and chemical inhibitors

Tables 5.4.1 and 5.4.2 list the morpholino and chemical inhibitors used.

All morpholinos were acquired from Gene-Tools, LLC, diluted in sterile H2O to 20µg/µl stock concentration and stored at RT. All morpholinos were co-injected with the

p53 morpholino. Unless otherwise stated, one-cell stage embryos were injected with the working concentration listed.

Table 5.4.1: Morpholinos

Target	Blocking Type	Sequence	Effective Concentration
p53	Translation	5'-GCGCCATTGCTTTGCAAGAATTG-3'	1.5 ng/nl
sdc4	Translation	5'-CGGACAACTTTATTCACTCGGGCTA-3'	4 ng/nl
fgf10	Translation	5'-GCTTTACTCACTGTACGGATCGTCC-3'	4 ng/nl
sdc3	Translation	5'-GTGCTGGGTGTGAATAAACCCTTCT-3'	4 ng/nl
cxcl12a	Translation	5'-TTGAGATCCATGTTTGCAGTGTGAA-3'	4ng/nl
hs3st3b1a	Translation	5'-ACACCCACAGCGAGAGCATGATGCA-3'	6ng/nl
hs3st3b1b	Translation	5'-GGTGACAGAACAGGCTATATTCCAT-3'	6ng/nl
hs3st3b1a	Splice	5'-TGTGTGGATAAAAAAACGTACCTGT-3'	2ng/nl
hs3st3b1b	Splice	5'-ATTAGTAGCATTCGTACCTGTACCA-3'	6ng/nl

Chemical inhibitors were diluted in DMSO, except for $NaClO_3$, which was diluted in egg water. Chemical treatment lasted 5-6 hours prior to fixation of embryos in 4% PFA.

Table 5.4.2: Chemical inhibitors

Inhibitor	Concentration	Inhibition Target	Source
DMSO	5µM	none - control	American Bioanalytical
IWR-1	10-30µM	TNKS1/PARP5a, TNKS2/PARP5b (suppresses Wnt)	Calbiochem
BIO	5µM	GSK-3α/β (activates Wnt)	Calbiochem
$NaClO_3$	200mM	formation of 3′-phosphoadenosine 5′-phosphosulfate (PAPS) (suppresses HSPG sulfation)	Sigma-Aldrich
K02288	30µM	Type I BMP receptors	Tocris
SU5402	10µM	VEGF and Fgf receptors	Tocris

5.5 *In situ* hybridization

In situ probes and hybridization protocol

Clones containing the pCS2+ vector with the full open reading frame of *sdc4*, *hs3st3b1a*, *hs3st3b1b*, were obtained from GenScript. In addition to probes generated from these clones, the *lef1* and *pea3* probes were also used [27]. RNA probes were synthesized using a DIG labeling kit (Roche). *In situ* hybrization was performed on embryos fixed in

4% PFA overnight at 4°C and stored in 100% methanol at -20°C. They were rehydrated in a descending series of methanol to PBST, permeabilized in 10 μg/ml proteinase K, and hybridized with DIG-labeled antisense RNA probes at 65°C overnight. Embryos were washed sequentially in 50% formamide/2x SSCT, 2x SSCT and 0.2x SSCT at 65°C, blocked for 1 hr in blocking solution, and then incubated with anti-DIG-AP antibody in blocking solution for 2 hr at RT. After washing with PBST and then NTMT staining buffer embryos were incubated in NTMT staining buffer with BCIP/NBT (Roche). To stop the color reaction, embryos were washed with PBST and then fixed in 4% PFA. To clearly delineate the boundaries of the PLLP in DIC images, embryos were stained after *in situ* with anti-GFP antibody (Abcam). For flat mounting, the yolk was dissected away and embryos were mounted for imaging in 100% glycerol.

In situ image analysis

All images were analyzed using ImageJ. For domain length quantification, expression domain lengths were measured and then normalized by comparison to PLLP length. Similarly, distance from the leading edge was measured and also normalized to PLLP length.

For quantification of expression intensity, color images were converted to 8-bit grayscale and inverted from positive to negative. The average gray value of all of the pixels within the PLLP was measured, as was the average gray value of the pixels in the background. The ratio of PLLP pixel gray value to background pixel gray value was taken and averaged for each experimental group.

5.6 Morpholino and mRNA microinjection

Clones containing the pCS2+ vector with the full open reading frame of sdc4, hs3st3b1a, hs3st3b1b, were obtained from GenScript. Plasmids were linearized using FastDigest NotI (ThermoFisher) and mRNA was transcribed using the mMessage mMachine SP6 RNA transcription kit (Ambion).

For microinjection, morpholinos were diluted to concentrations between 1.5-6ng/nl, depending on the efficacy of the morpholino, in DEPC-H_2O and phenol red dye. Similarly, mRNA was diluted to concentrations between 10-600pg in Ultra Pure Water and RNAse-free phenol red. Needles were loaded into a pneumatic injection rig and calibrated to inject 1nl of injection mix. One-cell stage embryos were aligned on a grooved agarose mold and injected prior to the first cleavage.

5.7 Microscopy

Still images of embryos were captured on a Leica MZ16F fluorescent microscope. *In situ* images were taken on Zeiss LSM 510 META confocal microscope. For time-lapse imaging, embryos were anesthetized at 26-28hpf in 600 μM MS-222 (Sigma) and mounted in 0.8% low melting temperature agarose (NuSieve GTG) and placed in a solution of egg water with 600 μM tricaine or imaging. On a Leica SP5 confocal microscope, 25 z-stack images were acquired at 5-minute intervals for between 5 and 24 hours. Time-lapse images were compressed and stitched into movies in ImageJ.

5.8 Statistical analysis

Unpaired, two-tailed t-tests were used to determine statistical significance. *p* values less than 0.05 were considered statistically significant. All statistical analysis was performed using Microsoft Excel or GraphPad Prism software.

References

1. Chitnis AB, Nogare DD: **Lessons from the Zebrafish Lateral Line System**. *Principles of Developmental Genetics, 2nd Edition* 2015:265-279.
2. Dijkgraaf S: **The functioning and significance of the lateral-line organs**. *Biol Rev Camb Philos Soc* 1963, **38**:51-105.
3. Pohlmann K, Atema J, Breithaupt T: **The importance of the lateral line in nocturnal predation of piscivorous catfish**. *J Exp Biol* 2004, **207**(Pt 17):2971-2978.
4. Montgomery JC, Baker CF, Carton AG: **The lateral line can mediate rheotaxis in fish**. *Nature* 1997, **389**:960-963.
5. Grant KA, Raible DW, Piotrowski T: **Regulation of latent sensory hair cell precursors by glia in the zebrafish lateral line**. *Neuron* 2005, **45**(1):69-80.
6. Sarrazin AF, Nunez VA, Sapede D, Tassin V, Dambly-Chaudiere C, Ghysen A: **Origin and early development of the posterior lateral line system of zebrafish**. *J Neurosci* 2010, **30**(24):8234-8244.
7. Wada H, Ghysen A, Satou C, Higashijima S, Kawakami K, Hamaguchi S, Sakaizumi M: **Dermal morphogenesis controls lateral line patterning during postembryonic development of teleost fish**. *Dev Biol* 2010, **340**(2):583-594.
8. Aman A, Piotrowski T: **Wnt/beta-catenin and Fgf signaling control collective cell migration by restricting chemokine receptor expression**. *Dev Cell* 2008, **15**(5):749-761.
9. Nechiporuk A, Raible DW: **FGF-dependent mechanosensory organ patterning in zebrafish**. *Science* 2008, **320**(5884):1774-1777.
10. Lecaudey V, Cakan-Akdogan G, Norton WH, Gilmour D: **Dynamic Fgf signaling couples morphogenesis and migration in the zebrafish lateral line primordium**. *Development* 2008, **135**(16):2695-2705.
11. Tsang M, Friesel R, Kudoh T, Dawid IB: **Identification of Sef, a novel modulator of FGF signalling**. *Nat Cell Biol* 2002, **4**(2):165-169.
12. Matsuda M, Nogare DD, Somers K, Martin K, Wang C, Chitnis AB: **Lef1 regulates Dusp6 to influence neuromast formation and spacing in the zebrafish posterior lateral line primordium**. *Development* 2013, **140**(11):2387-2397.
13. Valdivia LE, Young RM, Hawkins TA, Stickney HL, Cavodeassi F, Schwarz Q, Pullin LM, Villegas R, Moro E, Argenton F *et al*: **Lef1-dependent Wnt/beta-catenin signalling drives the proliferative engine that maintains tissue homeostasis during lateral line development**. *Development* 2011, **138**(18):3931-3941.
14. McGraw HF, Drerup CM, Culbertson MD, Linbo T, Raible DW, Nechiporuk AV: **Lef1 is required for progenitor cell identity in the zebrafish lateral line primordium**. *Development* 2011, **138**(18):3921-3930.
15. Raman D, Sobolik-Delmaire T, Richmond A: **Chemokines in health and disease**. *Exp Cell Res* 2011, **317**(5):575-589.
16. David NB, Sapede D, Saint-Etienne L, Thisse C, Thisse B, Dambly-Chaudiere C, Rosa FM, Ghysen A: **Molecular basis of cell migration in the fish lateral line: role of the chemokine receptor CXCR4 and of its ligand, SDF1**. *Proc Natl Acad Sci U S A* 2002, **99**(25):16297-16302.

17. Haas P, Gilmour D: **Chemokine signaling mediates self-organizing tissue migration in the zebrafish lateral line**. *Dev Cell* 2006, **10**(5):673-680.
18. Valentin G, Haas P, Gilmour D: **The chemokine SDF1a coordinates tissue migration through the spatially restricted activation of Cxcr7 and Cxcr4b**. *Curr Biol* 2007, **17**(12):1026-1031.
19. Li Q, Shirabe K, Kuwada JY: **Chemokine signaling regulates sensory cell migration in zebrafish**. *Dev Biol* 2004, **269**(1):123-136.
20. Dambly-Chaudiere C, Cubedo N, Ghysen A: **Control of cell migration in the development of the posterior lateral line: antagonistic interactions between the chemokine receptors CXCR4 and CXCR7/RDC1**. *BMC Dev Biol* 2007, **7**:23.
21. Dona E, Barry JD, Valentin G, Quirin C, Khmelinskii A, Kunze A, Durdu S, Newton LR, Fernandez-Minan A, Huber W *et al*: **Directional tissue migration through a self-generated chemokine gradient**. *Nature* 2013, **503**(7475):285-289.
22. Venkiteswaran G, Lewellis SW, Wang J, Reynolds E, Nicholson C, Knaut H: **Generation and dynamics of an endogenous, self-generated signaling gradient across a migrating tissue**. *Cell* 2013, **155**(3):674-687.
23. Dalle Nogare D, Somers K, Rao S, Matsuda M, Reichman-Fried M, Raz E, Chitnis AB: **Leading and trailing cells cooperate in collective migration of the zebrafish posterior lateral line primordium**. *Development* 2014, **141**(16):3188-3196.
24. Matsuda M, Chitnis AB: **Atoh1a expression must be restricted by Notch signaling for effective morphogenesis of the posterior lateral line primordium in zebrafish**. *Development* 2010, **137**(20):3477-3487.
25. Itoh M, Chitnis AB: **Expression of proneural and neurogenic genes in the zebrafish lateral line primordium correlates with selection of hair cell fate in neuromasts**. *Mech Dev* 2001, **102**(1-2):263-266.
26. Medeiros GF, Mendes A, Castro RA, Bau EC, Nader HB, Dietrich CP: **Distribution of sulfated glycosaminoglycans in the animal kingdom: widespread occurrence of heparin-like compounds in invertebrates**. *Biochim Biophys Acta* 2000, **1475**(3):287-294.
27. Kramer KL, Yost HJ: **Heparan sulfate core proteins in cell-cell signaling**. *Annu Rev Genet* 2003, **37**:461-484.
28. Hacker U, Nybakken K, Perrimon N: **Heparan sulphate proteoglycans: the sweet side of development**. *Nat Rev Mol Cell Biol* 2005, **6**(7):530-541.
29. Bernfield M, Gotte M, Park PW, Reizes O, Fitzgerald ML, Lincecum J, Zako M: **Functions of cell surface heparan sulfate proteoglycans**. *Annu Rev Biochem* 1999, **68**:729-777.
30. Lin X, Wei G, Shi Z, Dryer L, Esko JD, Wells DE, Matzuk MM: **Disruption of gastrulation and heparan sulfate biosynthesis in EXT1-deficient mice**. *Dev Biol* 2000, **224**(2):299-311.
31. Morio H, Honda Y, Toyoda H, Nakajima M, Kurosawa H, Shirasawa T: **EXT gene family member rib-2 is essential for embryonic development and heparan sulfate biosynthesis in Caenorhabditis elegans**. *Biochem Biophys Res Commun* 2003, **301**(2):317-323.
32. Turnbull J, Powell A, Guimond S: **Heparan sulfate: decoding a dynamic multifunctional cell regulator**. *Trends Cell Biol* 2001, **11**(2):75-82.

33. Zako M, Dong J, Goldberger O, Bernfield M, Gallagher JT, Deakin JA: **Syndecan-1 and -4 synthesized simultaneously by mouse mammary gland epithelial cells bear heparan sulfate chains that are apparently structurally indistinguishable**. *J Biol Chem* 2003, **278**(15):13561-13569.
34. Chakravarti R, Adams JC: **Comparative genomics of the syndecans defines an ancestral genomic context associated with matrilins in vertebrates**. *BMC Genomics* 2006, **7**:83.
35. Gupta M, Brand M: **Identification and expression analysis of zebrafish glypicans during embryonic development**. *PLoS One* 2013, **8**(11):e80824.
36. Venero Galanternik M, Kramer KL, Piotrowski T: **Heparan Sulfate Proteoglycans Regulate Fgf Signaling and Cell Polarity during Collective Cell Migration**. *Cell Rep* 2015.
37. Thisse B. PS, Fürthauer M., Loppin B., Heyer V., Degrave A., Woehl R., Lux A., Steffan T., Charbonnier X.Q., Thisse C.: **Expression of the zebrafish genome during embryogenesis**. 2001, **(NIH R01 RR15402). ZFIN Direct Data Submission (**http://zfin.org/**)**.
38. Zhang L, David G, Esko JD: **Repetitive Ser-Gly sequences enhance heparan sulfate assembly in proteoglycans**. *J Biol Chem* 1995, **270**(45):27127-27135.
39. Zhang L, Esko JD: **Amino acid determinants that drive heparan sulfate assembly in a proteoglycan**. *J Biol Chem* 1994, **269**(30):19295-19299.
40. Paulson JC, Colley KJ: **Glycosyltransferases. Structure, localization, and control of cell type-specific glycosylation**. *J Biol Chem* 1989, **264**(30):17615-17618.
41. Wei G, Bai X, Gabb MM, Bame KJ, Koshy TI, Spear PG, Esko JD: **Location of the glucuronosyltransferase domain in the heparan sulfate copolymerase EXT1 by analysis of Chinese hamster ovary cell mutants**. *J Biol Chem* 2000, **275**(36):27733-27740.
42. McCormick C, Duncan G, Goutsos KT, Tufaro F: **The putative tumor suppressors EXT1 and EXT2 form a stable complex that accumulates in the Golgi apparatus and catalyzes the synthesis of heparan sulfate**. *Proc Natl Acad Sci U S A* 2000, **97**(2):668-673.
43. Lidholt K, Lindahl U: **Biosynthesis of heparin. The D-glucuronosyl- and N-acetyl-D-glucosaminyltransferase reactions and their relation to polymer modification**. *Biochem J* 1992, **287 (Pt 1)**:21-29.
44. Lidholt K, Kjellen L, Lindahl U: **Biosynthesis of heparin. Relationship between the polymerization and sulphation processes**. *Biochem J* 1989, **261**(3):999-1007.
45. Toida T, Yoshida H, Toyoda H, Koshiishi I, Imanari T, Hileman RE, Fromm JR, Linhardt RJ: **Structural differences and the presence of unsubstituted amino groups in heparan sulphates from different tissues and species**. *Biochem J* 1997, **322 (Pt 2)**:499-506.
46. Filipek-Gorniok B, Carlsson P, Haitina T, Habicher J, Ledin J, Kjellen L: **The NDST gene family in zebrafish: role of NDST1B in pharyngeal arch formation**. *PLoS One* 2015, **10**(3):e0119040.
47. Duncan MB, Liu M, Fox C, Liu J: **Characterization of the N-deacetylase domain from the heparan sulfate N-deacetylase/N-sulfotransferase 2**. *Biochem Biophys Res Commun* 2006, **339**(4):1232-1237.

48. Kakuta Y, Sueyoshi T, Negishi M, Pedersen LC: **Crystal structure of the sulfotransferase domain of human heparan sulfate N-deacetylase/ N-sulfotransferase 1**. *J Biol Chem* 1999, **274**(16):10673-10676.
49. Jacobsson I, Lindahl U, Jensen JW, Roden L, Prihar H, Feingold DS: **Biosynthesis of heparin. Substrate specificity of heparosan N-sulfate D-glucuronosyl 5-epimerase**. *J Biol Chem* 1984, **259**(2):1056-1063.
50. Ghiselli G, Farber SA: **D-glucuronyl C5-epimerase acts in dorso-ventral axis formation in zebrafish**. *BMC Dev Biol* 2005, **5**:19.
51. Qin Y, Ke J, Gu X, Fang J, Wang W, Cong Q, Li J, Tan J, Brunzelle JS, Zhang C *et al*: **Structural and functional study of D-glucuronyl C5-epimerase**. *J Biol Chem* 2015, **290**(8):4620-4630.
52. Mulloy B, Forster MJ: **Conformation and dynamics of heparin and heparan sulfate**. *Glycobiology* 2000, **10**(11):1147-1156.
53. Jia J, Maccarana M, Zhang X, Bespalov M, Lindahl U, Li JP: **Lack of L-iduronic acid in heparan sulfate affects interaction with growth factors and cell signaling**. *J Biol Chem* 2009, **284**(23):15942-15950.
54. Safaiyan F, Lindahl U, Salmivirta M: **Structural diversity of N-sulfated heparan sulfate domains: distinct modes of glucuronyl C5 epimerization, iduronic acid 2-O-sulfation, and glucosamine 6-O-sulfation**. *Biochemistry* 2000, **39**(35):10823-10830.
55. Habuchi H, Tanaka M, Habuchi O, Yoshida K, Suzuki H, Ban K, Kimata K: **The occurrence of three isoforms of heparan sulfate 6-O-sulfotransferase having different specificities for hexuronic acid adjacent to the targeted N-sulfoglucosamine**. *J Biol Chem* 2000, **275**(4):2859-2868.
56. Habuchi H, Kimata K: **Mice deficient in heparan sulfate 6-O-sulfotransferase-1**. *Prog Mol Biol Transl Sci* 2010, **93**:79-111.
57. Colliec-Jouault S, Shworak NW, Liu J, de Agostini AI, Rosenberg RD: **Characterization of a cell mutant specifically defective in the synthesis of anticoagulantly active heparan sulfate**. *J Biol Chem* 1994, **269**(40):24953-24958.
58. Shworak NW, Shirakawa M, Colliec-Jouault S, Liu J, Mulligan RC, Birinyi LK, Rosenberg RD: **Pathway-specific regulation of the synthesis of anticoagulantly active heparan sulfate**. *J Biol Chem* 1994, **269**(40):24941-24952.
59. Cadwallader AB, Yost HJ: **Combinatorial expression patterns of heparan sulfate sulfotransferases in zebrafish: I. The 3-O-sulfotransferase family**. *Dev Dyn* 2006, **235**(12):3423-3431.
60. Nugent MA, Edelman ER: **Kinetics of basic fibroblast growth factor binding to its receptor and heparan sulfate proteoglycan: a mechanism for cooperactivity**. *Biochemistry* 1992, **31**(37):8876-8883.
61. Sperinde GV, Nugent MA: **Mechanisms of fibroblast growth factor 2 intracellular processing: a kinetic analysis of the role of heparan sulfate proteoglycans**. *Biochemistry* 2000, **39**(13):3788-3796.
62. Yayon A, Klagsbrun M, Esko JD, Leder P, Ornitz DM: **Cell surface, heparin-like molecules are required for binding of basic fibroblast growth factor to its high affinity receptor**. *Cell* 1991, **64**(4):841-848.

63. Matsuo I, Kimura-Yoshida C: **Extracellular modulation of Fibroblast Growth Factor signaling through heparan sulfate proteoglycans in mammalian development**. *Curr Opin Genet Dev* 2013, **23**(4):399-407.
64. Kuro-o M: **Endocrine FGFs and Klothos: emerging concepts**. *Trends Endocrinol Metab* 2008, **19**(7):239-245.
65. Mohammadi M, Olsen SK, Goetz R: **A protein canyon in the FGF-FGF receptor dimer selects from an a la carte menu of heparan sulfate motifs**. *Curr Opin Struct Biol* 2005, **15**(5):506-516.
66. Makarenkova HP, Hoffman MP, Beenken A, Eliseenkova AV, Meech R, Tsau C, Patel VN, Lang RA, Mohammadi M: **Differential interactions of FGFs with heparan sulfate control gradient formation and branching morphogenesis**. *Sci Signal* 2009, **2**(88):ra55.
67. Norton WH, Ledin J, Grandel H, Neumann CJ: **HSPG synthesis by zebrafish Ext2 and Extl3 is required for Fgf10 signalling during limb development**. *Development* 2005, **132**(22):4963-4973.
68. Elfenbein A, Lanahan A, Zhou TX, Yamasaki A, Tkachenko E, Matsuda M, Simons M: **Syndecan 4 regulates FGFR1 signaling in endothelial cells by directing macropinocytosis**. *Sci Signal* 2012, **5**(223):ra36.
69. Fuerer C, Habib SJ, Nusse R: **A study on the interactions between heparan sulfate proteoglycans and Wnt proteins**. *Dev Dyn* 2010, **239**(1):184-190.
70. Binari RC, Staveley BE, Johnson WA, Godavarti R, Sasisekharan R, Manoukian AS: **Genetic evidence that heparin-like glycosaminoglycans are involved in wingless signaling**. *Development* 1997, **124**(13):2623-2632.
71. Hacker U, Lin X, Perrimon N: **The Drosophila sugarless gene modulates Wingless signaling and encodes an enzyme involved in polysaccharide biosynthesis**. *Development* 1997, **124**(18):3565-3573.
72. Lin X, Perrimon N: **Dally cooperates with Drosophila Frizzled 2 to transduce Wingless signalling**. *Nature* 1999, **400**(6741):281-284.
73. Haerry TE, Heslip TR, Marsh JL, O'Connor MB: **Defects in glucuronate biosynthesis disrupt Wingless signaling in Drosophila**. *Development* 1997, **124**(16):3055-3064.
74. Song HH, Shi W, Xiang YY, Filmus J: **The loss of glypican-3 induces alterations in Wnt signaling**. *J Biol Chem* 2005, **280**(3):2116-2125.
75. Munoz R, Moreno M, Oliva C, Orbenes C, Larrain J: **Syndecan-4 regulates non-canonical Wnt signalling and is essential for convergent and extension movements in Xenopus embryos**. *Nat Cell Biol* 2006, **8**(5):492-500.
76. Giraldez AJ, Copley RR, Cohen SM: **HSPG modification by the secreted enzyme Notum shapes the Wingless morphogen gradient**. *Dev Cell* 2002, **2**(5):667-676.
77. Flowers GP, Topczewska JM, Topczewski J: **A zebrafish Notum homolog specifically blocks the Wnt/beta-catenin signaling pathway**. *Development* 2012, **139**(13):2416-2425.
78. Pisconti A, Cornelison DD, Olguin HC, Antwine TL, Olwin BB: **Syndecan-3 and Notch cooperate in regulating adult myogenesis**. *J Cell Biol* 2010, **190**(3):427-441.

79. Zhao N, Liu H, Lilly B: **Reciprocal regulation of syndecan-2 and Notch signaling in vascular smooth muscle cells**. *J Biol Chem* 2012, **287**(20):16111-16120.
80. Guo Y, Feng Y, Li Z, Lin X: **Drosophila heparan sulfate 3-O sulfotransferase B null mutant is viable and exhibits no defects in Notch signaling**. *J Genet Genomics* 2014, **41**(7):369-378.
81. Murakami M, Elfenbein A, Simons M: **Non-canonical fibroblast growth factor signalling in angiogenesis**. *Cardiovasc Res* 2008, **78**(2):223-231.
82. Brule S, Charnaux N, Sutton A, Ledoux D, Chaigneau T, Saffar L, Gattegno L: **The shedding of syndecan-4 and syndecan-1 from HeLa cells and human primary macrophages is accelerated by SDF-1/CXCL12 and mediated by the matrix metalloproteinase-9**. *Glycobiology* 2006, **16**(6):488-501.
83. Brule S, Friand V, Sutton A, Baleux F, Gattegno L, Charnaux N: **Glycosaminoglycans and syndecan-4 are involved in SDF-1/CXCL12-mediated invasion of human epitheloid carcinoma HeLa cells**. *Biochim Biophys Acta* 2009, **1790**(12):1643-1650.
84. Charnaux N, Brule S, Hamon M, Chaigneau T, Saffar L, Prost C, Lievre N, Gattegno L: **Syndecan-4 is a signaling molecule for stromal cell-derived factor-1 (SDF-1)/ CXCL12**. *FEBS J* 2005, **272**(8):1937-1951.
85. Hamon M, Mbemba E, Charnaux N, Slimani H, Brule S, Saffar L, Vassy R, Prost C, Lievre N, Starzec A *et al*: **A syndecan-4/CXCR4 complex expressed on human primary lymphocytes and macrophages and HeLa cell line binds the CXC chemokine stromal cell-derived factor-1 (SDF-1)**. *Glycobiology* 2004, **14**(4):311-323.
86. Thacker BE, Xu D, Lawrence R, Esko JD: **Heparan sulfate 3-O-sulfation: a rare modification in search of a function**. *Matrix Biol* 2014, **35**:60-72.
87. Patel VN, Lombaert IM, Cowherd SN, Shworak NW, Xu Y, Liu J, Hoffman MP: **Hs3st3-modified heparan sulfate controls KIT+ progenitor expansion by regulating 3-O-sulfotransferases**. *Dev Cell* 2014, **29**(6):662-673.
88. Lee D, Oh ES, Woods A, Couchman JR, Lee W: **Solution structure of a syndecan-4 cytoplasmic domain and its interaction with phosphatidylinositol 4,5-bisphosphate**. *J Biol Chem* 1998, **273**(21):13022-13029.
89. Horowitz A, Murakami M, Gao Y, Simons M: **Phosphatidylinositol-4,5-bisphosphate mediates the interaction of syndecan-4 with protein kinase C**. *Biochemistry* 1999, **38**(48):15871-15877.
90. Nakashima S: **Protein kinase C alpha (PKC alpha): regulation and biological function**. *J Biochem* 2002, **132**(5):669-675.
91. Burridge K, Wennerberg K: **Rho and Rac take center stage**. *Cell* 2004, **116**(2):167-179.
92. Gao Y, Li M, Chen W, Simons M: **Synectin, syndecan-4 cytoplasmic domain binding PDZ protein, inhibits cell migration**. *J Cell Physiol* 2000, **184**(3):373-379.
93. Elfenbein A, Rhodes JM, Meller J, Schwartz MA, Matsuda M, Simons M: **Suppression of RhoG activity is mediated by a syndecan 4-synectin-RhoGDI1 complex and is reversed by PKCalpha in a Rac1 activation pathway**. *J Cell Biol* 2009, **186**(1):75-83.

94. Tkachenko E, Elfenbein A, Tirziu D, Simons M: **Syndecan-4 clustering induces cell migration in a PDZ-dependent manner**. *Circ Res* 2006, **98**(11):1398-1404.
95. Tkachenko E, Simons M: **Clustering induces redistribution of syndecan-4 core protein into raft membrane domains**. *J Biol Chem* 2002, **277**(22):19946-19951.
96. Oh ES, Woods A, Couchman JR: **Multimerization of the cytoplasmic domain of syndecan-4 is required for its ability to activate protein kinase C**. *J Biol Chem* 1997, **272**(18):11805-11811.
97. Bass MD, Morgan MR, Humphries MJ: **Integrins and syndecan-4 make distinct, but critical, contributions to adhesion contact formation**. *Soft Matter* 2007, **3**(3):372-376.
98. Woods A, Longley RL, Tumova S, Couchman JR: **Syndecan-4 binding to the high affinity heparin-binding domain of fibronectin drives focal adhesion formation in fibroblasts**. *Arch Biochem Biophys* 2000, **374**(1):66-72.
99. Zhang Y, Li J, Partovian C, Sellke FW, Simons M: **Syndecan-4 modulates basic fibroblast growth factor 2 signaling in vivo**. *Am J Physiol Heart Circ Physiol* 2003, **284**(6):H2078-2082.
100. Volk R, Schwartz JJ, Li J, Rosenberg RD, Simons M: **The role of syndecan cytoplasmic domain in basic fibroblast growth factor-dependent signal transduction**. *J Biol Chem* 1999, **274**(34):24417-24424.
101. Cornelison DD, Wilcox-Adelman SA, Goetinck PF, Rauvala H, Rapraeger AC, Olwin BB: **Essential and separable roles for Syndecan-3 and Syndecan-4 in skeletal muscle development and regeneration**. *Genes Dev* 2004, **18**(18):2231-2236.
102. Horowitz A, Tkachenko E, Simons M: **Fibroblast growth factor-specific modulation of cellular response by syndecan-4**. *J Cell Biol* 2002, **157**(4):715-725.
103. Chua CC, Rahimi N, Forsten-Williams K, Nugent MA: **Heparan sulfate proteoglycans function as receptors for fibroblast growth factor-2 activation of extracellular signal-regulated kinases 1 and 2**. *Circ Res* 2004, **94**(3):316-323.
104. Hou S, Maccarana M, Min TH, Strate I, Pera EM: **The secreted serine protease xHtrA1 stimulates long-range FGF signaling in the early Xenopus embryo**. *Dev Cell* 2007, **13**(2):226-241.
105. Safaiyan F, Kolset SO, Prydz K, Gottfridsson E, Lindahl U, Salmivirta M: **Selective effects of sodium chlorate treatment on the sulfation of heparan sulfate**. *J Biol Chem* 1999, **274**(51):36267-36273.
106. Matthews HK, Marchant L, Carmona-Fontaine C, Kuriyama S, Larrain J, Holt MR, Parsons M, Mayor R: **Directional migration of neural crest cells in vivo is regulated by Syndecan-4/Rac1 and non-canonical Wnt signaling/RhoA**. *Development* 2008, **135**(10):1771-1780.
107. Jones CM, Dale L, Hogan BL, Wright CV, Smith JC: **Bone morphogenetic protein-4 (BMP-4) acts during gastrula stages to cause ventralization of Xenopus embryos**. *Development* 1996, **122**(5):1545-1554.
108. Maegawa S, Varga M, Weinberg ES: **FGF signaling is required for {beta}-catenin-mediated induction of the zebrafish organizer**. *Development* 2006, **133**(16):3265-3276.

109. Bedell VM, Westcot SE, Ekker SC: **Lessons from morpholino-based screening in zebrafish**. *Brief Funct Genomics* 2011, **10**(4):181-188.
110. Blum M, De Robertis EM, Wallingford JB, Niehrs C: **Morpholinos: Antisense and Sensibility**. *Dev Cell* 2015, **35**(2):145-149.
111. Hwang WY, Fu Y, Reyon D, Maeder ML, Tsai SQ, Sander JD, Peterson RT, Yeh JR, Joung JK: **Efficient genome editing in zebrafish using a CRISPR-Cas system**. *Nat Biotechnol* 2013, **31**(3):227-229.
112. Rossi A, Kontarakis Z, Gerri C, Nolte H, Holper S, Kruger M, Stainier DY: **Genetic compensation induced by deleterious mutations but not gene knockdowns**. *Nature* 2015, **524**(7564):230-233.
113. Winkler S, Stahl RC, Carey DJ, Bansal R: **Syndecan-3 and perlecan are differentially expressed by progenitors and mature oligodendrocytes and accumulate in the extracellular matrix**. *J Neurosci Res* 2002, **69**(4):477-487.
114. Fuentealba L, Carey DJ, Brandan E: **Antisense inhibition of syndecan-3 expression during skeletal muscle differentiation accelerates myogenesis through a basic fibroblast growth factor-dependent mechanism**. *J Biol Chem* 1999, **274**(53):37876-37884.
115. Echtermeyer F, Streit M, Wilcox-Adelman S, Saoncella S, Denhez F, Detmar M, Goetinck P: **Delayed wound repair and impaired angiogenesis in mice lacking syndecan-4**. *J Clin Invest* 2001, **107**(2):R9-R14.
116. Reizes O, Lincecum J, Wang Z, Goldberger O, Huang L, Kaksonen M, Ahima R, Hinkes MT, Barsh GS, Rauvala H *et al*: **Transgenic expression of syndecan-1 uncovers a physiological control of feeding behavior by syndecan-3**. *Cell* 2001, **106**(1):105-116.
117. Elfenbein A, Simons M: **Syndecan-4 signaling at a glance**. *J Cell Sci* 2013, **126**(Pt 17):3799-3804.
118. Forsten-Williams K, Chua CC, Nugent MA: **The kinetics of FGF-2 binding to heparan sulfate proteoglycans and MAP kinase signaling**. *J Theor Biol* 2005, **233**(4):483-499.
119. Kniss JS, Jiang L, Piotrowski T: **Insights into sensory hair cell regeneration from the zebrafish lateral line**. *Curr Opin Genet Dev* 2016, **40**:32-40.
120. Jiang L, Romero-Carvajal A, Haug JS, Seidel CW, Piotrowski T: **Gene-expression analysis of hair cell regeneration in the zebrafish lateral line**. *Proc Natl Acad Sci U S A* 2014, **111**(14):E1383-1392.
121. Ku YC, Renaud NA, Veile RA, Helms C, Voelker CC, Warchol ME, Lovett M: **The transcriptome of utricle hair cell regeneration in the avian inner ear**. *J Neurosci* 2014, **34**(10):3523-3535.
122. Lush ME, Piotrowski T: **Sensory hair cell regeneration in the zebrafish lateral line**. *Dev Dyn* 2014, **243**(10):1187-1202.
123. Marcum JA, Atha DH, Fritze LM, Nawroth P, Stern D, Rosenberg RD: **Cloned bovine aortic endothelial cells synthesize anticoagulantly active heparan sulfate proteoglycan**. *J Biol Chem* 1986, **261**(16):7507-7517.
124. Pejler G, Backstrom G, Lindahl U, Paulsson M, Dziadek M, Fujiwara S, Timpl R: **Structure and affinity for antithrombin of heparan sulfate chains derived from basement membrane proteoglycans**. *J Biol Chem* 1987, **262**(11):5036-5043.

125. de Agostini AI, Dong JC, de Vantery Arrighi C, Ramus MA, Dentand-Quadri I, Thalmann S, Ventura P, Ibecheole V, Monge F, Fischer AM *et al*: **Human follicular fluid heparan sulfate contains abundant 3-O-sulfated chains with anticoagulant activity**. *J Biol Chem* 2008, **283**(42):28115-28124.
126. Liu J, Shworak NW, Fritze LM, Edelberg JM, Rosenberg RD: **Purification of heparan sulfate D-glucosaminyl 3-O-sulfotransferase**. *J Biol Chem* 1996, **271**(43):27072-27082.
127. Kusche M, Oscarsson LG, Reynertson R, Roden L, Lindahl U: **Biosynthesis of heparin. Enzymatic sulfation of pentasaccharides**. *J Biol Chem* 1991, **266**(12):7400-7409.
128. Zhang L, Lawrence R, Schwartz JJ, Bai X, Wei G, Esko JD, Rosenberg RD: **The effect of precursor structures on the action of glucosaminyl 3-O-sulfotransferase-1 and the biosynthesis of anticoagulant heparan sulfate**. *J Biol Chem* 2001, **276**(31):28806-28813.
129. Shukla D, Liu J, Blaiklock P, Shworak NW, Bai X, Esko JD, Cohen GH, Eisenberg RJ, Rosenberg RD, Spear PG: **A novel role for 3-O-sulfated heparan sulfate in herpes simplex virus 1 entry**. *Cell* 1999, **99**(1):13-22.
130. Shworak NW, Liu J, Petros LM, Zhang L, Kobayashi M, Copeland NG, Jenkins NA, Rosenberg RD: **Multiple isoforms of heparan sulfate D-glucosaminyl 3-O-sulfotransferase. Isolation, characterization, and expression of human cdnas and identification of distinct genomic loci**. *J Biol Chem* 1999, **274**(8):5170-5184.
131. Liu J, Shworak NW, Sinay P, Schwartz JJ, Zhang L, Fritze LM, Rosenberg RD: **Expression of heparan sulfate D-glucosaminyl 3-O-sulfotransferase isoforms reveals novel substrate specificities**. *J Biol Chem* 1999, **274**(8):5185-5192.
132. Xia G, Chen J, Tiwari V, Ju W, Li JP, Malmstrom A, Shukla D, Liu J: **Heparan sulfate 3-O-sulfotransferase isoform 5 generates both an antithrombin-binding site and an entry receptor for herpes simplex virus, type 1**. *J Biol Chem* 2002, **277**(40):37912-37919.
133. Spillman D. LU: **Glycosaminoglycan-protein interactions: a question of specificity**. *Curr Opin Struct Biol* 1994, **4**(5):677-682.
134. Guimond S, Maccarana M, Olwin BB, Lindahl U, Rapraeger AC: **Activating and inhibitory heparin sequences for FGF-2 (basic FGF). Distinct requirements for FGF-1, FGF-2, and FGF-4**. *J Biol Chem* 1993, **268**(32):23906-23914.
135. Wu ZL, Zhang L, Yabe T, Kuberan B, Beeler DL, Love A, Rosenberg RD: **The involvement of heparan sulfate (HS) in FGF1/HS/FGFR1 signaling complex**. *J Biol Chem* 2003, **278**(19):17121-17129.
136. Thunberg L, Backstrom G, Lindahl U: **Further characterization of the antithrombin-binding sequence in heparin**. *Carbohydr Res* 1982, **100**:393-410.
137. Lindahl U, Backstrom G, Thunberg L, Leder IG: **Evidence for a 3-O-sulfated D-glucosamine residue in the antithrombin-binding sequence of heparin**. *Proc Natl Acad Sci U S A* 1980, **77**(11):6551-6555.
138. Hubbard S, Darmani NA, Thrush GR, Dey D, Burnham L, Thompson JM, Jones K, Tiwari V: **Zebrafish-encoded 3-O-sulfotransferase-3 isoform mediates herpes simplex virus type 1 entry and spread**. *Zebrafish* 2010, **7**(2):181-187.

139. Pempe EH, Xu Y, Gopalakrishnan S, Liu J, Harris EN: **Probing structural selectivity of synthetic heparin binding to Stabilin protein receptors**. *J Biol Chem* 2012, **287**(25):20774-20783.
140. Vanpouille C, Deligny A, Delehedde M, Denys A, Melchior A, Lienard X, Lyon M, Mazurier J, Fernig DG, Allain F: **The heparin/heparan sulfate sequence that interacts with cyclophilin B contains a 3-O-sulfated N-unsubstituted glucosamine residue**. *J Biol Chem* 2007, **282**(33):24416-24429.
141. Neugebauer JM, Cadwallader AB, Amack JD, Bisgrove BW, Yost HJ: **Differential roles for 3-OSTs in the regulation of cilia length and motility**. *Development* 2013, **140**(18):3892-3902.
142. Christianson HC, Belting M: **Heparan sulfate proteoglycan as a cell-surface endocytosis receptor**. *Matrix Biol* 2014, **35**:51-55.
143. Oh MJ, Akhtar J, Desai P, Shukla D: **A role for heparan sulfate in viral surfing**. *Biochem Biophys Res Commun* 2010, **391**(1):176-181.
144. Lopez-Schier H, Starr CJ, Kappler JA, Kollmar R, Hudspeth AJ: **Directional cell migration establishes the axes of planar polarity in the posterior lateral-line organ of the zebrafish**. *Dev Cell* 2004, **7**(3):401-412.
145. Mirkovic I, Pylawka S, Hudspeth AJ: **Rearrangements between differentiating hair cells coordinate planar polarity and the establishment of mirror symmetry in lateral-line neuromasts**. *Biol Open* 2012, **1**(5):498-505.
146. Devenport D: **The cell biology of planar cell polarity**. *J Cell Biol* 2014, **207**(2):171-179.
147. Escobedo N, Contreras O, Munoz R, Farias M, Carrasco H, Hill C, Tran U, Pryor SE, Wessely O, Copp AJ *et al*: **Syndecan 4 interacts genetically with Vangl2 to regulate neural tube closure and planar cell polarity**. *Development* 2013, **140**(14):3008-3017.
148. Karasneh GA, Ali M, Shukla D: **An important role for syndecan-1 in herpes simplex virus type-1 induced cell-to-cell fusion and virus spread**. *PLoS One* 2011, **6**(9):e25252.
149. Kimmel CB, Ballard WW, Kimmel SR, Ullmann B, Schilling TF: **Stages of embryonic development of the zebrafish**. *Dev Dyn* 1995, **203**(3):253-310.
150. Varshney GK, Pei W, LaFave MC, Idol J, Xu L, Gallardo V, Carrington B, Bishop K, Jones M, Li M *et al*: **High-throughput gene targeting and phenotyping in zebrafish using CRISPR/Cas9**. *Genome Res* 2015, **25**(7):1030-1042.

Curriculum Vitae

Caitlin Moira (Younts) Fox
Home: 8908 16th Street • Silver Spring, MD 20910
Cell: 301-609-0020 • Email: caitlinmoirafox@mail.com • Blog:
http://bioblogyscience.wordpress.com

Caitlin Moira Fox (née Younts), daughter of Steven Carroll Younts and Diana Joan Younts, was born on June 11, 1986 in San Francisco, California. Caitlin spent most of her childhood living in the Maryland suburbs of Washington, DC. She started her scientific career in 2007 as an intern at the National Institute of Mental Health in Bethesda, Maryland under the mentorship of Dr. Zheng Li.

Caitlin received her Bachelor of Arts (B.A.) in Biology and History from Oberlin College in Oberlin Ohio in May 2008. After graduation, she completed a two-year post-baccalaureate research fellowship at the National Institute on Aging in the Laboratory of Experimental Gerontology under the mentorship of Dr. Rafael de Cabo in Baltimore, Maryland.

In August 2010, she enrolled in the National Institutes of Health-Johns Hopkins University graduate partnership program. In 2011, she officially joined the lab of Dr. Ajay Chitnis at the National Institute of Child Health and Human Development in Bethesda, MD. Caitlin married Brett John Fox on October 19, 2013 in Adelphi, Maryland. During graduate school, Caitlin worked as an adjunct faculty member at the Community College of Baltimore County. Caitlin intends to pursue a career in teaching with a Lecturer position in the Department of Biology at the University of Maryland, College Park starting in August 2016.

Education:

Johns Hopkins University, Baltimore, MD, Sept 2016
Ph.D., Cellular, Molecular, Developmental Biology and Biophysics

Oberlin College, Oberlin, OH, May 2008
B.A., Biology and History

Semester at Sea, University of Pittsburgh, Jan-April 2006
Study Abroad Program

Research Experience:

National Institutes of Health, Predoctoral IRTA, Bethesda, MD Sept 2011 – Aug 2016
• Pre-doctoral research fellow under Dr. Ajay Chitnis in the Laboratory of Molecular Genetics at the National Institute of Child Health and Human Development, researching the development of the posterior lateral line in zebrafish.
• Investigating the role of heparan sulfate proteoglycans in lateral line pattern formation.

National Institutes of Health, Postbaccalaureate IRTA, Baltimore, MD, June 2008 – June 2010
• Research fellow under Dr. Rafael de Cabo in the Laboratory of Experimental Gerontology at the National Institute on Aging, investigating how calorie restriction and calorie restriction mimetics influence aging in laboratory mice and monkeys.
• Researched effects of maternal diet during gestation on offspring health and longevity.
• Studied physiological impact of resveratrol when combined with a high fat, high sugar diet.

Smithsonian Tropical Research Institute, Winter Term Intern, Panama City, Panama, Jan 2008
• Participated in ongoing research of invasive species in the Panama Canal in the lab of Dr. Mark Torchin.
• Documented decreased survival of an invasive species of crab at high water salinity levels.

National Institutes of Health, Summer Intern, Bethesda, MD, June – Aug 2007
• Interned in the lab of Dr. Zheng Li in the National Institute of Mental Health, researching the molecular and cellular mechanisms of synapse development and plasticity.
• Examined the role of microRNAs in neuron morphological development.

Teaching and Mentoring Experience:
Foundation for Advanced Education in the Sciences, Lecturer, Bethesda, MD,Jan 2015 – May 2015
• Co-taught two lectures for the course Research Tools in Studying Disease, a class of 15 students.
• In conjunction with another graduate student, planned and taught lectures in microscopy and protein structure determination. Also designed and graded homework assignments and exam questions.

Community College of Baltimore County, Adjunct Faculty, Baltimore, MD, Jan 2013 – May 2014
• Taught weekly lecture, recitation, and laboratory classes in undergraduate Introductory Cell and Molecular Biology to classes of 15-22 students.
• Wrote exams for both lecture and laboratory classes. Also designed assignments, including homework, lab reports, and extra credit. Graded all exams and assignments.
• Used Blackboard to give online quizzes, report student grades, and answer student inquiries.

Johns Hopkins Biology Department, Teaching Assistant, Baltimore, MD, Sept 2010 – May 2011
• Taught undergraduate laboratory classes of 25 students in General Biology I & II.
• Set up laboratory experiments prior to the start of class, gave introductory lecture for each lab, guided students through experiments, answered questions, and administered in-class quizzes.

• Graded quizzes and homework assignments. Also proctored and graded exams for the lecture course.
• Used Blackboard to report student grades and answer inquiries about homework assignments.

Oberlin College Biology Department, Teaching Assistant, Oberlin, OH, Sept 2007 – Dec 2007
• Assisted a professor in teaching 30 students in an undergraduate Organismal Biology laboratory course.
• Set up experiments prior to class, performed demonstration of techniques, and answered questions.
• Assisted students with coursework and conducted review sessions for quizzes.

Oberlin College Student Academic Services, Astronomy Tutor, Oberlin, OH, Sept 2007 – Dec 2007
• Assisted a professor in running a weekly help session for 100 students in Introductory Astronomy.
• Answered student questions about homework assignments and aided them in studying for exams.

Oberlin College Office of Career Services, Peer Career Advisor, Oberlin, OH, Oct 2004 – May 2008
• Advised fellow students on the composition of resumes, cover letters, and job applications.
• Maintained an online database of job and internship opportunities.

Publications:
1) Jimenez-Gomez Y, Mattison JA, Pearson KJ, Martin-Montalvo A, Palacios HH, Sossong AM, Ward TM, Younts CM, Lewis K, Allard JS, Longo DL, Belman JP, Malagon MM, Navas P, Sanghvi M, Moaddel R, Tilmont EM, Herbert RL, Morrell CH, Egan JM, Baur JA, Ferrucci L, Bogan JS, Bernier M, de Cabo R (2013) Resveratrol improves adipose insulin signaling and reduces the inflammatory response in adipose tissue of rhesus monkeys on high-fat, high-sugar diet. Cell Metab 18:533-45.

2) Minor RK, López M, Younts CM, Jones B, Pearson KJ, Anson RM, Diéguez C, de Cabo R (2011) The arcuate nucleus and neuropeptide Y contribute to the antitumorigenic effect of calorie restriction. Aging Cell 10:483-92.

3) Jódar L, Mercken EM, Ariza J, Younts C, González-Reyes JA, Alcaín FJ, Burón I, de Cabo R, Villalba JM (2011) Genetic deletion of Nrf2 promotes immortalization and decreases life span of murine embryonic fibroblasts. J Gerontol A Biol Sci Med Sci. 66: 247-276.

4) Minor RK, Allard JS, Younts CM, Ward TM, and de Cabo R (2010) Dietary aging interventions to extend lifespan and healthspan based on calorie restriction. J Gerontol A Biol Sci Med Sci. 65:

695-703.

Poster Presentations:

1) Fox CM and Chitnis AB "Syndecan4 facilitates Fgf signaling in trailing cells and cell migration in the zebrafish lateral line primordium." 12th International Conference on Zebrafish Development and Genetics. Orlando, FL. July 2016.

2) Fox CM and Chitnis AB "Heparan sulfate proteoglycan regulate FGF signaling in the zebrafish lateral line." 12th NIH Graduate Student Research Symposium. Bethesda, MD. January 2016.

3) Fox CM and Chitnis AB "Heparan sulfate proteoglycan regulate FGF signaling in the zebrafish lateral line." 74th Annual Meeting of the Society for Developmental Biology. Snowbird, UT. July 2015.

4) Fox CM and Chitnis AB "Fishing for factors in self-organization of biological systems." 11th NIH Graduate Student Research Symposium. Bethesda, MD. January 2015.

5) Fox CM and Chitnis AB "Heparan sulfate proteoglycan regulate FGF signaling in the zebrafish lateral line." 73rd Annual Meeting of the Society for Developmental Biology. Seattle, WA. July 2014.

6) Younts CM and Chitnis AB "The role of heparan sulfate proteoglycans in zebrafish lateral line morphogenesis." 10th NIH Graduate Student Research Symposium. Bethesda, MD. January 2014.

7) Younts CM and Chitnis AB "The role of heparan sulfate proteoglycans in the zebrafish lateral line." 9th NIH Graduate Student Research Symposium. Bethesda, MD. January 2013.

8) Younts CM and Chitnis AB "Establishing a gradient of Wnt activity in the zebrafish lateral line primordium." 8th NIH Graduate Student Research Symposium. Bethesda, MD. January 2012.

9) Younts CM, Pearson KJ, Lewis KN, Phillips-Boyer DL, Egan J, and de Cabo R "Maternal voluntary exercise during pregnancy improves glucose regulation in offspring." NIA Annual Retreat. Baltimore, MD. March 2010.

10) Younts CM, Pearson KJ, Phillips DL, and de Cabo R "Impact of perinatal maternal diet on health and longevity of the offspring." NIH Spring Research Festival, Bethesda, MD. May 2009.

11) Younts CM, Pearson KJ, Lewis KN, Allard JS, Tilmont E, Yount J, Kurdziel L, de Cabo R, and Mattison, J "Effects of resveratrol treatment with a high fat and sugar diet in

monkeys: Design and preliminary data." University of Texas Nathan Shock Center Conference on Aging, Bandera, TX. October 2008.

Trainings and Workshops:
Bridge to BCG Consulting Workshop, June 2015
Scientists Teaching Science Pedagogy Course, March 2015 – June 2015
Leadership and Management Training Certificate, May 2015

Honors, Awards, and Grants:
NIH Three Minute Talks Competition, Semifinalist, June 2015
11th Annual NIH Graduate Student Research Award, Jan 2015
10th Annual NIH Graduate Student Research Award, Jan 2014
Aging Cell Best Paper Prize 2011, May 2012
Pre-doctoral Intramural Research Training Award, NICHD/NIH, Oct 2011
Post-baccalaureate Intramural Research Training Award, NIA/NIH, June 2008
George & Carrie Life Fund Prize for Excellence in American History, Oberlin History Department, May 2008
Winter Term Grant, Oberlin College Winter Term Office, Dec 2007
Summer Internship Grant, Oberlin College Office of Career Services, May 2007

Academic Activities:
NIH GSChronicals, Writer and Editor-in-Chief, May 2012 – April 2015
• Solicited and edited articles by graduate students that were of interest to the NIH graduate student community.
• Organized and edited the monthly issue of the Chronicles.
• Wrote occasional features for publication in the Chronicles.

NIH Graduate Student Council, Secretary, Jan 2013 – Dec 2013
• Helped organize academic and social activities for graduate students at the NIH.
• Advocated for graduate students at the NIH.
• Attended monthly meetings and recorded meeting minutes.

9th NIH Graduate Student Research Symposium Planning Committee, May 2012 – Jan 2013
• Chose the keynote speaker and communicated with her to organize her talk.
• Reviewed student abstracts and selected four excellent graduate students to present their work.
• Wrote and edited the symposium booklet with the agenda and biographies of all the speakers.
• Organized a student-alumni networking event.

USA Science and Engineering Festival, Volunteer Captain, May 2012
• Organized registration desk volunteers, assigning tasks and directing activities.
• Staffed exhibitor booth registration desk, checking in exhibitors.
• Acted as move-in monitor overseeing exhibit setup.